Efficient Solvers and Error Estimators
for a Mixed Method in Elastoplasticity

Vom Fachbereich Mathematik der Universität Hannover
zur Erlangung des Grades

Doktor der Naturwissenschaften
Dr. rer. nat.

genehmigte Dissertation
von

Dipl.-Math. André Geilenkothen

geboren am 11.07.1972 in Mülheim an der Ruhr

Juli 2004

Referent: Prof. Dr. rer. nat. Gerhard Starke

Korreferent: Prof. Dr. rer. nat. Ernst P. Stephan

Tag der Promotion: 03. Mai 2004

Zusammenfassung

Diese Arbeit behandelt mathematische Formulierungen zur Beschreibung von elastischem und elastoplastischem Materialverhalten von Körpern unter der Einwirkung äußerer Kräfte, sowie numerische Verfahren zur Lösung der sich in diesem Zusammmenhang ergebenden partiellen Differentialgleichungssysteme. Schwerpunkt der Arbeit ist dabei die Entwicklung eines effizienten Lösungsverfahren, einerseits durch die Verwendung eines dem Problem angepassten vorkonditionierten Gleichungslösers, andererseits durch adaptive Gitterverfeinerungsstrategien auf der Basis eines residualen a posteriori Fehlerschätzers.

Nach einem kurzen allgemeinen Überblick über die Modellierung elastischer und elastoplastischer Problemstellungen werden verschiedene Finite–Elemente–Formulierungen zur Behandlung des elastischen Problems vorgestellt. Das Hauptaugenmerk liegt hierbei auf der Klasse gemischter Finite–Elemente–Methoden und speziell auf dem sogenannten $PEERS$–Ansatz ("plane elasticity element with reduced symmetry"), der für den numerisch interessanten Fall nahezu inkompressiblen Materials besonders geeignet ist. Dieser Ansatz wird im Weiteren so modifiziert, daß er auch auf den elastoplastischen Fall angewandt werden kann. Dabei werden die zusätzlichen Nebenbedingungen in der elastoplastischen Problemstellung durch ein sogenanntes Return–Mapping–Verfahren erfüllt, welches in der in dieser Arbeit präsentierten Formulierung mittels einer neuartigen Fixpunkt–Iteration realisiert wird. Konvergenz und Konsistenz dieser Fixpunkt–Iteration werden daher detailliert analysiert. Ferner wird ausgehend von den im $PEERS$–Ansatz auftretenden indefiniten Gleichungssystemen ein effizientes iteratives Lösungsverfahren entwickelt und vorgestellt, das auf einem sogenannten Sattelpunkts–Vorkonditionierer basiert und speziell der Struktur indefiniter Systeme Rechnung trägt. Ein besonderes Augenmerk gilt auch den a posteriori Fehlerschätzern. Mittels der Technik der Helmholtz–Zerlegung wird ein residualer Fehlerschätzer für die $PEERS$–Formulierung des elastischen Problems hergeleitet und dessen Zuverlässigkeit und Effizienz nachgewiesen. Dieser Fehlerschätzer für den elastischen Fall wird mit Hilfe der Konsistenz–Überlegungen zur o.g. Fixpunkt–Iteration auch zu einem Fehlerschätzer für den plastischen Fall ausgebaut. Die vorgestellten numerischen Verfahren werden schließlich anhand eines verbreiteten Benchmark-Problems getestet. Die Ergebnisse dieser Tests demonstrieren die Effizienz und Effektivität der präsentierten Algorithmen.

Stichworte: *Elastizität, Elastoplastizität, gemischte Finite–Elemente–Methoden, Return–Mapping–Verfahren, Sattelpunkts–Vorkonditionierer, residuale Fehlerschätzer.*

Abstract

This thesis considers mathematical formulations that describe elastic and elastoplastic behavior of a material body subjected to external forces and tractions, and it considers as well numerical algorithms for the solution of the related partial differential equations. The main focus of this thesis is the development of efficient solution methods by applying problem-related preconditioned iterative solvers and also by adaptive grid refinement based on a residual a posteriori error estimator.

After a short review on modeling elastic and elastoplastic problems various finite element formulations for the elastic case will be presented. Considerations will concentrate on mixed finite element methods and especially on the $PEERS$ ('plane elasticity element with reduced symmetry') approach that was developed for the numerically interesting case of nearly incompressible materials. This approach will be modified to also fit to the elastoplastic case that poses additional constraints which can be fulfilled applying a return mapping procedure. In this thesis the return mapping is realized via a new fixed point iteration scheme. Convergence and consistency of this scheme will be analyzed in detail. Furthermore, the linear systems resulting from the $PEERS$ formulation lead to an efficient iterative solution method based on a so-called constraint preconditioner that uses the saddle-point pattern of such indefinite systems. We also focus on a posteriori error estimators. By applying the Helmholtz decomposition a reliable and efficient residual error estimator for the $PEERS$ approach in elasticity is deduced and proved. This estimator is also extended to an estimator for the plastic case using considerations on the consistency of the above mentioned fixed point iteration scheme. The presented numerical methods are finally tested for a common benchmark problem. The results show efficiency and effectiveness of the proposed algorithms.

Keywords: *Elasticity, Elastoplasticity, Mixed Finite Element Methods, Return Mapping, Constraint Preconditioner, Residual Error Estimators.*

Contents

List of Figures

List of Tables

Introduction

The mathematical modeling and description of elastic and elastoplastic material behavior and the numerical treatment of these topics is of large interest in science and industry. Every building and structure, every vehicle and machine has to be tested in numerical simulations to verify whether it can stand various external forces and tractions that are deemed important for the specimen. Such simulations are also necessary to find criteria for the failure of a material, a building or a machine. Hence, the detailed and problem-related modeling of the underlying physical and mechanical processes is a very advanced field of research.

The constitutive equations describing elasticity in its various forms (e.g. the linear small-strain model or any nonlinear model) are well-known for a long time. There are also many models for elastoplasticity due to the different forms of plasticity as e.g. plasticity with hardening or viscoplasticity but also owing to different flow rules as for example the *von Mises* yield criterion or the *Tresca* flow rule. All these formulations were introduced in the first half or the middle of the last century and are therefore also a well-researched topic.

Naturally, the numerical treatment of elasticity and elastoplasticity problems is of paramount importance, too. Any simulations or computations that are related to engineering applications are far too complex and of such a large scale that ***efficient*** numerical solution methods are essential. The main numerical tool are of course finite element methods that yield computable approximations to the idealized solution in finite dimensional spaces. These finite spaces have to be of course subspaces of the infinite dimensional space that contains the true solution. The computation of these approximations usually leads to very large linear equation systems with millions of unknowns. Therefore these problems require efficient iterative solution techniques combined – if possible – with problem-related preconditioners.

Furthermore, the finite element method yields *a priori* error estimates that guarantee a convergence of the method if we choose finer and finer discretizations, thus enlarging

the finite dimensional approximation space and the corresponding linear system. On the other hand the application of a finite element method on a very fine mesh is also a very costly process in terms of numerical resources such as time and computer capacity. Due to the fact that usually the discretization error arising in a finite element scheme is not uniformly distributed on a mesh it is reasonable to use a finer discretization only in regions where the error is large. This consideration leads to the important topic of *a posteriori* error estimators.

Such an error estimator is determined in the post-processing of the computation of an finite element approximation and it has to have two properties: *efficiency* and *reliability*. By efficiency we mean that the estimator yields locally (i.e. on each element or on a patch of elements) a lower bound of the error. Consequently, this bound can be used in an adaptive strategy that refines the match in such regions where the lower bound is relatively large. Reliability on the other hand yields a global upper bound on the error which of course describes the maximal error on the whole discretization and is therefore used as a termination criterion for the refinement algorithm.

The idea of *a posteriori* error estimation was developed and published first in [BR1'78, BR2'78] starting a new branch of research interest that developed several kinds of such estimators for the diverse forms of variational formulations and dicretizations. We refer at this point to e.g. [BW'85, ZZ'87, ZZ'88, Do'96] for general considerations on such estimators and to [Ve'96, Ve'97] for estimators for the elastic problem. However, all the referenced work consider only so-called primal finite element methods in one variable. Such a primal approach formulates all quantities of interest in a partial differential equation system in terms of the primal variable and solves the problem for that variable. The other quantities are recovered via post-processing. This finite element approach is very useful in such cases that have a primal variable of main interest. In problems of elasticity and elastoplasticity however we are primarily interested in the dual variable of the stress within a material besides the primal variable describing the material's deformation. In a saddle-point setting we can formulate such problems with two or more variables of interest as a minimization problem under constraints. Such formulations lead finally to the so-called mixed finite element methods that approximate multiple variables simultaneously in 'mixed' (i.e different) ansatz spaces. Mixed methods for the elastic problem are e.g. the *Hellinger-Reissner* principle, the *Hu-Washizu* principle or the *PEERS* ('plane elasticity element with reduced symmetry') approach. For these methods in general we refer to [Bz'74, BF'91] while considerations on the mixed methods for elasticity can be found in [Re'50, Wa'68, ABD'84, Br'97]. The topic of error estimation for those mixed methods on the other hand is not that extensively researched as estimators for primal methods are. Literature on this topic can nevertheless be found e.g. in [BV'96, WH'99],

in [Ca'97, CD'98, CDFH'00] or in [BGS'02, GS'02] while there exists a broad variety of error **indicators** for such problems in engineering literature. We cite for example [SR'90, KSSM'94, BKNSW'95, SKSM'97, B'98]. The most recent work on error estimation for a mixed method in elasticity is presented in [Lo'02, LoV'04] where an efficient and reliable error estimator for the *PEERS* approach is developed and proved.

The topic of mixed finite methods for plasticity is also of eminent interest in the literature. In the elastoplastic case the mixed methods developed for elasticity have to be complemented with an iterative procedure that solves the nonlinearities introduced to the system via additional constraints. This can be done by Newton-type methods as for example in [ACZ'99] or via return mapping techniques as analyzed in e.g. [Bl'97, SH'98, Wie1'99, Wie2'99]. The problem of error estimation in the elastoplastic problem however is not fully researched. The main efforts in this direction are still due to [Jo'77, Jo'78].

There are three main contributions of this thesis in the research area of efficient solution methods for elasticity and elastoplasticity. The first contribution is the development and implementation of an efficient *GMRES* scheme for the indefinite linear systems arising from mixed finite element methods such as e.g. the *PEERS* approach. In such a scheme efficiency depends on a good preconditioner for the indefinite system in question. Following an idea only theoretically examined in [KGW'00] we therefore apply a so-called *constraint preconditioner* that has to resemble the saddle-point structure of the mixed method. This iterative method and the related numerical results that show its efficiency are already published in [Ge'03]. As a second contribution we derive similar to [Lo'02] a residual *a posteriori error estimator* for linear elasticity based on the well-known *Helmholtz-decomposition*, cf. [WH'99]. Contrary to [Lo'02] we use in our derivation an especially appropriate Helmholtz decomposition for the case of linear elasticity proposed in [CS'03]. The third contribution finally is the development of a new fixed point iteration scheme in the return mapping algorithm needed for the solution of the plastic problem and the proof of its convergence and consistency. By applying this fixed point method we can reduce the nonlinear plasticity problem to a series of elastic problems. Furthermore, the consistency criterion of the proposed method yields a natural error measure for the plastic problem. Combining this error measure with the error estimator in the elastic case leads finally to an error estimator for the elastoplastic case.

Therefore we will consider in this thesis the above mentioned topics focusing on efficient solution algorithms for a mixed finite element method in elastoplasticity. Step by step we will introduce an idealized linear elastic and also an idealized elastoplastic

problem and their mathematical formulation. We begin in Chapter 1 by introducing the basic notation as well as some important definitions and theorems that are needed later on. The physical and mechanical background for elastic and plastic material behavior and furthermore the constitutive equations for the problems in question are presented in Chapter 2. Subsequently in Chapter 3, we examine different finite element formulations for the solution of the elastic problem and we give a short introduction in the theory of mixed methods. This leads to the derivation of the above mentioned *PEERS* approach that is well suited for the elastic problem in consideration, e.g. also for the numerically interesting case of elastic and nearly incompressible materials. This mixed approach will finally be extended to plastic material behavior using the above mentioned newly developed fixed point iteration scheme in the necessary return mapping procedure. Thereafter (in Chapter 4) we will examine adequate iterative solvers for the indefinite linear systems arising from the discretization of the *PEERS* method in elasticity (leading to the *constraint preconditioners* already mentioned). Furthermore we will analyze in this chapter the fixed point iteration scheme used in the plastic case. At this point the proof for convergence and consistency of the scheme will also be given. Chapter 5 considers the error estimation for the *PEERS* approach in elasticity and elastoplasticity. In this context we prove the reliable and efficient a posteriori error estimator similar to the one proposed in [Lo'02] and we also extend it from the elastic case to the elastoplastic one. The thesis is concluded in Chapter 6 with a review on numerical tests of the solution algorithms developed in this thesis. These tests are implemented for a common benchmark problem that is very well documented in [S+'02].

André Geilenkothen, Hannover, 14. Januar 2004

Acknowledgements

---

[1]   German Research Foundation

Chapter 1

Notations and Terminology

The common notations and definitions as well as the terminology used throughout this thesis will be shortly recalled or otherwise introduced in brief in this chapter. The content of this chapter is therefore considered to be well-known in the further chapters and will usually not be cited or referenced again.

1.1 Notations

In this section the mathematical symbolism as well as the most common operators used in this work are presented.

Notation 1.1 (Scalars, Vectors and Tensors) *A scalar $c \in \mathbb{R}$ or $\lambda \in \mathbb{R}$ is always printed in the normal italic face, while vectors or tensors are printed in* **bold face**. *Furthermore, vectors $\mathbf{v} \in \mathbb{R}^n$ are denoted by Roman letters while tensors $\boldsymbol{\sigma} \in \mathbb{R}^{m \times n}$ are denoted mostly Greek; only tensors of special importance as for example the elasticity tensor $\mathcal{C}$ are denoted by calligraphic letters and are thus not in bold face.*

Notation 1.2 (Operators, Bilinear Forms, Functionals) *Operators like* div *or* tr *as well as bilinear forms* a$(\,\cdot\,,\,\cdot\,)$ *and functionals* J *are always printed in* Sans Serif.

Definition 1.3 (Nabla-Operator ∇) *The operator ∇ is formally a differential operator and it represents the following differentiation in $\mathbb{R}^n$:*

$$\nabla \ := \ \begin{bmatrix} \dfrac{\partial}{\partial x_1} \\ \vdots \\ \dfrac{\partial}{\partial x_n} \end{bmatrix} \ .$$

Definition 1.4 (Gradient) *With* $\nabla \mathbf{v}$ *we will denote the gradient of any vector (or vector-valued function)* $\mathbf{v} = (v_1, v_2, \ldots, v_n) \in \mathbb{R}^n$. *The gradient of* $\mathbf{v}$ *is given by*

$$
\nabla \mathbf{v} := \begin{bmatrix} \dfrac{\partial v_1}{\partial x_1} & \cdots & \dfrac{\partial v_n}{\partial x_1} \\ \vdots & \ddots & \vdots \\ \dfrac{\partial v_1}{\partial x_n} & \cdots & \dfrac{\partial v_n}{\partial x_n} \end{bmatrix} .
$$

Definition 1.5 (Divergence) *We denote the divergence operator by* div. *The divergence of any vector* $\mathbf{v} = (v_1, v_2, \ldots, v_n) \in \mathbb{R}^n$ *is given through the scalar value*

$$
\operatorname{div} \mathbf{v} := \sum_{i=1}^{n} \frac{\partial v_i}{\partial x_i} .
$$

Hence, the divergence can also be understood as the scalar product of the operator ∇ *and a vector* $\mathbf{v}$:

$$
\operatorname{div} \mathbf{v} = \nabla \cdot \mathbf{v}.
$$

The divergence of any tensor $\boldsymbol{\sigma} \in \mathbb{R}^{m \times n}$ *is meant row-wise and thus* div $\boldsymbol{\sigma}$ *returns a vector in* $\mathbb{R}^m$:

$$
\operatorname{div} \boldsymbol{\sigma} = \operatorname{div} \begin{bmatrix} \boldsymbol{\sigma}_1 \\ \vdots \\ \boldsymbol{\sigma}_n \end{bmatrix} = \begin{bmatrix} \operatorname{div} \boldsymbol{\sigma}_1 \\ \vdots \\ \operatorname{div} \boldsymbol{\sigma}_n \end{bmatrix} = \begin{bmatrix} \displaystyle\sum_{i=1}^{n} \frac{\partial \sigma_{1i}}{\partial x_i} \\ \vdots \\ \displaystyle\sum_{i=1}^{n} \frac{\partial \sigma_{mi}}{\partial x_i} \end{bmatrix} .
$$

Definition 1.6 (Rotation) *The rotation operator is denoted by* rot. *It is defined through the vector product of the* ∇-*operator and a vector* $\mathbf{v} = (v_1, v_2, \ldots, v_n) \in \mathbb{R}^n$:

$$
\operatorname{rot} \mathbf{v} := \nabla \times \mathbf{v} .
$$

Therefore, rot $\mathbf{v}$ *takes the following form in* $\mathbb{R}^2$ *and* $\mathbb{R}^3$:

$$
\operatorname{rot} \mathbf{v} = \frac{\partial v_2}{\partial x_1} - \frac{\partial v_1}{\partial x_2} \qquad \forall\, \mathbf{v} \in \mathbb{R}^2 ,
$$

$$
\operatorname{rot} \mathbf{v} = \begin{bmatrix} \dfrac{\partial v_3}{\partial x_2} - \dfrac{\partial v_2}{\partial x_3} \\ \dfrac{\partial v_1}{\partial x_3} - \dfrac{\partial v_3}{\partial x_1} \\ \dfrac{\partial v_2}{\partial x_1} - \dfrac{\partial v_1}{\partial x_2} \end{bmatrix} \qquad \forall\, \mathbf{v} \in \mathbb{R}^3 .
$$

In the literature one often finds also the operators curl *and* $\nabla^{\perp}$ *that are connected to the* rot-*operator. Therefore we also use these operators at some essential points in this thesis to remain within the usual notation in the standard literature. For a vector-valued* $\mathbf{v} \in \mathbb{R}^n$ *we define* curl *through the identity*

$$\mathsf{curl}\,\mathbf{v} \ := \ \mathsf{rot}\,\mathbf{v} \ ,$$

while for a scalar value c we define by curl *a vector in* $\mathbb{R}^2$

$$\mathsf{curl}\,c \ := \ \left[\begin{array}{c} \dfrac{\partial c}{\partial x_2} \\[2mm] -\dfrac{\partial c}{\partial x_1} \end{array}\right] \ .$$

Note that we have

$$\mathsf{curl}\,(\nabla \mathbf{v}) \ = \ 0 \ ,$$

which is the reason why we sometimes also denote curl *by the operator* $\nabla^{\perp}$*:*

$$\nabla^{\perp}\mathbf{v} \ := \ \mathsf{curl}\,\mathbf{v} \ .$$

Finally, the curl *of any tensor* $\boldsymbol{\sigma} \in \mathbb{R}^{m \times n}$ *is meant row-wise (analogously to the divergence) and returns also a vector in* $\mathbb{R}^m$*.*

Definition 1.7 (Trace) *The trace operator* tr *for a tensor* $\boldsymbol{\sigma} \in \mathbb{R}^{n \times n}$ *is given through*

$$\mathsf{tr}\,\boldsymbol{\sigma} \ := \ \sum_{i=1}^{n} \sigma_{ii} \ .$$

Definition 1.8 (Scalar Product for Tensors) *For tensors* $\boldsymbol{\sigma}, \boldsymbol{\tau} \in \mathbb{R}^{n \times n}$ *we also define a special scalar product*

$$\boldsymbol{\sigma} : \boldsymbol{\tau} \ := \ \sum_{i,j} \sigma_{ij}\tau_{ij} \ = \ \mathsf{tr}\,(\boldsymbol{\sigma}\boldsymbol{\tau}^T) \ ,$$

associated with the Frobenius norm $\|\cdot\|_F$*:*

$$\|\boldsymbol{\sigma}\|_F \ := \ \left(\sum_{i,j} \sigma_{ij}^2\right)^{\frac{1}{2}} \ .$$

Definition 1.9 (The symbols $\lesssim$ and $\eqsim$) *In the course of deriving error estimates this thesis has to deal with a lot of equalities and inequalities that relate different dependent quantities. Often these equalities and inequalities hold only true when multiplying one side with specific constants that are independent of the quantities of interest. Thus, in general we use the symbols* $\lesssim$ *and* $\eqsim$ *in estimates denoting that an equality or inequality holds only true up to some positive constants that are of no further importance.*

1.2   Analytical tools

The standard analytical tools necessary for the setup of finite element methods are briefly
described in the following definitions.

Definition 1.10 (Lipschitz Continuity and Lipschitz Domain) *We call a function*
$\mathbf{f} : D \longrightarrow \mathbb{R}^n$ *'Lipschitz continuous' if there exists a constant $c \in \mathbb{R}$ such that*

$$\|\mathbf{f}(x) - \mathbf{f}(y)\| \ \leq \ c\, \|x - y\| \qquad \forall \ x, y \in D(\mathbf{f}) \ .$$

*A domain $\Omega \in \mathbb{R}^n$ is called a 'Lipschitz domain' if for every $x \in \partial\Omega$ on the boundary
$\partial\Omega$ of Ω there exists a ball $B_\varepsilon(x)$ such that $B_\varepsilon(x) \cap \partial\Omega$ can be expressed as a graph of a
Lipschitz continuous function. Here, by 'graph' we mean a $(n-1)$-dimensional subset of
the $\mathbb{R}^n$ that can be represented as the image of a function on $\mathbb{R}^{n-1}$. If not stated otherwise
we assume a domain Ω always to be a bounded Lipschitz domain.*

Definition 1.11 (Lebesgue Integration Spaces) *If not stated otherwise in this thesis
any domain Ω is meant to be a Lebesgue measurable subset of $\mathbb{R}^d$ and any function $\mathbf{f}$ on
Ω is meant to be a Lebesgue function which means it is Lebesgue integrable. The Lebesgue
integral of $\mathbf{f}$ is of course denoted as*

$$\int_\Omega \mathbf{f} \ dx \ ,$$

*and we define for any $p \in \mathbb{Z}, 1 \leq p \leq \infty$ the following norm and its associated space
(identifying functions that differ only on sets with measure zero as the same function)*

$$\|\mathbf{f}\|_{L^p(\Omega)} \ := \ \begin{cases} \left(\int_\Omega |\mathbf{f}(x)|^p \ dx \right)^{\frac{1}{p}} & \text{for } p < \infty \ , \\[2ex] \sup_{x \in \Omega} |\mathbf{f}(x)| & \text{for } p = \infty \ , \end{cases}$$

$$L^p(\Omega) \ := \ \left\{ \mathbf{f} \ : \ \|\mathbf{f}\|_{L^p(\Omega)} < \infty \right\} \ .$$

*These spaces together with their associated norm are Banach spaces; L^2 is even a Hilbert
space.*

Definition 1.12 (Locally Integrable Functions) *We define the space of locally inte-
grable functions through*

$$L^1_{loc}(\Omega) \ := \ \left\{ \mathbf{f} \ : \ \mathbf{f} \in L^1(K) \ \ \forall \text{ compact } K \subset (\Omega \setminus \partial\Omega) \right\} \ .$$

Definition 1.13 (Multi-Index Derivatives) *Assume we are given a function* $\mathbf{f}$ *on* $\mathbb{R}^d$ *and an index vector* $\boldsymbol{\alpha} = (\alpha_1, \alpha_2, \dots, \alpha_n) \in \mathbb{N}_0^d$ *. With*

$$|\boldsymbol{\alpha}| := \sum_{i=1}^{d} \alpha_i \,,$$

we define the partial derivative $D^{\boldsymbol{\alpha}}$ *of* $\mathbf{f}$ *via*

$$D^{\boldsymbol{\alpha}}\mathbf{f} := \frac{\partial^{|\boldsymbol{\alpha}|}\mathbf{f}}{\partial^{\alpha_1}x_1 \, \partial^{\alpha_2}x_2 \, \dots \, \partial^{\alpha_n}x_n} \,.$$

Definition 1.14 (Sobolev Spaces) *Let* $m \in \mathbb{N}_0$ *and* $p \in \mathbb{Z}$, $1 \le p \le \infty$ *be given. We define a Sobolev space through*

$$W^{m,p}(\Omega) := \left\{ \mathbf{f} \in L^1_{loc}(\Omega) : \forall\, |\boldsymbol{\alpha}| \le m \,,\, \exists\, D^{\boldsymbol{\alpha}}\mathbf{f}\,,\, \|D^{\boldsymbol{\alpha}}\mathbf{f}\|_{L^p(\Omega)} < \infty \right\} \,.$$

Again we identify functions that differ only on a set of measure zero with each other and define a norm on these Sobolev spaces through

$$\|\mathbf{f}\|_{m,p,\Omega} := \begin{cases} \left(\displaystyle\sum_{|\boldsymbol{\alpha}| \le m} \|D^{\boldsymbol{\alpha}}\mathbf{f}(x)\|_{L^p(\Omega)}^p \right)^{\frac{1}{p}} & \text{for } p < \infty \,, \\[2em] \displaystyle\max_{|\boldsymbol{\alpha}| \le m} \|D^{\boldsymbol{\alpha}}\mathbf{f}(x)\|_{L^\infty(\Omega)} & \text{for } p = \infty \,. \end{cases}$$

The spaces $W^{m,p}(\Omega)$ *together with their associated norm are Banach spaces and the spaces* $W^{m,2}(\Omega)$ *are Hilbert spaces. Therefore, these spaces will be denoted* $H^m(\Omega)$ *throughout the rest of this thesis.*

The scalar product induced by the above norm in $H^m(\Omega)$ *is denoted by* $(\,\cdot\,,\,\cdot\,)_{m,\Omega}$ *and is defined through*

$$(\mathbf{f}, \mathbf{g})_{m,\Omega} := \sum_{|\boldsymbol{\alpha}| \le m} \int_{\Omega} D^{\boldsymbol{\alpha}}\mathbf{f}(x) D^{\boldsymbol{\alpha}}\mathbf{g}(x) \ dx \,.$$

Note that $H^0(\Omega) = L^2(\Omega)$*. Thus, the* L^2 *inner products for vector-valued functions*

$$(\mathbf{f}, \mathbf{g})_{0,\Omega} = \int_{\Omega} \mathbf{f}\,\mathbf{g} \ dx$$

or for tensor-valued functions

$$(\boldsymbol{\sigma}, \boldsymbol{\tau})_{0,\Omega} = \int_{\Omega} \boldsymbol{\sigma} : \boldsymbol{\tau} \ dx$$

are used in both notations in this thesis but mostly in the Sobolev form instead of the integral form.

Definition 1.15 (The Space $H(\mathsf{div}, \Omega)$) *We define furthermore a Sobolev space* $H(\mathsf{div}, \Omega)$ *via*

$$H(\mathsf{div}, \Omega) \ := \ \left\{ \mathbf{x} \in L^2(\Omega) \ : \ \mathsf{div}\, \mathbf{x} \in L^2(\Omega) \right\} \ .$$

The associated norm $\| \cdot \|_{H(\mathsf{div}, \Omega)}$ *is given through*

$$\| \mathbf{x} \|_{H(\mathsf{div}, \Omega)} \ := \ \left(\| \mathbf{x} \|_{0,\Omega}^2 \ + \ \| \mathsf{div}\, \mathbf{x} \|_{0,\Omega}^2 \right)^{\frac{1}{2}} \ .$$

Definition 1.16 (Sobolev Spaces and Boundary Conditions) *Let* Γ_D *be the part of the boundary* $\partial\Omega$ *of a domain* Ω *that is subjected to Dirichlet boundary conditions and* $\Gamma_N \subset \partial\Omega$ *the part that is subjected to Neumann boundary conditions. We often call* Γ_D *the Dirichlet part and* Γ_N *the Neumann part of the boundary.*
Sobolev spaces that incorporate a zero Dirichlet boundary condition are then defined by

$$H_{\Gamma_D}^m(\Omega) \ := \ \left\{ \mathbf{x} \in H^m(\Omega) \ : \ \mathbf{x} = 0 \text{ on } \Gamma_D \right\} \ ,$$

while a Sobolev space that incorporates Neumann boundary conditions is given via

$$H_{\Gamma_N}(\mathsf{div}, \Omega) \ := \ \left\{ \mathbf{x} \in H(\mathsf{div}, \Omega) \ : \ \mathbf{x} \cdot \mathbf{n} = 0 \text{ on } \Gamma_N \right\} \ .$$

Notation 1.17 (Spatial Dimensions) *The number of spatial dimensions is always represented by the parameter d. Thus, Sobolev spaces of the form* $H^m(\Omega)^d$ *or* $H^m(\Omega)^{d \times d}$ *indicate the spatial dimensions of the elements they contain.*

Definition 1.18 (Continuous Bilinear Form) *Let* X *be a Hilbert space. A bilinear form* $\mathsf{a} : X \times X \longrightarrow \mathbb{R}$ *is called 'continuous' if there exists a constant* $c > 0$ *such that*

$$| \mathsf{a}\, (\mathbf{v}, \mathbf{x}) | \ \leq \ c \, \| \mathbf{v} \| \, \| \mathbf{x} \| \qquad \forall \, \mathbf{v}, \mathbf{x} \in X$$

holds true.

Definition 1.19 (Coercivity) *Let* X *be a Hilbert space. A symmetric continuous bilinear form* $\mathsf{a} : X \times X \longrightarrow \mathbb{R}$ *is called 'coercive' with respect to* X *if there exists a constant* $\alpha > 0$ *such that*

$$\mathsf{a}\, (\mathbf{x}, \mathbf{x}) \ \geq \ \alpha \, \| \mathbf{x} \|^2 \qquad \forall \, \mathbf{x} \in X$$

holds true. In the literature such bilinear forms are often also called 'X-elliptic' or just 'elliptic'. Each coercive bilinear form defines the well-known energy norm:

$$\| \mathbf{x} \|_{\mathsf{a}} \ := \ \left(\mathsf{a}\, (\mathbf{x}, \mathbf{x}) \right)^{\frac{1}{2}} \ .$$

Definition 1.20 (Dual Space) *Let Y be a vector space associated with a norm. We define the dual space Y' of Y as the space of all bounded linear operators f from Y in $\mathbb{R}$:*

$$Y' := \{\mathsf{f} : Y \longrightarrow \mathbb{R} : \mathsf{f} \text{ linear }, \sup_{\substack{x \\ \|x\|_Y \leq 1}} \|\mathsf{f}(x)\|_{\mathbf{R}} < \infty\} .$$

Note that a Hilbert space can be identified with its dual space.

1.3 Lemmata and theorems

We shortly recall in this section some basic results of calculus and the theory of partial differential equations that will be used later on.

Lemma 1.21 (Green's Formula) *With given $\mathbf{v} \in H^1(\Omega)^d$ and given $\boldsymbol{\tau} \in H(\mathsf{div}, \Omega)^{d \times d}$ the following equation holds:*

$$-\int_\Omega \mathbf{v} \cdot (\mathsf{div}\, \boldsymbol{\tau})\, dx = \int_\Omega (\nabla \mathbf{v}) : \boldsymbol{\tau}\, dx - \int_{\partial\Omega} \mathbf{v} \cdot (\boldsymbol{\tau} \cdot \mathbf{n})\, dx .$$

This equality is called 'Green's Formula' and a proof of it can be found in a broad variety of books (e.g. in [BF'91, He'95]).

Lemma 1.22 (Partial Integration for the curl-Operator) *Let Ω be an open subset of $\mathbb{R}^2$. For given $\mathbf{v} \in H^1(\Omega)^2$, $\boldsymbol{\tau} \in H^1(\Omega)^{2\times 2}$ and a scalar function $c \in H^1(\Omega)$ the following partial integrations hold true:*

$$\int_\Omega c\,(\mathsf{curl}\, \mathbf{v})\, dx - \int_\Omega \mathbf{v} \cdot (\mathsf{curl}\, c)\, dx = \int_{\partial\Omega} c\,(\mathbf{v} \cdot \mathbf{t})\, dx ,$$

$$\int_\Omega c\,(\mathsf{curl}\, \boldsymbol{\tau})\, dx - \int_\Omega \boldsymbol{\tau} \cdot (\mathsf{curl}\, c)\, dx = \int_{\partial\Omega} c\,(\boldsymbol{\tau} \cdot \mathbf{t})\, dx ,$$

where $\mathbf{v} \cdot \mathbf{t}$ and $\boldsymbol{\tau} \cdot \mathbf{t}$ denote the tangential components of $\mathbf{v}$ and $\boldsymbol{\tau}$ respectively. These results follow directly from the Integral Theorem of Gauss and the product rule

$$\mathsf{curl}\,(c\,\mathbf{v}) = c\,(\mathsf{curl}\, \mathbf{v}) - \mathbf{v} \cdot (\mathsf{curl}\, c) .$$

Lemma 1.23 *Let $K \subset \mathbb{R}^n$ be a convex set and let $P_K : \mathbb{R}^n \longrightarrow K$ be the orthogonal projection onto the set K, e.g. it is*

$$\| P_K(x) - x \| = \min_{z \in K} \| z - x \| \qquad \forall\, x \in \mathbb{R}^n .$$

Then the following three statements hold true:

$(i) \quad (x - P_K(x), z - P_K(x)) \; \leq \; 0 \qquad \forall \; x \in \mathbb{R}^n, z \in K \; ,$

$(ii) \quad (P_K(y) - P_K(x), y - x) \; \geq \; \| P_K(y) - P_K(x) \|^2 \qquad \forall \; x, y \in \mathbb{R}^n \; ,$

$(iii) \quad \| P_K(y) - P_K(x) \| \; \leq \; \| y - x \| \qquad \forall \; x, y \in \mathbb{R}^n \; .$

Statement (i) results from the convex nature of K and the minimisation property of P_K while the other two statements follow directly from the first one. A detailed proof can be found in [JS'04].

1.4   Finite element framework

In this section some general terminology concerning finite elements is introduced such as the triangulation of a domain Ω and the finite dimensional ansatz spaces which are used as subspaces of the infinite dimensional Sobolev spaces for discretization purposes. In the following we always denote by $\mathcal{P}^k$ the space of polynomials of degree k.

Definition 1.24 (Triangulation) *Let $\Omega \in \mathbb{R}^2$ be a bounded Lipschitz domain. By a triangulation $\mathcal{T}$ of Ω we mean a finite set of bounded Lipschitz domains with polygonal boundary that has the following properties:*

(i) The closure $\bar{\Omega}$ of Ω is overlapped by $\mathcal{T}$, e.g.

$$\bigcup_{T \in \mathcal{T}} T \; = \; \bar{\Omega} \; .$$

(ii) The interior $int(T_1) := T_1 \setminus \partial T_1$ of any element $T_1 \in \mathcal{T}$ is disjunct to the interior $int(T_2)$ of any other element $T_1 \neq T_2 \in \mathcal{T}$, e.g.

$$int(T_1) \cap int(T_2) \; = \; \emptyset \; .$$

This definition of a triangulation assumes $\Omega \subset \mathbb{R}^2$ because the discrete problems considered in this thesis will be problems reduced to a 2D model.

Definition 1.25 (Triangles, Edges, Vertices) *An element T of a triangulation $\mathcal{T}$ is often also called 'triangle' although it does not have to be a triangle necessarily. A maximal closed and straight subset of the boundary ∂T of an element T is called an edge E of T. The set of all edges E of all elements T of $\mathcal{T}$ is denoted as $\mathcal{E}$. An end point of an edge is*

called a vertex V and the set of all vertices is denoted as $\mathcal{V}$. By h_E we denote the size or length of an edge E, e.g.

$$h_E \; := \; |E| \, ,$$

while h_T is the diameter of T and therefore a measure for the size of the triangle. It is defined as

$$h_T \; := \; \max_{E \subset \partial T} h_E \, ,$$

Definition 1.26 (Regular Triangulation) *Let $\mathcal{T}$ be a triangulation of a bounded Lipschitz domain $\Omega \in \mathbb{R}^2$ with boundary $\partial \Omega = \Gamma_D \cup \Gamma_N$. Furthermore, let the Dirichlet part Γ_D be a non-empty and closed subset of the boundary and let Γ_N also be a closed (and possibly empty) subset of $\partial \Omega$. We call a triangulation $\mathcal{T}$ 'regular' if it has the following four properties for all $T_1, T_2 \in \mathcal{T}$:*

(i) $\operatorname{int}(T_1) \; \neq \; \emptyset$,

(ii) either $\quad T_1 \cap T_2 \; = \; \emptyset \quad$ or $\quad T_1 \cap T_2 \; \in \; \mathcal{E} \quad$ or $\quad T_1 \cap T_2 \; \in \; \mathcal{V}$,

(iii) either $\quad T_1 \cap \Gamma_D \; = \; \emptyset \quad$ or $\quad T_1 \cap \Gamma_D \; \in \; \mathcal{E} \quad$ or $\quad T_1 \cap \Gamma_D \; \in \; \mathcal{V}$,

(iv) either $\quad T_1 \cap \Gamma_N \; = \; \emptyset \quad$ or $\quad T_1 \cap \Gamma_N \; \in \; \mathcal{E} \quad$ or $\quad T_1 \cap \Gamma_N \; \in \; \mathcal{V}$.

Definition 1.27 (Shape-Regular Triangulation) *For every T in a regular triangulation $\mathcal{T}$ let ρ_T be the diameter of the inner circle of T. The triangulation $\mathcal{T}$ is also called 'shape-regular' if there exists a $\kappa > 0$ such that for all $T \in \mathcal{T}$*

$$\frac{h_T}{\rho_T} \; \leq \; \kappa \, .$$

Throughout this thesis we will mostly skip the descriptions 'regular' and 'shape-regular' when we speak of triangulations but denote all such triangulations in the form $\mathcal{T}_h$ with an additional parameter h that describes the associated mesh width according to

$$h \; := \; \max_{T \in \mathcal{T}} h_T \, .$$

Definition 1.28 (Standard Ansatz Spaces) *Let Ω be a bounded Lipschitz domain and let $\mathcal{T}_h$ be a regular triangulation on Ω. We define a standard ansatz space on this triangulation via*

$$\mathcal{M}_h^k \; := \; \{ \, x \in L^2(\Omega) \, : \, x|_T \in \mathcal{P}^k \quad \forall \, T \in \mathcal{T}_h \, \} \, .$$

If we demand additional continuity on triangle edges we need modified ansatz spaces defined through

$$\mathcal{M}_{0,h}^k \; := \; \mathcal{M}_h^k \cap H^1(\Omega) \, ,$$

$$\mathcal{M}_{0,\Gamma_D,h}^k \; := \; \mathcal{M}_h^k \cap H_{\Gamma_D}^1(\Omega) \, .$$

Definition 1.29 (Raviart-Thomas Ansatz Spaces) *Let Ω be a bounded Lipschitz domain and let $\mathcal{T}_h$ be a regular triangulation on Ω. Raviart-Thomas spaces are special ansatz spaces constructed to fit the space $H(\mathrm{div}, \Omega)$; they are defined by*

$$
\mathcal{RT}_h^k \;:=\; \Big\{ x \in (\mathcal{M}_h^{k+1})^2 \cap H(\mathrm{div}, \Omega) \;:\; x|_T \;=\; \begin{bmatrix} p_1 \\ p_2 \end{bmatrix} + p_3 \begin{bmatrix} y \\ z \end{bmatrix} \;,\; p_i \in \mathcal{P}^k, \;\; \forall \, T \in \mathcal{T}_h \Big\} \,.
$$

Definition 1.30 (Bubble Ansatz Functions) *Let Ω be a bounded Lipschitz domain and let $\mathcal{T}_h$ be a regular triangulation on Ω. A space of bubble functions is defined through*

$$
\mathcal{B}_{0,h}^3 \;:=\; \big\{ x \in \mathcal{M}_{0,h}^3 \;:\; x|_E \;=\; 0 \;\; \forall \, E \in \mathcal{T}_h \big\} \,.
$$

Chapter 2

Elastoplasticity: A Short Overview

This chapter is meant to give a short impression of what *elastoplasticity* is all about. Looking around we experience everyday that things in the material world are subjected to various forces (or more general: to various loads). Examples are countless and reach from constant and ubiquitous loads like gravity over bridge constructions that have to withstand singular loads – implied by e.g. a heavy storm – and periodic loads – as daily traffic – up to simple cushions deformed by someone sitting on it. All such loads in general can cause various effects. One of them is damage or deterioration of material that can be understood as the development of tiny fractures on the microscopic material scale. These micro-fractures finally alter the material properties of the work-piece in consideration and in the end lead to major cracks or fractures on the macroscopic scale. Naturally, this is an important topic in engineering science, but it will not be tackled here.

Instead this thesis focuses on two other effects: *elastic* and *plastic deformations.* Elastic material behavior means that all deformations resulting from a load are reversible and the material returns to its initial configuration once the load is removed. Plastic behavior on the other hand describes irreversible deformations of a material that still remain after the load has vanished. This is expressed in a simplified way by Fig. 2.1 on the following page depicting the relation between *stresses* and *strains* for an 1D example. In this context, *stresses* represent the internal 'forces' that build up within the material in response to the external loads and *strains* are the change rates of the deformations between the initial and the deformed state.

Elastic material behavior is characterized by a linear relation between the stresses $\boldsymbol{\sigma}$ and the strains $\boldsymbol{\epsilon}$ (the red line in Fig. 2.1). But once the stresses within a material body reach a material dependent yield stress $\sigma^{\star}$ the material does not react elastic any more; instead it reacts plastic, that is, the relation between stress and strain changes. The new
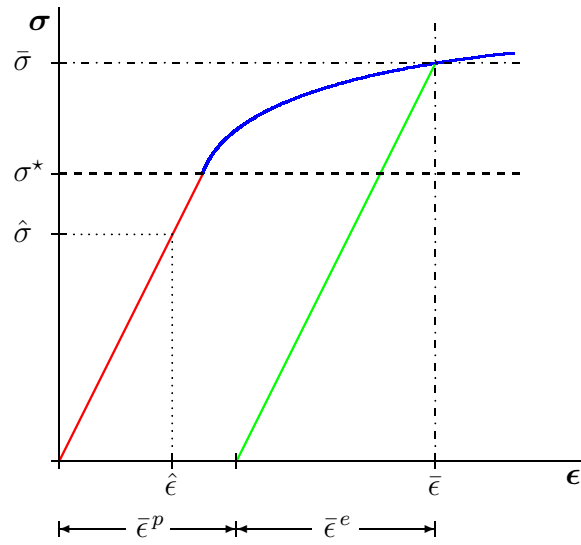
Figure 2.1: *Example for the relation between stress $\boldsymbol{\sigma}$ and strain $\boldsymbol{\epsilon}$ in 1D-elastoplasticity with nonlinear hardening*

relation can be e.g. nonlinear as the blue line in Fig. 2.1 indicates (*plasticity with nonlinear hardening*) or it can be linear again with a different factor of linearity (*plasticity with linear hardening*) or even constant (*perfect plasticity*); the latter two are depicted by the blue lines in Fig. 2.2. The most important thing concerning elastoplasticity however is the fact that plastically deformed material reacts elastic again once the loads are decreased again (cf. the green line in Fig. 2.1). Furthermore, this 'new' elastic relation is the just a translation of the linear relation during the first elastic phase. Thus, for plastic deformations we can split the total strain $\boldsymbol{\epsilon}$ in an elastic part $\boldsymbol{\epsilon}^e$ and a plastic part $\boldsymbol{\epsilon}^p$ and it is obvious that a plastically deformed material body is still subjected to strains even with no loads applied.
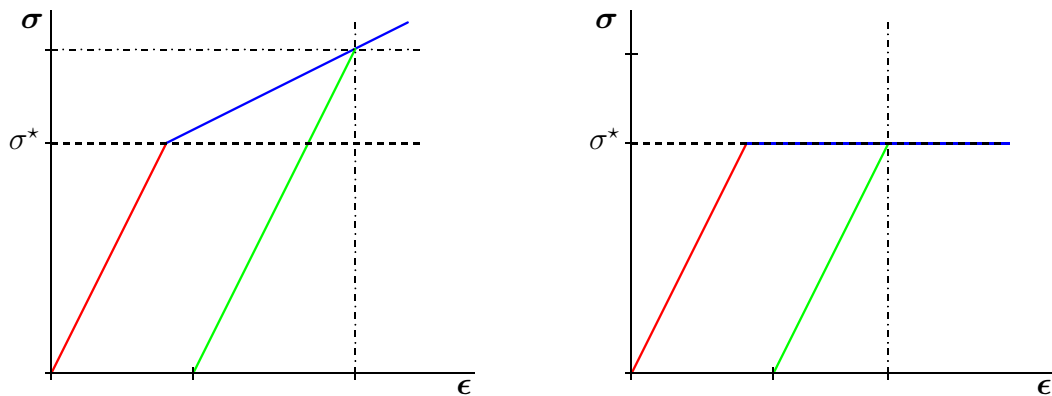

Figure 2.2: *Relation between stress and strain in 1D-elastoplasticity with linear hardening (left) and perfect 1D-elastoplasticity (right)*

In the following sections the basic mechanical theory of elastoplasticity as well as its common mathematical formulation will be introduced. We focus only on a very small part of the theory that will be needed in the examined problems later on. Thus, this thesis is generally restricted to *linear* elasticity and *perfect* plasticity. For further reading on this topic we refer to [Br'97, SH'98, HR'99, RPD'03].

2.1 Linear elasticity in 3D

A material body occupies a bounded Lipschitz domain $\Omega \subset \mathbb{R}^3$. The domain Ω is the so-called *reference configuration* and in general we assume that in this state the body is undeformed and in equilibrium. A point $x \in \Omega$ is called a *material point*. We assume that the reference configuration of a material body is given at a time $t_0 = 0$. Furthermore let us assume that this material body deforms in a time interval $I_t = (\,0\,;\,T\,]$ under the action of applied volume and surface loads. The deformed configuration of the material body is described by a mapping $\mathbf{\Phi}$ with

$$\mathbf{\Phi}_t : \Omega \longrightarrow \mathbb{R}^3 \ ,$$

i.e. $\mathbf{\Phi}_t$ maps an old point x to its new position $\mathbf{\Phi}_t(x)$. One can write $\mathbf{\Phi}$ also as

$$\mathbf{\Phi}_t \;=\; \mathsf{id} + \mathbf{u} \ ,$$

with identity id and some *displacement* $\mathbf{u}$. Thus, we can keep track of the changing configuration of a material body by evaluating $\mathbf{\Phi}_t(x)$ at some time $t \in I_t$.

Figure 2.3: *Rigid body motion: simple translation (left) and deformation: indention (right)*

In elastoplasticity we are mainly interested in the *deformation* (and the related strains and stresses) within a body and not so much in its displacement in general. That is why we distinguish between *rigid body motions* that describe just translations and rotations of Ω and deformations that occur when a body assumes a new shape (cf. Fig. 2.3).

The quantity to measure these 'true' deformations is the *strain tensor* $\epsilon(\mathbf{u})$ (cf. [Br'97]). We call $\mathbf{\Phi}$ a *deformation* provided it is a locally injective mapping and

$$\mathsf{det}\,(\nabla\mathbf{\Phi}) \leq 0\,.$$

This definition guarantees that parts of the material body with positive volume are mapped to the deformed state with still positive volume. The gradient of deformation is of course

$$\nabla\mathbf{\Phi} \;=\; \begin{bmatrix} \dfrac{\partial\Phi_1}{\partial x_1} & \dfrac{\partial\Phi_2}{\partial x_1} & \dfrac{\partial\Phi_3}{\partial x_1} \\[3mm] \dfrac{\partial\Phi_1}{\partial x_2} & \dfrac{\partial\Phi_2}{\partial x_2} & \dfrac{\partial\Phi_3}{\partial x_2} \\[3mm] \dfrac{\partial\Phi_1}{\partial x_3} & \dfrac{\partial\Phi_2}{\partial x_3} & \dfrac{\partial\Phi_3}{\partial x_3} \end{bmatrix}\,.$$

With these definitions we can describe the deformation of a line within Ω and its Euklidian measure by

$$\mathbf{\Phi}(x+z) \,-\, \mathbf{\Phi}(x) \;\;=\;\; \nabla\mathbf{\Phi}\,\cdot\,z \,+\, \mathcal{O}(z)$$

$$\|\mathbf{\Phi}(x+z) \,-\, \mathbf{\Phi}(x)\|^2 \;\;=\;\; z'\,\nabla\mathbf{\Phi}^T\,\nabla\mathbf{\Phi}\,z \,+\, \mathcal{O}(\|z\|^2)\,.$$

The tensor $\nabla\mathbf{\Phi}^T\,\nabla\mathbf{\Phi}$ is called the *right Cauchy-Green strain tensor*. Using this tensor we can define the strain tensor $\mathcal{E}$ that measures the deviation from identity through

$$\mathcal{E} \;:=\; \frac{1}{2}\,(\nabla\mathbf{\Phi}^T\,\nabla\mathbf{\Phi} \,-\, \mathcal{I})\,.$$

Recalling that $\mathbf{\Phi} \;=\; \mathsf{id}+\mathbf{u}$ and doing some straight forward computations we can represent $\mathcal{E}$ in the following way:

$$\mathcal{E} \;=\; \frac{1}{2}\,(\nabla\mathbf{u} \,+\, \nabla\mathbf{u}^T \,+\, \nabla\mathbf{u}^T\,\nabla\mathbf{u})\,.$$

As was said in the beginning of this chapter we will focus on a linear elasticity model. Thus, we assume that in all our models the deformations are small and then the so-called *symmetric gradient*

$$\epsilon(\mathbf{u}) \;:=\; \nabla^{\mathsf{s}}\mathbf{u} \;:=\; \frac{(\nabla\mathbf{u} + (\nabla\mathbf{u})^T)}{2}\,, \tag{2.1}$$

is a sufficient linear approximation for $\mathcal{E}$.

Together with the deformation and the strains one is also interested in the aforementioned stresses that 'connect' the applied loads with the resulting strains. These quantities themselves are coupled in linear elasticity via the following material law, the *stress-strain-relationship*

$$\boldsymbol{\epsilon}(\mathbf{u}) = \mathcal{C}^{-1}\boldsymbol{\sigma} \ , \tag{2.2}$$

where $\boldsymbol{\epsilon} \in \mathbb{R}^{3\times3}$ is the so-called *linear Green strain tensor*, $\boldsymbol{\sigma} \in \mathbb{R}^{3\times3}$ is the stress tensor and $\mathcal{C}^{-1}$ denotes the *compliance tensor*, the inverse of the symmetric positive definite elasticity tensor[1] of fourth order $\mathcal{C}$, which depends on the Lamé constants (or: moduli) $\lambda > 0$ and $\mu > 0$ through Hooke's Law

$$\boldsymbol{\sigma} \ = \ \mathcal{C}\boldsymbol{\epsilon} \ = \ \lambda \operatorname{tr}\boldsymbol{\epsilon}\,\mathcal{I} \ + \ 2\mu\,\boldsymbol{\epsilon} \ . \tag{2.3}$$

Here, the tensor $\mathcal{I}$ represents the identity tensor of fourth order. The Lamé constants are coupled with three other material constants, *Young's modulus E*, *Poisson's ratio ν* and the *bulk modulus G*, that can be found quite often in engineering literature. They are connected via the equations

$$\lambda \ = \ \frac{E\,\nu}{(1+\nu)\,(1-2\nu)} \qquad \text{and} \qquad \mu \ = \ \frac{E}{2\,(1+\nu)} \ ,$$

or

$$E \ = \ \frac{\mu\,(2\mu+3\lambda)}{\mu+\lambda} \qquad \text{and} \qquad \nu \ = \ \frac{\lambda}{2\,(\mu+\lambda)} \ ,$$

with $0 < \nu < 0.5$ and $E > 0$ and

$$G \ = \ \lambda + \frac{2}{3}\,\mu \ .$$

To explain the meaning of these material parameters it is useful to decompose stress and strain orthogonally in their spherical and deviatoric components. Both stresses and strains are tensors of second order and each such tensor $\boldsymbol{\tau}$ of dimension n can thus be written in the form

$$\boldsymbol{\tau} \ = \ \frac{1}{n}\operatorname{tr}\boldsymbol{\tau}\,\mathcal{I} \ + \ \operatorname{dev}\boldsymbol{\tau} \ ,$$

with

$$\operatorname{dev}\boldsymbol{\tau} \ := \ \boldsymbol{\tau} \ - \ \frac{1}{n}\operatorname{tr}\boldsymbol{\tau}\,\mathcal{I} \ . \tag{2.4}$$

The spherical component (the trace-depending part) describes volumetric changes within material while the deviatoric part represents shearing and deformations. To show that this decomposition is truly orthogonal with respect to the scalar product for tensors we

---

[1]   We will see later why $\mathcal{C}$ is truly positive definite and symmetric.

perform some simple calculations for $n = 3$ (the orthogonality holds of course for all $n \in \mathbb{N}$):

$$\operatorname{dev}\boldsymbol{\tau} : \frac{1}{3}\operatorname{tr}\boldsymbol{\tau}\,\mathcal{I} \;=\; (\boldsymbol{\tau} - \frac{1}{3}\operatorname{tr}\boldsymbol{\tau}\,\mathcal{I}) : \frac{1}{3}\operatorname{tr}\boldsymbol{\tau}\,\mathcal{I}$$

$$= \frac{1}{3}\begin{bmatrix} 2\,\tau_{11} - \tau_{22} - \tau_{33} & \tau_{12} & \tau_{13} \\ \tau_{21} & 2\,\tau_{22} - \tau_{11} - \tau_{33} & \tau_{23} \\ \tau_{31} & \tau_{32} & 2\,\tau_{33} - \tau_{11} - \tau_{22} \end{bmatrix}$$

$$: \frac{1}{3}\begin{bmatrix} \tau_{11} + \tau_{22} + \tau_{33} & 0 & 0 \\ 0 & \tau_{11} + \tau_{22} + \tau_{33} & 0 \\ 0 & 0 & \tau_{11} + \tau_{22} + \tau_{33} \end{bmatrix}$$

$$= \frac{\tau_{11} + \tau_{22} + \tau_{33}}{9}\,\underbrace{(2\,\tau_{11} - \tau_{22} - \tau_{33} + 2\,\tau_{22} - \tau_{11} - \tau_{33} + 2\,\tau_{33} - \tau_{11} - \tau_{22})}_{=\,0}$$

$$= \; 0 \; .$$

Applying this orthogonal decomposition to Hooke's Law (2.3) we can find an uncoupled relation for the deviatoric as well as the spherical part of stress and strain:

$$\operatorname{dev}\boldsymbol{\sigma} \;=\; 2\,\mu\operatorname{dev}\boldsymbol{\epsilon} \qquad \text{and} \qquad \operatorname{tr}\boldsymbol{\sigma}\,\mathcal{I} \;=\; 3\,G\operatorname{tr}\boldsymbol{\epsilon}\,\mathcal{I} \; .$$

Thus, it becomes obvious why μ is also called the *shear modulus* as it measures shearing. Furthermore, we see that the bulk modulus G represents the ratio between spherical stresses and volume change. The meaning of Young's modulus E and Poisson's ration ν can be demonstrated with a very simple 2D test example. Let us assume an isotropic elastic rod parallel to the x_1-axis which is subjected to a stress with $\sigma_{11} \neq 0$. Consecutively, one can compute the strain $\boldsymbol{\epsilon}$ by straight forward computations. We will skip that here, but these computations lead to the result

$$E \;=\; \frac{\sigma_{11}}{\epsilon_{11}} \qquad \text{and} \qquad \nu \;=\; -\frac{\epsilon_{22}}{\epsilon_{11}} \; .$$

In this case Young's modulus gives a measure for the stress-strain-relationship or its slope, respectively. Thus, it is often described as a kind of stiffness parameter similar as in a spring. An introduction to elasticity as a model of coupled springs is described very detailed in [SH'98]. Poisson's ratio finally measures the lateral contraction of the work-piece. These physical interpretations also clarify why in this thesis we assume these

constants to be positive.[2]

Next, we have to take into account the above mentioned relation between the stresses and the applied forces. Stresses and volume forces have to fulfill an equilibrium equation (the balance of forces), which reads

$$\operatorname{div} \boldsymbol{\sigma} + \mathbf{f} = 0 \qquad \text{and} \qquad \boldsymbol{\sigma}^T = \boldsymbol{\sigma} \tag{2.5}$$

with stress tensor $\boldsymbol{\sigma} \in \mathbb{R}^{3\times3}$ and volume force $\mathbf{f} \in \mathbb{R}^3$. Note that the divergence operator has to be understood row-wise in this context. The symmetry condition $\boldsymbol{\sigma}^T = \boldsymbol{\sigma}$ is a result of the balance of momentum and fits into the framework of the stress-strain-relationship (2.2) and the symmetric nature of $\boldsymbol{\epsilon}(\mathbf{u})$ in (2.1). Often, the second part of (2.5) is skipped and one just demands $\boldsymbol{\sigma} \in \mathbb{R}^{3\times3}_{sym}$. A detailed derivation of these equilibrium equations can be found in e.g. [RPD'03].

Finally, we incorporate boundary conditions. Let Γ be the boundary of Ω. On parts of the boundary Dirichlet and Neumann conditions are assumed, so that the Dirichlet part Γ_D is a closed and nonempty subset of Γ. The Neumann part Γ_N may be empty. Furthermore, on some parts of the boundary one may have Dirichlet conditions in the x-direction and Neumann conditions in the y-direction (or vice versa). For simplicity reasons only zero Dirichlet conditions are considered throughout this paper, and with a given traction (or surface load) $\mathbf{g} \in \mathbb{R}^3$ we have

$$\mathbf{u} = 0 \quad \text{on } \Gamma_D \qquad \text{and} \qquad \boldsymbol{\sigma} \cdot \mathbf{n} = \mathbf{g} \quad \text{on } \Gamma_N , \tag{2.6}$$

where $\mathbf{n}$ represents the normal component of the stresses. Due to the fact that the tensors $\boldsymbol{\sigma}$ and $\boldsymbol{\epsilon}$ are symmetric these 3×3-matrizes can also be identified with vectors in $\mathbb{R}^6$:

$$\boldsymbol{\sigma} = \begin{bmatrix} \sigma_{xx} \\ \sigma_{yy} \\ \sigma_{zz} \\ \sigma_{xy} \\ \sigma_{xz} \\ \sigma_{yz} \end{bmatrix} \qquad \text{and} \qquad \boldsymbol{\epsilon} = \begin{bmatrix} \epsilon_{xx} \\ \epsilon_{yy} \\ \epsilon_{zz} \\ \epsilon_{xy} \\ \epsilon_{xz} \\ \epsilon_{yz} \end{bmatrix} . \tag{2.7}$$

With this notation there exists also a quite simple and elegant representation of the

---

[2] Actually, one can also construct certain exotic foams – sometimes called anti-rubber, auxetic or dilatational materials – that experience a negative Poisson's ratio ν. Nevertheless, such materials will not be considered in this thesis.

so-called compliance tensor $\mathcal{C}^{-1} \in \mathbb{R}^{6 \times 6}$ in terms of the material parameters E and ν:

$$
\mathcal{C}^{-1} = \frac{1}{E} \begin{bmatrix}
1 & -\nu & -\nu & & & \\
-\nu & 1 & -\nu & & 0 & \\
-\nu & -\nu & 1 & & & \\
& & & 1+\nu & & \\
& 0 & & & 1+\nu & \\
& & & & & 1+\nu
\end{bmatrix} .
\tag{2.8}
$$

Realize that under the above assumption $0 < \nu < 0.5$ (which is reasonable) the matrix $\mathcal{C}^{-1}$ is symmetric positive definite[3] while for $\nu = 0.5$ it would be singular. Thus, for $\nu \longrightarrow 0.5$ (which means that the material becomes more and more incompressible) this matrix poses numerical problems that any approximation scheme has to take into account. Consequently, we will tackle this problem in the following chapters. We close this section by giving also a representation of $\mathcal{C}^{-1}$ in terms of the *Lamé constants* that will be used later on in this thesis:

$$
\boldsymbol{\epsilon} = \mathcal{C}^{-1} \boldsymbol{\sigma} = \frac{1}{2\,\mu} \boldsymbol{\sigma} - \frac{\lambda}{4\,\mu\,(\mu + \lambda)} \operatorname{tr} \boldsymbol{\sigma}\, \mathcal{I} .
\tag{2.9}
$$

2.2   Plane stress and plane strain: models in 2D

Considering a material body which is 'very small' in one spatial direction (e.g. in z-direction) compared to the other two dimensions and considering loads that do not depend on z one can reduce the 3D model to 2D model with some additional assumptions. One possible 2D model is the plane stress model where there are stresses only in the x-y-plane. All other stresses in the z-direction are vanishing. The other model is the plane strain model that will be used throughout this thesis. In this case there is no displacement in the z-direction. Therefore, the strain vector and the related stress vector from (2.7) are now given by

$$
\boldsymbol{\sigma} = \begin{bmatrix}
\sigma_{xx} \\
\sigma_{yy} \\
\sigma_{zz} \\
\sigma_{xy} \\
0 \\
0
\end{bmatrix}
\quad \text{and} \quad
\boldsymbol{\epsilon} = \begin{bmatrix}
\epsilon_{xx} \\
\epsilon_{yy} \\
0 \\
\epsilon_{xy} \\
0 \\
0
\end{bmatrix} .
\tag{2.10}
$$

---

[3]   That $\mathcal{C}^{-1}$ (and then of course $\mathcal{C}$) is positive definite can be seen by applying the *Theorem of Gerschgorin*. The largest eigenvalue of $\mathcal{C}^{-1}$ is by the way $1/\mu$; cf. [Lo'02].

Note that the σ_{zz} component can be expressed through the σ_{xx} and σ_{yy} components. By inserting (2.10) and (2.8) in (2.2) we get deduce the equation

$$\sigma_{zz} = \nu \left(\sigma_{xx} + \sigma_{yy} \right) . \tag{2.11}$$

Hence, we can eliminate the zz-stress-component from the system and get the following reduced matrix $\mathcal{C}^{-1}$:

$$\mathcal{C}^{-1} = \frac{1+\nu}{E} \begin{bmatrix} 1-\nu & -\nu & 0 \\ -\nu & 1-\nu & 0 \\ 0 & 0 & 1 \end{bmatrix} , \tag{2.12}$$

while the reduced stress and strain vectors read

$$\boldsymbol{\sigma} = \begin{bmatrix} \sigma_{xx} \\ \sigma_{yy} \\ \sigma_{xy} \end{bmatrix} \quad \text{and} \quad \boldsymbol{\epsilon} = \begin{bmatrix} \epsilon_{xx} \\ \epsilon_{yy} \\ \epsilon_{xy} \end{bmatrix} . \tag{2.13}$$

The reduced system is of course a major simplification of the true problem. Its main advantage is that it is a valid model problem to study the general behavior of elastic and elastoplastic materials combined with the fact that it is easy to implement and solvable with very reasonable resources in short time.

2.3 Quasi-static perfect plasticity

In this section the aforementioned linear elastic problem is extended to some relatively simple elastoplastic problem. In an elastic problem all deformations of the material body under consideration are reversible while in a plastic problem we also have to model irreversible effects. These effects are modeled by additional **nonlinear** constraints in the form of an inequality that bounds the stresses within an admissible convex set K (this set will be described in detail further below). The nonlinearity is the main difficulty of plasticity. Furthermore, plasticity in general is a time dependent problem due to the irreversible effects.

Considering plastic deformations, it seems natural that every work-piece reacts elastic first (within a – sometimes quite small, sometimes very large – range of applied loads). Nevertheless it is also obvious that loads large enough can yield irreversible deformation to any material or specimen in consideration. The reasons for these effects can be found on the atomic and on the crystalline level. Electrostatic forces maintain a certain attraction between atoms while on the other hand there are also forces of repulsion that keep atoms at a 'safe' distance. Between these forces finally an equilibrium is obtained defining
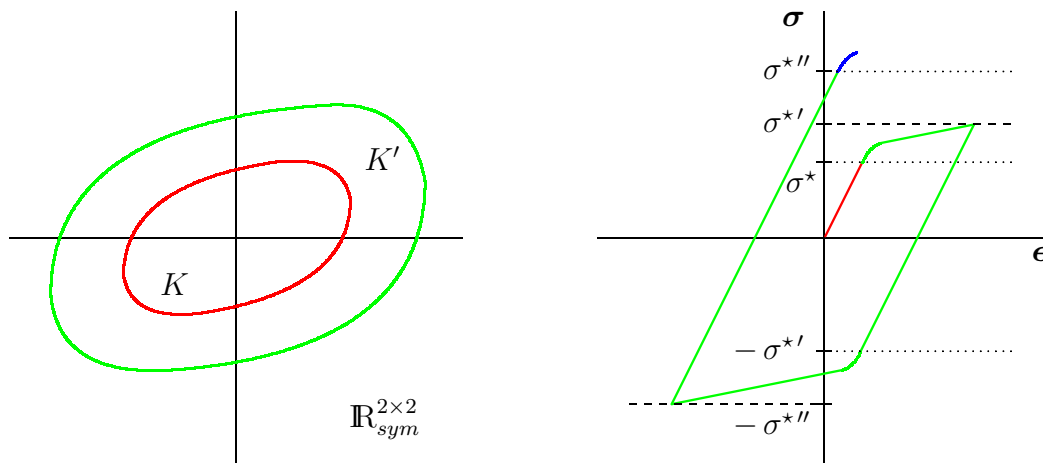
Figure 2.4: *Admissible sets K and K′ in 2D and the hysteresis curve of a full load cycle for isotropic plasticity*

the normal state of the specific matter. Applied forces can influence this equilibrium and a new equilibrium will arise. These are elastic material effects; after the removal of the external forces the old equilibrium takes its place again. On the other hand, the equilibrium is also challenged on the crystalline level, because even the most homogeneous materials experience tiny imperfections on the microscopic level. Confronted with loads large enough, these imperfections can break the atomic equilibrium apart and e.g. a whole layer of crystalline material may slip along the edges of another layer resulting in a dilatation of the imperfection. In such a case even material failure and fracture may happen but the material can also find a new equilibrium. If a new equilibrium is established we have plastic effects. As it was said before, plasticity can be 'instant' and irreversible without any change in the critical yield stress that marks the transition from elastic to plastic behavior or it can incorporate *hardening* effects. By *hardening* we mean that the material changes only 'slowly' and fits itself to the applied loads such that the critical yield stress grows allowing even larger loads in a new elastic range. Of course, there is also a material behavior called softening, but this is of only small importance in engineering sciences and will be skipped here. Hardening in elastoplasticity is represented by additional variables; as already mentioned hardening effects can be linear as well as nonlinear. Furthermore, we distinguish between isotropic and kinematic hardening (and a combined variant). Isotropic hardening means that the yield stress for both compression and traction is growing in the hardening process; this leads to an increasing region K' of admissible stresses. It is a characteristic for this kind of hardening that the yield stress for compression is initially equal to the negative yield stress for traction and that it stays this way even after plastic deformation happened (cf. Fig. 2.4).

Pure kinematic hardening on the other hand results in a set of admissible stresses that does not grow but that gets just translated in the stress-space during the hardening process. This phenomenon is called *Bauschinger effect* and it resembles the fact that some material is affected differently if compression and traction are applied in different order within a load cycle. That means that a rise of the yield stress for tensile forces $\sigma_T^\star$ leads to decrease of the yield stress for compressive forces $\sigma_C^\star$ (cf. Fig. 2.5). Admissible sets for combined kinematic and isotropic hardening is depicted in Fig. 2.6.
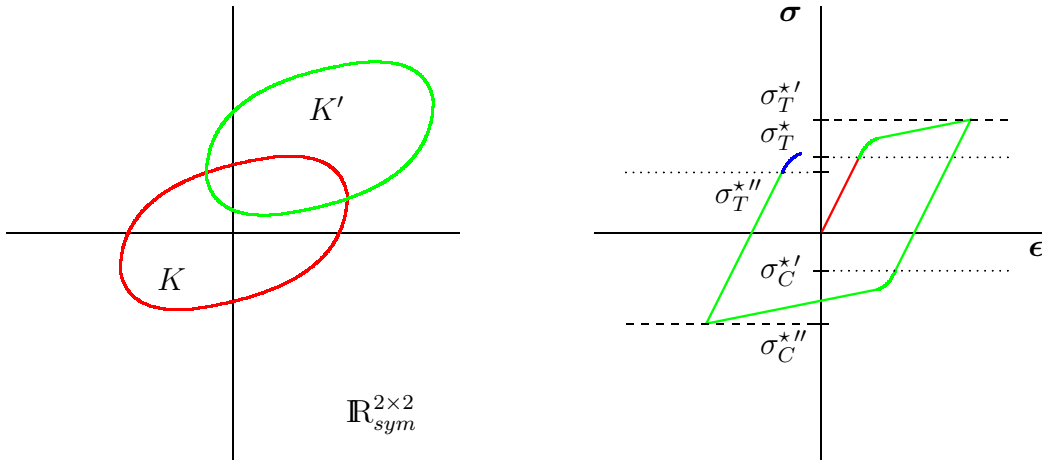
Figure 2.5: *Admissible sets K and K' in 2D and the hysteresis curve of a full load cycle for kinematic plasticity*

In this thesis we focus on the quite simple material behavior mentioned above: 'instant' and 'unchanging' or so-called *perfect plasticity*. That means that any deformations resulting in stresses beyond some trial stress $\sigma^\star$ are assumed irreversible. Furthermore it is assumed that there are no internal forces that lead to hardening or other similar effects. Thus, no additional variables have to be incorporated and the so-called yield condition that models the nonlinear constraint depends only on the trial stress. In this model the admissible set K does not change in any way but remains in its initial state. The introduced perfect plasticity will also be quasi-static so that time dependencies are of relatively small concern. In each time step variable increments have to be just added up.

In engineering science a broad variety of yield conditions is known, e.g. the *Tresca* or the *von-Mises* yield condition. Here, *von-Mises perfect plasticity* will be applied. This defines a convex set K of admissible stresses through

$$K := \{\boldsymbol{\sigma} \in \mathbb{R}^{3\times3}_{sym} \quad : \quad \|\,\mathsf{dev}\,\boldsymbol{\sigma}\,\|_F \ \leq \ \sqrt{\frac{2}{3}}\ \sigma^\star \quad a.e.\ \text{in}\ \Omega\}, \qquad (2.14)$$
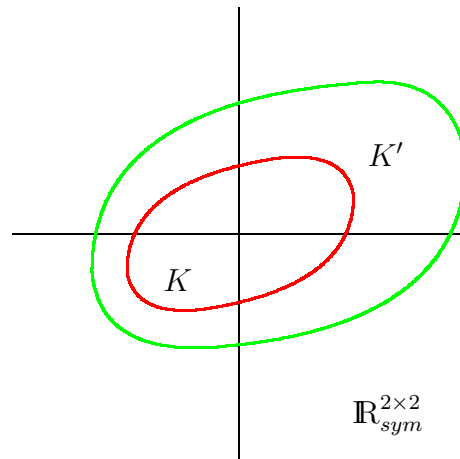
Figure 2.6: *Admissible sets K and K' for combined kinematic and isotropic plasticity*

where $\| \cdot \|_F$ is the Frobenius norm and $\mathsf{dev}\,\boldsymbol{\sigma}$ denotes again the deviatoric part of $\boldsymbol{\sigma}$ with

$$\mathsf{dev}\,\boldsymbol{\sigma} \;:=\; \boldsymbol{\sigma} - \frac{1}{3}\,\mathsf{tr}\,\boldsymbol{\sigma}\,\mathcal{I}\;. \tag{2.15}$$

If the stresses resulting from some loads $\mathbf{f}$ or $\mathbf{g}$ fulfill the constraint condition implied by (2.14) the problem is still elastic. If on the other hand the stresses computed according to the constitutive relations of elasticity violate the constraint on the deviatoric part of $\boldsymbol{\sigma}$ the problem is in the plastic region and a method called *return mapping* has to be applied to model the plastic effects and to compute the correct stresses. Perfectly plastic material behavior in a full load cycle is depicted in the Fig. 2.7.
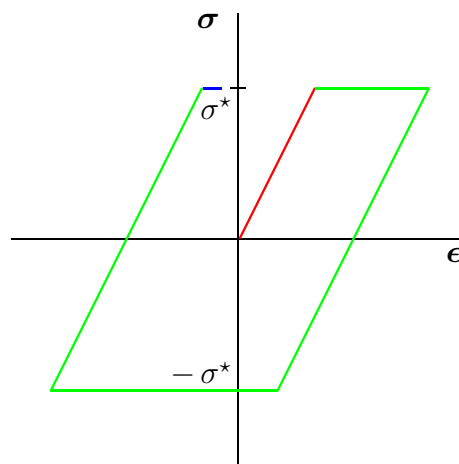
Figure 2.7: *Full load cycle for perfect plasticity*

The return mapping is an orthogonal projection of the so-called *elastic trial stress* $\boldsymbol{\sigma}^{tr}$ (the solution stress of a special assumed elastic problem) onto the set of admissible

stresses K. In the case of static and quasi-static perfect plasticity this projection P_K can be explicitly represented pointwise by

$$P_K(\boldsymbol{\sigma}^{tr}) \;:=\; \boldsymbol{\sigma}^{tr} \;-\; \max\{0\,;\, \|\,\mathsf{dev}\,\boldsymbol{\sigma}^{tr}\,\|_F \;-\; \sqrt{\frac{2}{3}}\;\sigma^\star\} \; \frac{\mathsf{dev}\,\boldsymbol{\sigma}^{tr}}{\|\,\mathsf{dev}\,\boldsymbol{\sigma}^{tr}\,\|_F}\;. \qquad (2.16)$$

If we have a mere elastic problem and the stresses are in the admissible set K the trial stress is equal to the elastic solution stress. Note that therefore $P_K(\cdot)$ is the identity in the elastic case and thus, the *return mapping* procedure via this projection generally yields the solution stress $\boldsymbol{\sigma}^{pl}$ of the elastoplastic problem independently whether it is in the elastic or in the plastic region:

$$\boldsymbol{\sigma}^{pl} \;=\; P_K(\boldsymbol{\sigma}^{tr})\;. \qquad (2.17)$$

This topic will be examined more closely later on in the Sections 3.4 and 4.2 where we present a variational setting and a computable solution algorithm for the elastoplastic problem.

Chapter 3

Mixed Finite Element Methods in Elastoplasticity

In this chapter we will first present a standard variational approach to elasticity following the general variational theory (as e.g. in [Br'97]) until we focus on approaches better suited for this kind of problems: *mixed methods*. In this context we will also give an introduction into the theory of mixed finite element methods and present the necessary definitions, lemmas and theorems to set up such a method successfully. However, the main emphasis of this chapter will be a specific mixed method: the so-called *PEERS* approach which will be used and examined throughout the rest of this thesis. We conclude the chapter by extending the *PEERS* method from the mere elastic problem to the *elastoplastic* problem. For all problems and equations considered in this chapter and in the following chapters we are using the plane strain model from Section 2.2. Thus, it suffices to study linear elasticity in only two spatial dimensions. Only in the elastoplastic case we have to take the third dimension into account.

To derive a finite element method for elasticity we first have to formulate a variational problem for the following partial differential equation (PDE) that recalls the equations (2.2), (2.5) and (2.6):

$$
\begin{aligned}
\boldsymbol{\epsilon}(\mathbf{u}) &= \mathcal{C}^{-1}\boldsymbol{\sigma} & &\text{on } \Omega \ , \\
\operatorname{div}\boldsymbol{\sigma} + \mathbf{f} &= 0 & &\text{on } \Omega \ , \\
\mathbf{u} &= 0 & &\text{on } \Gamma_D \ , \\
\boldsymbol{\sigma}\cdot\mathbf{n} &= \mathbf{g} & &\text{on } \Gamma_N \ ,
\end{aligned}
\tag{3.1}
$$

where $\mathbf{f}$ and $\mathbf{g}$ are quantities in $L^2(\Omega)$ while $\mathbf{u}$ and $\boldsymbol{\sigma}$ have to be at least H^1-functions. In this PDE only the strain $\boldsymbol{\epsilon}$ is expressed in terms of the displacement $\mathbf{u}$ while the stress $\boldsymbol{\sigma}$ is represented in an additional equation, called *constraint*. Such a formulation leads to

a *saddle-point problem* where we have at least two quantities that depend on each other and that we want to determine simultaneously (instead of computing one quantity by the other via some kind of post-processing). The family of *mixed* finite element methods was developed to deal with those *saddle-point problems* and will be introduced in detail later on in this chapter.

We want to start by developing a standard variational formulation that has to cope with only one solution variable. To do so, we introduce an approach that eliminates also the stress $\boldsymbol{\sigma}$ from the system (3.1).

3.1 The displacement approach

The PDE in equation (3.1) can also be written in other forms, for example as the *Lamé Equation*

$$
\begin{aligned}
\lambda \, \nabla \operatorname{div} \mathbf{u} \, + \, 2 \, \mu \operatorname{div} \boldsymbol{\epsilon}(\mathbf{u}) \, + \, \mathbf{f} \, &= \, 0 \qquad \text{on } \Omega \; , \\
\mathbf{u} \, &= \, 0 \qquad \text{on } \Gamma_D \; , \\
\boldsymbol{\sigma}(\mathbf{u}) \cdot \mathbf{n} \, &= \, \mathbf{g} \qquad \text{on } \Gamma_N \; .
\end{aligned}
\tag{3.2}
$$

The two systems (3.1) and (3.2) are equivalent. In the second PDE the stress tensor is eliminated and appears only as a functional depending on the displacement in the *Neumann* boundary conditions. The equivalence can be shown by replacing[1] $\boldsymbol{\sigma}$ in the equilibrium equation (2.5) by $\mathcal{C} \, \boldsymbol{\epsilon}(\mathbf{u})$ which leads to

$$
\operatorname{div} \boldsymbol{\sigma} \, + \, \mathbf{f} \, = \, \operatorname{div} \mathcal{C} \, \boldsymbol{\epsilon}(\mathbf{u}) \, + \, \mathbf{f} \, = \, 0 \; .
$$

Furthermore, using *Hooke's Law* from equality (2.3),

$$
\mathcal{C} \boldsymbol{\epsilon} \, = \, \lambda \operatorname{tr} \boldsymbol{\epsilon} \, \mathcal{I} \, + \, 2 \, \mu \, \boldsymbol{\epsilon} \; ,
$$

we get

$$
\operatorname{div} \left(\lambda \operatorname{tr} \boldsymbol{\epsilon}(\mathbf{u}) \, \mathcal{I} \right) \, + \, \operatorname{div} \left(2 \, \mu \, \boldsymbol{\epsilon}(\mathbf{u}) \right) \, + \, \mathbf{f} \, = \, 0 \; .
$$

Finally, the *Lamé Equation* follows from the equality

$$
\operatorname{div} \left(\operatorname{tr} \boldsymbol{\epsilon}(\mathbf{u}) \, \mathcal{I} \right) \, = \, \nabla \operatorname{div} \mathbf{u} \; ,
$$

which can easily be obtained by straight forward computations.

Following the general variational theory we can formulate this PDE also in the so-called *weak form* as a variational integral equation using test functions $\mathbf{v}$. The weak formulation of (3.2) reads

$$
\mathsf{a} \left(\mathbf{u}, \mathbf{v} \right) \, = \, \mathsf{F} \left(\mathbf{v} \right) \qquad \forall \, \mathbf{v} \in X \; ,
\tag{3.3}
$$

---

[1]   To do so we of course have to assume $\mathbf{u} \in H^2(\Omega)^2$.

with a continuous symmetric positive definite bilinear form $\mathsf{a}\,(\,\cdot\,,\,\cdot\,) : X \times X \longrightarrow \mathbb{R}^2$ and a linear functional (incorporating also the Neumann boundary conditions) $\mathsf{F}\,(\,\cdot\,) : X \longrightarrow \mathbb{R}^2$ with an 'appropriate' space X defined through

$$\mathsf{a}\,(\mathbf{u}, \mathbf{v}) \quad := \quad - \lambda \int_\Omega \nabla \operatorname{div} \mathbf{u}\,\mathbf{v}\,\,dx \;-\; 2\,\mu \int_\Omega \operatorname{div} \epsilon(\mathbf{u})\,\mathbf{v}\,\,dx$$

$$= \quad - \lambda \,(\nabla \operatorname{div} \mathbf{u}, \mathbf{v})_{0,\Omega} \;-\; 2\,\mu \,(\operatorname{div} \epsilon(\mathbf{u}), \mathbf{v})_{0,\Omega}\,,$$

$$\mathsf{F}\,(\mathbf{v}) \quad := \quad \int_\Omega \mathbf{f}\,\mathbf{v}\,\,dx \;-\; \int_{\Gamma_N} \mathbf{g}\,\mathbf{v}\,\,dx$$

$$= \quad (\mathbf{f}, \mathbf{v})_{0,\Omega} \;-\; (\mathbf{g}, \mathbf{v})_{0,\Gamma_N}\,.$$

Due to the *Characterization Theorem* (cf. [Br'97]) we know that the solution $\mathbf{u}$ of equation (3.3) is the minimum of the functional

$$\mathsf{J}\,(\mathbf{u}) \quad := \quad - \frac{\lambda}{2}\,(\nabla \operatorname{div} \mathbf{u}, \mathbf{u})_{0,\Omega} \;-\; \mu\,(\operatorname{div} \epsilon(\mathbf{u}), \mathbf{u})_{0,\Omega} \;-\; (\mathbf{f}, \mathbf{u})_{0,\Omega} \;+\; (\mathbf{g}, \mathbf{u})_{0,\Gamma_N}\,. \qquad (3.4)$$

Obtaining the following two equalities (by the use of *Green's Formula*)

$$(\nabla \operatorname{div} \mathbf{u}, \mathbf{u})_{0,\Omega} \quad = \quad - (\operatorname{div} \mathbf{u}, \operatorname{div} \mathbf{u})_{0,\Omega}$$

$$(\operatorname{div} \epsilon(\mathbf{u}), \mathbf{u})_{0,\Omega} \quad = \quad - (\epsilon(\mathbf{u}), \epsilon(\mathbf{u}))_{0,\Omega}$$

we can write the first two inner products of (3.4) in a much more symmetric way which results in

$$\mathsf{J}\,(\mathbf{u}) \quad = \quad \frac{\lambda}{2}\,(\operatorname{div} \mathbf{u}, \operatorname{div} \mathbf{u})_{0,\Omega} \;+\; \mu\,(\epsilon(\mathbf{u}), \epsilon(\mathbf{u}))_{0,\Omega} \;-\; (\mathbf{f}, \mathbf{u})_{0,\Omega} \;+\; (\mathbf{g}, \mathbf{u})_{0,\Gamma_N}\,. \qquad (3.5)$$

With the functional in the above equation in mind we can also rewrite the weak form in equation (3.3) more conveniently as

$$\underbrace{\lambda\,(\operatorname{div} \mathbf{u}, \operatorname{div} \mathbf{v})_{0,\Omega} \;+\; 2\,\mu\,(\epsilon(\mathbf{u}), \epsilon(\mathbf{v}))_{0,\Omega}}_{\mathsf{a}\,(\mathbf{u}, \mathbf{v})} \;=\; \underbrace{(\mathbf{f}, \mathbf{v})_{0,\Omega} \;-\; (\mathbf{g}, \mathbf{v})_{0,\Gamma_N}}_{\mathsf{F}\,(\mathbf{v})} \qquad \forall\,\mathbf{v} \in X\,. \quad (3.6)$$

Furthermore, from equality (3.6) we know that the 'appropriate' space X for the test functions $\mathbf{v}$ has to be at least $H^1_{\Gamma_D}(\Omega)^2$ such that for every $\mathbf{v} \in X$ the terms $\operatorname{div} \mathbf{v}$ and $\epsilon(\mathbf{v})$ exist.

This mere displacement approach is the easiest way to formulate a variational problem for elasticity and to set up a finite element method to approximate the solution for an elastic problem. It is also quite easy to prove that there exists a unique solution to the

equivalent problems (3.5) and (3.6); for the proof cf. [Br'97]. The drawback of this approach is the fact that the stress is only computed via post-processing and is thus less accurate than the displacement. In practice however, engineers are more interested in an accurate approximation of the stress (or sometimes the strain) than of the displacement. Thus, mixed methods which compute the stress directly are of great importance even though they are much more complicated to handle.

3.2   An introduction to mixed methods

Mixed methods arose from the need to develop a finite element approach suited to naturally solve the above-mentioned saddle-point problems as e.g. the system (3.1). We will therefore explain shortly the nature of such constrained problems.

3.2.1   Saddle-point problems

We consider a minimization problem with constraints. Let two Hilbert spaces X_1 and X_2 be given and two continuous bilinear forms

$$
\begin{aligned}
\mathsf{a} \,&:\, X_1 \times X_1 \longrightarrow \mathbb{R} \;, \\
\mathsf{b} \,&:\, X_1 \times X_2 \longrightarrow \mathbb{R} \;.
\end{aligned}
\tag{3.7}
$$

Given these bilinear forms we state the following problem: find the minimum of the functional

$$
\mathsf{J}(\mathbf{x}) \;=\; \frac{1}{2}\,\mathsf{a}(\mathbf{x},\mathbf{x}) \;-\; \mathsf{F}(\mathbf{x}) \qquad (\mathbf{x} \in X_1)
\tag{3.8}
$$

under the constraint

$$
\mathsf{b}(\mathbf{x},\mathbf{w}) \;=\; \mathsf{G}(\mathbf{w}) \qquad \forall\, \mathbf{w} \in X_2 \;.
\tag{3.9}
$$

Defining the so-called *Lagrange function* $\mathsf{L}(\mathbf{x},\mathbf{l})$ with $\mathbf{x} \in X_1$ and $\mathbf{l} \in X_2$ through

$$
\mathsf{L}(\mathbf{x},\mathbf{l}) \;:=\; \mathsf{J}(\mathbf{x}) \;+\; \mathsf{b}(\mathbf{x},\mathbf{l}) \;-\; \mathsf{G}(\mathbf{l}) \;,
\tag{3.10}
$$

we know that for every $\mathbf{x}$ that fulfills the constraint (3.9) we have the equality

$$
\mathsf{L}(\mathbf{x},\mathbf{l}) \;=\; \mathsf{J}(\mathbf{x}) \;.
$$

Thus, it seems natural to minimize $\mathsf{L}(\,\cdot\,,\mathbf{l})$ for some fixed $\mathbf{l} \in X_2$. For such a procedure however we have to be sure that there exists such an $\mathbf{l}$ for which the minimum of $\mathsf{L}(\,\cdot\,,\mathbf{l})$

in X_1 fulfills the constraint (3.9) for all $\mathbf{w} \in X_2$. To analyze this in further detail we formulate a saddle-point problem that results from the minimization of $\mathsf{L}(\mathbf{x}, \mathbf{l})$. As L is a quadratic form in two variables the weak form of its partial derivatives gives us a system of two equations:

$$\begin{aligned}
\mathsf{a}(\mathbf{x}, \mathbf{v}) + \mathsf{b}(\mathbf{v}, \mathbf{l}) &= \mathsf{F}(\mathbf{v}) && \forall \, \mathbf{v} \in X_1 \,, \\
\mathsf{b}(\mathbf{x}, \mathbf{w}) &= \mathsf{G}(\mathbf{w}) && \forall \, \mathbf{w} \in X_2 \,.
\end{aligned} \tag{3.11}$$

With a non-negative bilinear form a one can verify the *saddle-point property*

$$\mathsf{L}(\mathbf{x}, \mathbf{w}) \; \leq \; \mathsf{L}(\mathbf{x}, \mathbf{l}) \; \leq \; \mathsf{L}(\mathbf{v}, \mathbf{l}) \qquad \forall \, (\mathbf{v}, \mathbf{w}) \in X_1 \times X_2$$

for every solution $(\mathbf{x}, \mathbf{l})$ of (3.11). Thus, the $\mathbf{x}$ of such a saddle-point $(\mathbf{x}, \mathbf{l})$ is a solution of the original problem represented by the equations (3.8) and (3.9). The inverse however is not true in general. There are solutions to the constrained problem that do not guarantee the existence of such a unique so-called *Lagrangian parameter* $\mathbf{l}$ (for a counter-example cf. [Br'97]). That is why we have to postulate some properties for the bilinear forms $\mathsf{a}(\cdot, \cdot)$ and especially $\mathsf{b}(\cdot, \cdot)$.

These properties are first of all the usual continuity and coercivity demands for $\mathsf{a}(\cdot, \cdot)$. Furthermore, to fulfill the constraints represented in $\mathsf{b}(\cdot, \cdot)$ one deduces that linear independence of the system (3.11) is necessary. However, this is not sufficient (cf. [Bz'74, BF'91, Br'97]). In fact it is even necessary that the bounded linear mapping $\mathcal{L}$ from $X_1 \times X_2$ into its dual space which is defined through the system (3.11) via

$$\begin{aligned}
\mathcal{L} \, : \, X_1 \times X_2 \; &\longrightarrow \; X_1' \times X_2' \,, \\
(\mathbf{x}, \mathbf{l}) \; &\longmapsto \; (\mathsf{F}, \mathsf{G}) \,,
\end{aligned} \tag{3.12}$$

is an *isomorphism*. To guarantee this property we need the so-called *inf-sup condition* that will be introduced in the following definition.

Definition 3.1 (The inf-sup Condition) *Let two Hilbert spaces X_1 and X_2 be given. We say that a bilinear form $\mathsf{b} : X_1 \times X_2 \longrightarrow \mathbb{R}$ fulfills the inf-sup condition if there exists a constant $\beta > 0$ such that we have*

$$\inf_{\mathbf{w} \in X_2} \sup_{\mathbf{v} \in X_1} \frac{\mathsf{b}(\mathbf{v}, \mathbf{w})}{\|\mathbf{v}\| \|\mathbf{w}\|} \; \geq \; \beta \,. \tag{3.13}$$

This inequality is sometimes also called *Brezzi condition*. In the literature one can often find an equivalent formulation for (3.13), namely that there exists a constant $\beta > 0$ such that

$$\sup_{\mathbf{v} \in X_1} \frac{\mathsf{b}(\mathbf{v}, \mathbf{w})}{\|\mathbf{v}\|} \; \geq \; \beta \|\mathbf{w}\| \qquad \forall \, \mathbf{w} \in X_2 \tag{3.14}$$

holds true. However, throughout this thesis we will use the first formulation (3.13) which represents the name *'inf-sup condition'* and the whole topic of *saddle-point problems* in a natural way.

Given the condition (3.13) we can state the central main theorem for *saddle-point problems* that goes back to the important work of BREZZI and FORTIN. We will not prove this standard theorem and refer for a proof either to ([Bz'74, BF'91]) or to ([Br'97]). In these books there can also be found more detailed information on the derivation of the *inf-sup condition* and the whole framework of *saddle-point problems*.

Theorem 3.2 *Let two Hilbert spaces X_1 and X_2 and two continuous bilinear forms $\mathsf{a}\left(\cdot,\cdot\right)$ and $\mathsf{b}\left(\cdot,\cdot\right)$ as in (3.7) be given. Furthermore, using the continuity of $\mathsf{b}\left(\cdot,\cdot\right)$ we define a closed subset $Z \subset X_1$ via*

$$Z \ := \ \left\{ \mathbf{v} \in X_1 \, : \, \mathsf{b}\left(\mathbf{v},\mathbf{w}\right) \, = \, 0 \quad \forall \, \mathbf{w} \in X_2 \right\} . \tag{3.15}$$

The saddle-point problem given by the system (3.11) defines the mapping $\mathcal{L}$ in (3.12). This mapping is an isomorphism if and only if both of the following two conditions are fulfilled:

(i) The bilinear form a is coercive with respect to the subspace $Z \in X_1$, which means (cf. Definition 1.19):

$$\mathsf{a}\left(\mathbf{v},\mathbf{v}\right) \ \geq \ \alpha \left\| \mathbf{v} \right\|^2 \quad \forall \, \mathbf{v} \in Z . \tag{3.16}$$

(ii) The bilinear form b fulfills the inf-sup condition (3.13).

This theorem guarantees a unique solution for a variational problem under constraints in an infinite dimensional space. Thus, we finally have to tackle the question of an appropriate finite element method that can deal with this kind of problems successfully. This will be done in the next subsection.

3.2.2   Mixed finite element methods

A natural way to solve the system (3.11) as a finite dimensional problem is to choose subspaces $X_{h,1} \subset X_1$ and $X_{h,2} \subset X_2$ and solve the discrete problem

$$\begin{aligned}
\mathsf{a}\left(\mathbf{x}_h,\mathbf{v}_h\right) + \mathsf{b}\left(\mathbf{v}_h,\mathbf{l}_h\right) \ &= \ \mathsf{F}\left(\mathbf{v}_h\right) && \forall \, \mathbf{v}_h \in X_{h,1} , \\
\mathsf{b}\left(\mathbf{x}_h,\mathbf{w}_h\right) \ &= \ \mathsf{G}\left(\mathbf{w}_h\right) && \forall \, \mathbf{w}_h \in X_{h,2} ,
\end{aligned} \tag{3.17}$$

for a pair of variables $(\mathbf{x}_h, \mathbf{l}_h) \in X_{h,1} \times X_{h,2}$. Due to the fact that we have two distinct and most likely also *different* ansatz spaces such an finite element method is called a *mixed method*.

The theory of BREZZI and FORTIN as presented in [Bz'74, BF'91] and also shortly in [Br'97] shows that the bilinear forms $\mathsf{a}(\cdot, \cdot)$ and $\mathsf{b}(\cdot, \cdot)$ not only have to fulfill the conditions in Theorem 3.2 on the spaces X_1 and X_2 but also on the discrete spaces. This is stated in the so-called *Babuska-Brezzi condition* that is defined below.

Definition 3.3 *Analogously to (3.15) we define $Z_h \subset X_{h,1}$ via*

$$Z_h \; := \; \left\{ \mathbf{v}_h \in X_{h,1} \, : \, \mathsf{b}(\mathbf{v}_h, \mathbf{w}_h) \, = \, 0 \quad \forall \; \mathbf{w}_h \in X_{h,2} \right\} . \tag{3.18}$$

With this notation a pair of finite element spaces $X_{h,1}$ and $X_{h,2}$ is said to fulfill the Babuska-Brezzi condition, if there exist constants $\alpha > 0$ and $\beta > 0$ such that

$$\mathsf{a}(\mathbf{v}_h, \mathbf{v}_h) \; \geq \; \alpha \, \| \, \mathbf{v}_h \, \|^2 \qquad \quad \forall \; \mathbf{v}_h \in Z_h \, , \tag{3.19}$$

and

$$\inf_{\mathbf{w}_h \in X_{h,2}} \; \sup_{\mathbf{v}_h \in X_{h,1}} \; \frac{\mathsf{b}(\mathbf{v}_h, \mathbf{w}_h)}{\| \, \mathbf{v}_h \, \| \, \| \, \mathbf{w}_h \, \|} \; \geq \; \beta \, . \tag{3.20}$$

Applying the theory presented here to practical problems one will note that it is not trivial to meet the requirements in Theorem 3.2 for the variational spaces and those of the *Babuska-Brezzi condition* for the discrete ones. However, it is necessary for the setup of a stable finite element method to find especially discrete spaces that match these conditions. Only then we can be sure to find reasonable approximations for the saddle-point problem of interest. Furthermore, we have to note that in general the space Z_h is not a subset of the space Z. This is not a necessary condition for a successful mixed method but it usually grants the better results (cf. [Br'97]). Thus, we often demand the *additional conformity condition* for mixed methods:

$$Z_h \; \subset \; Z \, . \tag{3.21}$$

The topic of adjusting the variational and the discrete spaces to the problem under consideration will be examined later on in greater detail when we discuss and setup the *PEERS* method. For now, we have given an introduction to mixed methods and can thus finally apply the presented framework to elasticity.

3.3   Mixed methods in linear elasticity

There are different possibilities to set up a mixed method for the problem of linear elasticity depending on the quantities of interest and on the used ansatz spaces. We will present

two general and well-known mixed approaches in elasticity in the variational framework only, before we finally turn to the *PEERS* method on which we will focus more closely. For this method we will present also a suitable discrete setting that will be used throughout the rest of this thesis.

3.3.1   The Hellinger-Reissner principle

To set up a mixed method for linear elasticity we first have to understand at least two of the quantities stress, strain and displacement as separate variables that we want to determine – contrary to the mere displacement approach where we eliminated all but one variable. This will lead to a saddle-point problem in which one quantity will be the *Lagrangian parameter* in the sense of section 3.2.1. Usual mixed approaches in elasticity determine simultaneously stress and displacement (which is sometimes also called the *dual problem* of elasticity) or strain and displacement (called the *primal problem*).

A very common method is an approach by Hellinger and Reissner that focuses on the stress tensor. Analogous formulations for the strain tensor are possible but will not be introduced within this thesis. Keeping stress and displacement as separate variables and understanding the strain as a dependent quantity we end up with the usual PDE system for elasticity (3.1). Following the Hellinger-Reissner principle and the general theory of mixed methods the variational system for the PDE of linear elasticity reads:

$$
\begin{aligned}
(\mathcal{C}^{-1}\boldsymbol{\sigma}, \boldsymbol{\tau})_{0,\Omega} - (\boldsymbol{\tau}, \boldsymbol{\epsilon}(\mathbf{u}))_{0,\Omega} &= 0 & \forall\, \boldsymbol{\tau} \in L^2(\Omega)^{2\times2}_{sym} \ , \\
(\boldsymbol{\sigma}, \boldsymbol{\epsilon}(\mathbf{v}))_{0,\Omega} &= (\mathbf{f}, \mathbf{v})_{0,\Omega} - (\mathbf{g}, \mathbf{v})_{0,\Gamma_N} & \forall\, \mathbf{v} \in H^1_{\Gamma_D}(\Omega)^2 \ .
\end{aligned}
\tag{3.22}
$$

To fit this variational formulation into the terminology of saddle-point problems as presented in (3.11) we define shortly:

$$
\begin{aligned}
\mathsf{a}\,(\boldsymbol{\sigma}, \boldsymbol{\tau}) &:= (\mathcal{C}^{-1}\boldsymbol{\sigma}, \boldsymbol{\tau})_{0,\Omega} \ , \\
\mathsf{b}\,(\boldsymbol{\sigma}, \mathbf{v}) &:= -(\boldsymbol{\sigma}, \boldsymbol{\epsilon}(\mathbf{v}))_{0,\Omega} \ , \\
\mathsf{F}\,(\boldsymbol{\tau}) &:= 0 \ , \\
\mathsf{G}\,(\mathbf{v}) &:= -(\mathbf{f}, \mathbf{v})_{0,\Omega} + (\mathbf{g}, \mathbf{v})_{0,\Gamma_N} \ , \\
X_1 &:= L^2(\Omega)^{2\times2}_{sym} \ , \\
X_2 &:= H^1_{\Gamma_D}(\Omega)^2 \ .
\end{aligned}
\tag{3.23}
$$

Here, the displacement $\mathbf{u}$ obviously takes the role of the *Lagrangian parameter*. Under the assumption that both variational forms (3.6) and (3.22) have a unique solution their

equivalence can easily be seen. We can write equality (3.22) more generally as

$$(\boldsymbol{\epsilon}(\mathbf{u}) : \mathcal{C}\boldsymbol{\epsilon}(\mathbf{v}))_{0,\Omega} \;=\; (\mathbf{f}, \mathbf{v})_{0,\Omega} - (\mathbf{g}, \mathbf{v})_{0,\Gamma_N} \;,$$

and due to the symmetry of the tensor $\mathcal{C}$ also as

$$(\boldsymbol{\epsilon}(\mathbf{v}) : \mathcal{C}\boldsymbol{\epsilon}(\mathbf{u}))_{0,\Omega} \;=\; (\mathbf{f}, \mathbf{v})_{0,\Omega} - (\mathbf{g}, \mathbf{v})_{0,\Gamma_N} \;.$$

Replacing $\mathcal{C}\boldsymbol{\epsilon}(\mathbf{u})$ by $\boldsymbol{\sigma}$ leads to the second part of (3.22) while the first equation is just the weak expression of the additional equality $\boldsymbol{\sigma} = \mathcal{C}\boldsymbol{\epsilon}(\mathbf{u})$. For further details concerning existence and uniqueness of a solution to (3.22) we again refer to e.g. [Br'97].

3.3.2   The Hu-Washizu principle

This approach following an ansatz of Hu and Washizu (cf. [Wa'68]) keeps all three quantities stress $\boldsymbol{\sigma}$, strain $\boldsymbol{\epsilon}$ and displacement $\mathbf{u}$ as separate variables in the variational system. Note that thus in this method $\boldsymbol{\epsilon}$ is not just a tensor depending on the variable $\mathbf{u}$ but another variable that one has to solve for. To emphasize this we do not denote the symmetric gradient of the displacement as usual throughout this thesis by $\boldsymbol{\epsilon}(\mathbf{u})$ but write it as $\nabla^s \mathbf{u}$. The associated version of (3.1) for this formulation reads

$$
\begin{aligned}
\boldsymbol{\epsilon} &= \mathcal{C}^{-1}\boldsymbol{\sigma} & &\text{on } \Omega \;, \\
\boldsymbol{\epsilon} &= \nabla^s \mathbf{u} & &\text{on } \Omega \;, \\
\operatorname{div}\boldsymbol{\sigma} + \mathbf{f} &= 0 & &\text{on } \Omega \;, \\
\mathbf{u} &= 0 & &\text{on } \Gamma_D \;, \\
\boldsymbol{\sigma}\cdot\mathbf{n} &= \mathbf{g} & &\text{on } \Gamma_N \;,
\end{aligned}
\tag{3.24}
$$

and thus the variational form given by the system

$$
\begin{aligned}
(\mathcal{C}\boldsymbol{\epsilon}, \boldsymbol{\eta})_{0,\Omega} \qquad\qquad -(\boldsymbol{\eta}, \boldsymbol{\sigma})_{0,\Omega} &= 0 & &\forall\, \boldsymbol{\eta} \in L^2(\Omega)^{2\times 2} \;, \\
(\nabla^s \mathbf{v}, \boldsymbol{\sigma})_{0,\Omega} &= \mathsf{R}(\mathbf{v}) & &\forall\, \mathbf{v} \in H^1_{\Gamma_D}(\Omega)^2 \;, \\
(\boldsymbol{\epsilon}, \boldsymbol{\tau})_{0,\Omega} - (\nabla^s \mathbf{u}, \boldsymbol{\tau})_{0,\Omega} \qquad\qquad &= 0 & &\forall\, \boldsymbol{\tau} \in L^2(\Omega)^{2\times 2} \;,
\end{aligned}
\tag{3.25}
$$

where we denote $\mathsf{R}(\mathbf{v}) := (\mathbf{f}, \mathbf{v})_{0,\Omega} - (\mathbf{g}, \mathbf{v})_{0,\Gamma_N}$.

The equivalence of (3.1) to (3.24) and (3.22) to (3.25) is obvious due to the fact that there is only one additional equation in the PDE system that has its weak expression in the third equality of (3.25). The first equation of the variational system (3.22) is multiplied by the tensor $\mathcal{C}$ and thus results in the first equation of (3.25). To fit this formulation

again in the context of Section 3.2.1 we set

$$
\begin{aligned}
\mathsf{a}\left((\boldsymbol{\epsilon},\mathbf{u}),(\boldsymbol{\eta},\mathbf{v})\right) &:= (\mathcal{C}\boldsymbol{\epsilon},\boldsymbol{\eta})_{0,\Omega} \ , \\
\mathsf{b}\left((\boldsymbol{\epsilon},\mathbf{u}),\boldsymbol{\tau}\right) &:= -(\boldsymbol{\epsilon},\boldsymbol{\tau})_{0,\Omega} + (\nabla^{\mathsf{s}}\mathbf{u},\boldsymbol{\tau})_{0,\Omega} \ , \\
\mathsf{F}\left((\boldsymbol{\eta},\boldsymbol{\tau})\right) &:= (\mathbf{f},\mathbf{v})_{0,\Omega} - (\mathbf{g},\mathbf{v})_{0,\Gamma_N} \ , \\
\mathsf{G}\left(\mathbf{v}\right) &:= 0 \ , \\
X_1 &:= L^2(\Omega)^{2\times 2} \times H^1_{\Gamma_D}(\Omega)^2 \ , \\
X_2 &:= L^2(\Omega)^{2\times 2} \ .
\end{aligned}
\tag{3.26}
$$

We see that in this formulation the stress $\boldsymbol{\sigma}$ is the *Lagrangian parameter*. Remarks concerning existence and uniqueness of a solution of the Hu-Washizu approach can again be found in [Br'97].

3.3.3   The *PEERS* approach

After presenting two quite general mixed approaches we will finally focus on the *PEERS* method which is based on a modification of the Hellinger-Reissner principle. This modification is necessary in practical applications due to the fact that the advantages of mixed methods (e.g. better approximation of the stress tensor) can not be realized very well with the proposed ansatz spaces in (3.22). A better suited equivalent approach makes use of the Sobolev space $H(\mathsf{div},\Omega)^{2\times 2}_{sym}$ by applying integration by parts on the bilinear form $\mathsf{b}\left(\cdot,\cdot\right)$. Thus, contrary to (3.23) we get

$$
\begin{aligned}
\mathsf{a}\left(\boldsymbol{\sigma},\boldsymbol{\tau}\right) &:= (\mathcal{C}^{-1}\boldsymbol{\sigma},\boldsymbol{\tau})_{0,\Omega} \ , \\
\mathsf{b}\left(\boldsymbol{\sigma},\mathbf{v}\right) &:= -(\boldsymbol{\sigma},\boldsymbol{\epsilon}(\mathbf{v}))_{0,\Omega} = (\mathsf{div}\,\boldsymbol{\sigma},\mathbf{v})_{0,\Omega} \ , \\
\mathsf{F}\left(\boldsymbol{\tau}\right) &:= 0 \ , \\
\mathsf{G}\left(\mathbf{v}\right) &:= -(\mathbf{f},\mathbf{v})_{0,\Omega} \ , \\
X_1 &:= H_{\Gamma_N}(\mathsf{div},\Omega)^{2\times 2}_{sym} \ , \\
X_2 &:= L^2(\Omega)^2 \ ,
\end{aligned}
\tag{3.27}
$$

and the variational form – equivalent to (3.22) – reads

$$
\begin{aligned}
(\mathcal{C}^{-1}\boldsymbol{\sigma},\boldsymbol{\tau})_{0,\Omega} + (\mathsf{div}\,\boldsymbol{\tau},\mathbf{u})_{0,\Omega} &= 0 & \forall\,\boldsymbol{\tau} \in H_{\Gamma_N}(\mathsf{div},\Omega)^{2\times 2}_{sym} \ , \\
(\mathsf{div}\,\boldsymbol{\sigma},\mathbf{v})_{0,\Omega} &= -(\mathbf{f},\mathbf{v})_{0,\Omega} & \forall\,\mathbf{v} \in L^2(\Omega)^2 \ , \\
\boldsymbol{\sigma}\cdot\mathbf{n} &= \mathbf{g} & \text{on } \Gamma_N \ .
\end{aligned}
\tag{3.28}
$$

In this formulation it is more complicate to incorporate the *Neumann boundary conditions* correctly. One way how this can be done will be described later on and thus we will keep the boundary conditions first as the additional equation $\boldsymbol{\sigma} \cdot \mathbf{n} = \mathbf{g}$ on Γ_N.

However, even this modification does not grant a stable mixed method for linear elasticity in general. There are still two hurdles that remain. The first is the difficulty of *locking*. With *locking* the engineering literature describes the phenomenon that for some kind of problems finite element computations in elasticity yield approximation results that underestimate the true solution. This is due to the fact that various parameters can have a large influence on the continuity constant c and the coercivity constant α which both are of great importance in the error estimates of the *Céa Lemma* (cf. e.g. [Br'97]). Thus, for finer and finer triangulations ($h \longrightarrow 0$) a finite element method can loose uniform convergence with respect to these parameters.

Locking effects occur e.g. in problems with *nearly incompressible material*. Such materials (as for example rubber) have in common that the associated *Lamé constants* differ very much from each other as a result of *Poisson's ratio* $\nu \longrightarrow 0.5$, which means we usually have

$$\lambda \gg \mu \,.$$

Remember that in the limit case $\nu = 0.5$ the matrix $\mathcal{C}^{-1}$ would be singular. Therefore, the variational system is badly conditioned if $\nu \longrightarrow 0.5$. Furthermore, in such problems we get the following estimates for the coercivity constant α (cf. Definition 1.19) and the continuity constant c (cf. Definition 1.18):

$$\alpha \leq \mu \qquad \text{and} \qquad \lambda + \mu \leq c \,.$$

This results in a large quotient c/α which yields a significantly bad error estimation within the *Céa Lemma* and also bad approximation results for very large values of λ. Nevertheless, there are various ways to deal with the *locking* problem. In general they rely on penalty terms in the form of additional constraints that can be introduced elegantly in the *saddle-point problem* setting. For further information concerning the *locking* phenomenon we refer to [Br'97] for a short introduction or to [Ar'81, BS1'92, BS2'92] for more detailed examinations.

However, besides the *locking* effects we have the paramount hurdle that it is quite difficult to find appropriate spaces to match the *Babuska-Brezzi condition* in Definition 3.3 and especially the *additional conformity condition* (3.21), cf. Section 3.2.2. As was shown in [BF'91] this is mostly due to the demanded symmetry of the stress tensor. The *PEERS* approach in [ABD'84] which slightly modifies the equations in (3.27) and (3.28) is thus based on the idea, that we fulfill the symmetry condition for the stress tensor only

via an additional constraint[2] similar to the techniques to deal with *locking*. Furthermore, this approach does not only yield very good ansatz spaces to fulfill the *inf-sup condition* but it also works very well for *nearly incompressible material.*

To reduce the symmetry in the system (3.28) we do not demand any more that the stress tensor is necessarily symmetric, e.g. $\boldsymbol{\sigma} \in H_{\Gamma_N}(\mathsf{div}, \Omega)^{2\times 2}_{sym}$, but only $\boldsymbol{\sigma} \in H_{\Gamma_N}(\mathsf{div}, \Omega)^{2\times 2}$. Thus, we violate the equilibrium equation (2.5) that states

$$\boldsymbol{\sigma}^T \;=\; \boldsymbol{\sigma} \;. \tag{3.29}$$

This violation is mended by including equation (3.29) as an additional constraint that we want to fulfill in the weak sense. We therefore define an *anti-symmetric part* of a tensor $\boldsymbol{\tau} \in H_{\Gamma_N}(\mathsf{div}, \Omega)^{2\times 2}$ via

$$\mathsf{as}\,\boldsymbol{\tau} \;:=\; \boldsymbol{\tau} - \boldsymbol{\tau}^T \;. \tag{3.30}$$

Note that $\mathsf{as}\,\boldsymbol{\tau}$ is completely given trough $\tau_{12} - \tau_{21}$ and thus, we will identify the anti-symmetric part with this difference:

$$\mathsf{as}\,\boldsymbol{\tau} \;:=\; (\tau_{12} - \tau_{21}) \;\in L^2(\Omega) \;. \tag{3.31}$$

This leads us to the weak expression $(\mathsf{as}\,\boldsymbol{\sigma}, \eta)_{0,\Omega} \;=\; 0 \quad \forall\, \eta \in L^2(\Omega)$ that we add to the system (3.28) which leads us to the following definitions in the *saddle-point problem* framework:

$$\begin{aligned}
\mathsf{a}\,(\boldsymbol{\sigma}, \boldsymbol{\tau}) &\;:=\; (\mathcal{C}^{-1}\boldsymbol{\sigma}, \boldsymbol{\tau})_{0,\Omega} \;, \\
\mathsf{b}\,(\boldsymbol{\sigma}, (\mathbf{v}, \eta)) &\;:=\; (\mathsf{div}\,\boldsymbol{\sigma}, \mathbf{v})_{0,\Omega} + (\mathsf{as}\,\boldsymbol{\sigma}, \eta)_{0,\Omega} \;, \\
\mathsf{F}\,(\boldsymbol{\tau}) &\;:=\; 0 \;, \\
\mathsf{G}\,((\mathbf{v}, \eta)) &\;:=\; -(\mathbf{f}, \mathbf{v})_{0,\Omega} \;, \\
X_1 &\;:=\; H_{\Gamma_N}(\mathsf{div}, \Omega)^{2\times 2} \;, \\
X_2 &\;:=\; L^2(\Omega)^2 \times L^2(\Omega) \;.
\end{aligned} \tag{3.32}$$

The variational form now reads: find a triple $(\boldsymbol{\sigma}, \mathbf{u}, \gamma) \in H_{\Gamma_N}(\mathsf{div}, \Omega)^{2\times 2} \times L^2(\Omega)^2 \times L^2(\Omega)$ such that the system

$$\begin{aligned}
(\mathcal{C}^{-1}\boldsymbol{\sigma}, \boldsymbol{\tau})_{0,\Omega} + (\mathsf{div}\,\boldsymbol{\tau}, \mathbf{u})_{0,\Omega} + (\mathsf{as}\,\boldsymbol{\tau}, \gamma)_{0,\Omega} &\;=\; 0 \;, \\
(\mathsf{div}\,\boldsymbol{\sigma}, \mathbf{v})_{0,\Omega} &\;=\; -(\mathbf{f}, \mathbf{v})_{0,\Omega} \;, \\
(\mathsf{as}\,\boldsymbol{\sigma}, \eta)_{0,\Omega} &\;=\; 0 \;, \\
\boldsymbol{\sigma} \cdot \mathbf{n} &\;=\; \mathbf{g} \quad \text{on } \Gamma_N \;.
\end{aligned} \tag{3.33}$$

---

[2] This idea of 'reduced' symmetry gave the approach its name: *PEERS* stands for '*P*lane *E*lasticity *E*lement with *R*educed *S*ymmetry'.

holds true for all $(\boldsymbol{\tau}, \mathbf{v}, \eta) \in H_{\Gamma_N}(\mathsf{div}, \Omega)^{2 \times 2} \times L^2(\Omega)^2 \times L^2(\Omega)$. The equivalence of (3.28) and (3.33) can be seen easily. Let $(\boldsymbol{\sigma}, \mathbf{u}, \gamma)$ be a solution of (3.33). Consequently, $\boldsymbol{\sigma}$ is a symmetric tensor and the third equation in (3.33) can be omitted. For symmetric $\boldsymbol{\tau}$ we also have $(\mathsf{as}\,\boldsymbol{\tau}, \gamma)_{0,\Omega} = 0$ and thus the system (3.33) is reduced to the system (3.28) with a solution $(\boldsymbol{\sigma}, \mathbf{u})$. Assuming on the other hand that $(\boldsymbol{\sigma}, \mathbf{u})$ is a solution of (3.28) the equivalence of the two systems (3.22) and (3.28) yields $\mathbf{u} \in H_{\Gamma_D}^1(\Omega)^2$ and we have the equality

$$(\mathcal{C}^{-1}\boldsymbol{\sigma} - \boldsymbol{\epsilon}(\mathbf{u}), \boldsymbol{\tau})_{0,\Omega} = 0 , \tag{3.34}$$

that holds true for all symmetric $\boldsymbol{\tau}$. This equation however is true also for skew-symmetric $\boldsymbol{\tau}$ due to the symmetry of the two tensors $\mathcal{C}^{-1}\boldsymbol{\sigma}$ and $\boldsymbol{\epsilon}(\mathbf{u})$. To deduce the first equation of (3.33) from (3.34) for $\boldsymbol{\tau} \in H_{\Gamma_N}(\mathsf{div}, \Omega)^{2 \times 2}$ we decompose $\boldsymbol{\epsilon}(\mathbf{u})$ in the following way:

$$\boldsymbol{\epsilon}(\mathbf{u}) = \nabla\mathbf{u} - \frac{1}{2}\,\mathsf{as}\,(\nabla\mathbf{u})$$

$$= \nabla\mathbf{u} - \frac{1}{2}\left(\frac{\partial u_2}{\partial x_1} - \frac{\partial u_1}{\partial x_2}\right)\begin{bmatrix} 0 & -1 \\ 1 & 0 \end{bmatrix}$$

$$= \nabla\mathbf{u} - \frac{1}{2}\,\mathsf{curl}\,\mathbf{u}\begin{bmatrix} 0 & -1 \\ 1 & 0 \end{bmatrix} .$$

Applying this decomposition and afterwards *Green's Formula* to equation (3.34) we get

$$(\mathcal{C}^{-1}\boldsymbol{\sigma}, \boldsymbol{\tau})_{0,\Omega} + (\mathsf{div}\,\boldsymbol{\tau}, \mathbf{u})_{0,\Omega} + \frac{1}{2}\,(\mathsf{as}\,\boldsymbol{\tau}, \mathsf{curl}\,\mathbf{u})_{0,\Omega} = 0 . \tag{3.35}$$

This equation defines γ via

$$\gamma := \frac{1}{2}\,\mathsf{curl}\,\mathbf{u} , \tag{3.36}$$

and together with the symmetry of $\boldsymbol{\sigma}$ which yields $(\mathsf{as}\,\boldsymbol{\sigma}, \eta)_{0,\Omega} = 0 \ \ \forall\ \eta \in L^2(\Omega)$ we end up with system (3.33) and its solution $(\boldsymbol{\sigma}, \mathbf{u}, \gamma)$. Consequently, we have proven the equivalence of the systems (3.28) and (3.33).

It remains to show that the *saddle point problem* defined by (3.32) and (3.33) meets the requirements of Theorem 3.2 to guarantee existence and uniqueness of the solution. First of all continuity is demanded for both bilinear forms. Due to the fact that $1/\mu$ is the largest eigenvalue (cf. e.g. [Lo'02]) of the positive definite tensor $\mathcal{C}^{-1}$ (cf. Section 2.1) we deduce for the bilinear form $\mathsf{a}\,(\,\cdot\,,\,\cdot\,)$

$$\mathsf{a}\,(\boldsymbol{\sigma}, \boldsymbol{\tau}) = (\mathcal{C}^{-1}\boldsymbol{\sigma}, \boldsymbol{\tau})_{0,\Omega} \leq \frac{1}{\mu}\,\|\,\boldsymbol{\sigma}\,\|_{H(\mathsf{div},\Omega)}^2\,\|\,\boldsymbol{\tau}\,\|_{H(\mathsf{div},\Omega)}^2 ,$$

while for $\mathsf{b}\,(\,\cdot\,,\,\cdot\,)$ the inequality

$$\mathsf{b}\,(\boldsymbol{\tau}, (\mathbf{v}, \eta)) = (\mathsf{div}\,\boldsymbol{\tau}, \mathbf{v})_{0,\Omega} + (\mathsf{as}\,\boldsymbol{\tau}, \eta)_{0,\Omega} \leq \|\,\boldsymbol{\tau}\,\|_{H(\mathsf{div},\Omega)}^2\,(\|\,\mathbf{v}\,\|_{0,\Omega} + \|\,\eta\,\|_{0,\Omega})$$

obviously hold true. We continue with a proof of the coercivity of $\mathsf{a}\,(\,\cdot\,,\,\cdot\,)$ and define the subset $Z \in H_{\Gamma_N}(\mathsf{div}, \Omega)^{2 \times 2}$ through

$$Z := \{\boldsymbol{\tau} \in H_{\Gamma_N}(\mathsf{div}, \Omega)^{2 \times 2} : \mathsf{b}\,(\boldsymbol{\tau}, (\mathbf{v}, \eta)) = 0 \quad \forall\, (\mathbf{v}, \eta) \in L^2(\Omega)^2 \times L^2(\Omega)\}\;.$$

It is $\|\mathsf{div}\,\boldsymbol{\tau}\|_{0,\Omega}^2 = 0 \;\; \forall\, \boldsymbol{\tau} \in Z$ and consequently we get

$$\|\boldsymbol{\tau}\|_{H(\mathsf{div}, \Omega)}^2 = \|\boldsymbol{\tau}\|_{0,\Omega}^2 + \|\mathsf{div}\,\boldsymbol{\tau}\|_{0,\Omega}^2 = \|\boldsymbol{\tau}\|_{0,\Omega}^2 \lesssim (\mathcal{C}^{-1}\boldsymbol{\tau}, \boldsymbol{\tau})_{0,\Omega} = \mathsf{a}\,(\boldsymbol{\tau}, \boldsymbol{\tau})$$

for all $\boldsymbol{\tau} \in Z$. Therefore, coercivity of the bilinear form $\mathsf{a}\,(\,\cdot\,,\,\cdot\,)$ is provided. The proof that also the *inf-sup condition* is fulfilled is a little more complicated, especially if we consider Neumann boundary conditions. If we assume just mere Dirichlet boundary conditions it suffices to show that for each pairing $(\mathbf{v}, \eta) \in L^2(\Omega)^2 \times L^2(\Omega)$ we can find a $\boldsymbol{\tau} \in H(\mathsf{div}, \Omega)^{2 \times 2}$ such that we have

$$\begin{aligned} \mathsf{div}\,\boldsymbol{\tau} &= \mathbf{v}\;, \\ \mathsf{as}\,\boldsymbol{\tau} &= \eta\;, \\ \|\boldsymbol{\tau}\|_{H(\mathsf{div}, \Omega)} &\lesssim \|\mathbf{v}\|_{0,\Omega} + \|\eta\|_{0,\Omega}\;. \end{aligned} \tag{3.37}$$

With such $\boldsymbol{\tau}$ we would have

$$\begin{aligned} \|\boldsymbol{\tau}\|_{H(\mathsf{div}, \Omega)}\,(\|\mathbf{v}\|_{0,\Omega} + \|\eta\|_{0,\Omega}) &\lesssim (\|\mathbf{v}\|_{0,\Omega} + \|\eta\|_{0,\Omega})^2 \\ &\lesssim \|\mathbf{v}\|_{0,\Omega}^2 + \|\eta\|_{0,\Omega}^2 \\ &= (\mathsf{div}\,\boldsymbol{\tau}, \mathbf{v})_{0,\Omega} + (\mathsf{as}\,\boldsymbol{\tau}, \eta)_{0,\Omega} \\ &= \mathsf{b}\,(\boldsymbol{\tau}, (\mathbf{v}, \eta)) \\ &\lesssim \sup_{\boldsymbol{\tau}} \mathsf{b}\,(\boldsymbol{\tau}, (\mathbf{v}, \eta))\;, \end{aligned}$$

which is a representation of the *inf-sup condition* in the form of (3.14). To construct a $\boldsymbol{\tau}$ as it is needed, we start with a $\hat{\boldsymbol{\tau}} \in H(\mathsf{div}, \Omega)^{2 \times 2}$ that fulfills

$$\mathsf{div}\,\hat{\boldsymbol{\tau}} = \mathbf{v}\;, \tag{3.38}$$

for example

$$\hat{\boldsymbol{\tau}} := \nabla \mathbf{w}\;,$$

where $\mathbf{w} \in H_0^1(\Omega)$ is the well-known solution of *Poisson's Equation*

$$\triangle \mathbf{w} = \mathbf{v}\;.$$

We know from the general theory that

$$\|\mathbf{w}\|_{1,\Omega} \lesssim \|\mathbf{v}\|_{0,\Omega}\;,$$

and hence $\hat{\boldsymbol{\tau}}$ also fulfills

$$
\begin{aligned}
\|\hat{\boldsymbol{\tau}}\|_{H(\mathsf{div},\Omega)} &= \|\hat{\boldsymbol{\tau}}\|_{0,\Omega} + \|\mathsf{div}\,\hat{\boldsymbol{\tau}}\|_{0,\Omega} = \|\nabla\mathbf{w}\|_{0,\Omega} + \|\mathbf{v}\|_{0,\Omega} \\
&\lesssim \|\mathbf{v}\|_{0,\Omega} \lesssim \|\mathbf{v}\|_{0,\Omega} + \|\eta\|_{0,\Omega} .
\end{aligned}
\tag{3.39}
$$

Now, we define the defect d as

$$
d := \eta - \mathsf{as}\,\hat{\boldsymbol{\tau}} ,
$$

and construct similar to $\hat{\boldsymbol{\tau}}$ a vector $\mathbf{q} \in H^1(\Omega)^2$ such that

$$
\mathsf{div}\,\mathbf{q} = d
\tag{3.40}
$$

holds true. This also gives us the following estimate:

$$
\|\mathbf{q}\|_{1,\Omega} \lesssim \|d\|_{0,\Omega} \lesssim \|\eta\|_{0,\Omega} \lesssim \|\mathbf{v}\|_{0,\Omega} + \|\eta\|_{0,\Omega} .
\tag{3.41}
$$

Finally, we define the $\boldsymbol{\tau}$ we seek as

$$
\boldsymbol{\tau} := \hat{\boldsymbol{\tau}} + \begin{bmatrix} \mathsf{curl}\,q_1 & \mathsf{curl}\,q_2 \end{bmatrix} .
\tag{3.42}
$$

It remains to show that the $\boldsymbol{\tau}$ in (3.42) fulfills the demands from (3.37). First, due to the fact that the divergence of a rotation vanishes we have

$$
\mathsf{div}\,\boldsymbol{\tau} = \mathsf{div}\,\hat{\boldsymbol{\tau}} = \mathbf{v} ,
$$

and furthermore it is

$$
\begin{aligned}
\mathsf{as}\,\boldsymbol{\tau} &= \mathsf{as}\,\hat{\boldsymbol{\tau}} + \mathsf{as} \begin{bmatrix} \dfrac{\partial q_1}{\partial x_2} & \dfrac{\partial q_2}{\partial x_2} \\[2mm] \dfrac{\partial q_1}{\partial x_1} & \dfrac{\partial q_2}{\partial x_1} \end{bmatrix} \\
&= \mathsf{as}\,\hat{\boldsymbol{\tau}} + \mathsf{div}\,\mathbf{q} = \mathsf{as}\,\hat{\boldsymbol{\tau}} + d = \eta .
\end{aligned}
$$

We conclude this considerations with the remark that the inequalities (3.39) and (3.41) together imply also the inequality in (3.37).

For Neumann boundary conditions we have to modify the solutions $\hat{\boldsymbol{\tau}}$ and $\mathbf{q}$ of (3.40) and (3.38) further to match the condition

$$
\mathsf{div}\,\boldsymbol{\tau} \cdot \mathbf{n} = 0 \qquad \text{on } \Gamma_N .
\tag{3.43}
$$

It is easy to accomplish $\mathsf{div}\,\hat{\boldsymbol{\tau}} = 0$ on Γ_N if we demand related boundary conditions for the associated *Poisson's Equation*. But to fulfill (3.43) we have to force also $\mathsf{curl}\,q_i \cdot \mathbf{n} = 0$ on Γ_N which is nothing else than $\nabla q_i \cdot \mathbf{t} = 0$ on Γ_N. Thus, we have to find a $\mathbf{q}$ that fulfills

equation (3.40) and has constant components q_i on the boundary Γ_N. This problem can also be formulated as a saddle-point problem, namely the so-called *Stokes Problem*

$$
\begin{aligned}
\triangle \mathbf{q} + \nabla p &= 0 && \text{on } \Omega \\
\operatorname{div} \mathbf{q} &= d && \text{on } \Omega \\
\mathbf{q} &= 0 && \text{on } \Gamma_N \,,
\end{aligned}
\tag{3.44}
$$

with a scalar function $p \in L_0^2(\Omega) := \{ x \in L^2(\Omega) \,:\, (x,1)_{0,\Omega} = 0 \}$. Finally the *inf-sup condition* that holds for the *Stokes Problem* grants the *inf-sup condition* for the *PEERS* method. Details concerning the *Stokes Problem* and the associated *inf-sup condition* can be found in [Br'97, DL'76]. Therefore, Theorem 3.2 is finally proven for this approach and existence and uniqueness of the solution in this kind of *saddle-point problem* is guaranteed.

For the discretization of the problem in the *PEERS* approach we can now fulfill also the *additional conformity condition* $Z_h \subset Z$. We define the following ansatz spaces for a *PEERS* method of lowest order:

$$
\begin{aligned}
S_h &:= (\mathcal{RT}_h^0)^2 \oplus (\operatorname{curl} \mathcal{B}_{0,h}^3)^2 \\
V_h &:= (\mathcal{M}_h^0)^2 \\
Q_h &:= \mathcal{M}_{0,h}^1 \,.
\end{aligned}
\tag{3.45}
$$

Thus, the ansatz space for the discrete approximation of the stress tensor S_h is the Raviart-Thomas space of lowest order enriched by rotations of cubic bubble functions (which is a result from (3.42) to fulfill the *inf-sup-condition*), while we want to approximate the displacement variable in V_h in each component with piecewise constant functions. The space Q_h for the *Lagrangian multiplier* finally contains continuous piecewise linear ansatz functions. With these discrete spaces one can verify (similar to the verification of the demands from Theorem 3.2) the *Babuska-Brezzi condition* from Definition 3.3 which finally guarantees reasonable approximations $(\boldsymbol{\sigma}_h, \mathbf{u}_h, \gamma_h) \in S_h \times V_h \times Q_h$ to the true solution $(\boldsymbol{\sigma}, \mathbf{u}, \gamma)$.

In the further chapters of this thesis we will always consider the presented *PEERS* formulation and the presented discrete spaces with some simplifications. Thus, from now on we will always assume vanishing volume forces $\mathbf{f}$ and we will furthermore assume that the Neumann boundary conditions are extended and represented via a suitable function $\boldsymbol{\sigma}^N \in H(\operatorname{div}, \Omega)^{2 \times 2}$ that fulfills

$$
\boldsymbol{\sigma}^N \cdot \mathbf{n} = \mathbf{g} \qquad \text{on } \Gamma_N \,.
\tag{3.46}
$$

This leads to the following slightly modified variational formulation of linear elasticity:

$$(\mathcal{C}^{-1}(\boldsymbol{\sigma}^N + \boldsymbol{\sigma}), \boldsymbol{\tau})_{0,\Omega} \; + \; (\mathbf{u}, \operatorname{div} \boldsymbol{\tau})_{0,\Omega} \; + \; (\gamma, \operatorname{as} \boldsymbol{\tau})_{0,\Omega} \;\; = \;\; 0 \qquad \forall \, \boldsymbol{\tau} \in H_{\Gamma_N}(\operatorname{div}, \Omega)^{2 \times 2} \; ,$$

$$(\operatorname{div}(\boldsymbol{\sigma}^N + \boldsymbol{\sigma}), \mathbf{v})_{0,\Omega} \;\; = \;\; 0 \qquad \forall \, \mathbf{v} \in L^2(\Omega)^2 \; , \qquad (3.47)$$

$$(\operatorname{as}(\boldsymbol{\sigma}^N + \boldsymbol{\sigma}), \eta)_{0,\Omega} \;\; = \;\; 0 \qquad \forall \, \eta \in L^2(\Omega) \; ,$$

and its discrete version

$$(\mathcal{C}^{-1}(\boldsymbol{\sigma}^N + \boldsymbol{\sigma}_h), \boldsymbol{\tau}_h)_{0,\Omega} \; + \; (\mathbf{u}_h, \operatorname{div} \boldsymbol{\tau}_h)_{0,\Omega} \; + \; (\gamma_h, \operatorname{as} \boldsymbol{\tau}_h)_{0,\Omega} \;\; = \;\; 0 \qquad \forall \, \boldsymbol{\tau}_h \in S_h \; ,$$

$$(\operatorname{div}(\boldsymbol{\sigma}^N + \boldsymbol{\sigma}_h), \mathbf{v}_h)_{0,\Omega} \;\; = \;\; 0 \qquad \forall \, \mathbf{v}_h \in V_h \; , \quad (3.48)$$

$$(\operatorname{as}(\boldsymbol{\sigma}^N + \boldsymbol{\sigma}_h), \eta_h)_{0,\Omega} \;\; = \;\; 0 \qquad \forall \, \eta_h \in Q_h \; .$$

3.4 The *PEERS* approach in plasticity

In this section we want to extend the *PEERS* mixed method from the mere linear elasticity to also static and quasi-static perfect plasticity. Recalling Section 2.3 we know that we can compute the solution stress in the elastoplastic case generally via an orthogonal projection $P_K(\,\cdot\,)$ from a special *elastic trial stress* $\boldsymbol{\sigma}^{tr}$ onto the convex set of admissible stresses K. This procedure is generally called *return mapping*. Here, the projection was given explicitly through

$$P_K(\boldsymbol{\sigma}^{tr}) \;\; = \;\; \boldsymbol{\sigma}^{tr} \; - \; \max\{0 \, ; \, \| \operatorname{dev} \boldsymbol{\sigma}^{tr} \|_F \; - \; \sqrt{\frac{2}{3}} \, \sigma^\star \} \, \frac{\operatorname{dev} \boldsymbol{\sigma}^{tr}}{\| \operatorname{dev} \boldsymbol{\sigma}^{tr} \|_F} \; . \qquad (3.49)$$

Due to the fact that we can compute $P_K(\boldsymbol{\sigma}^{tr})$ explicitly (and also quite easily) if given $\boldsymbol{\sigma}^{tr}$ it remains to explain the nature of the *trial stress* and to find a way to compute it, especially in our variational *PEERS* setting. We will present this elastoplastic framework following mainly the work of SIMO and HUGHES as presented in [SH'98], while the notation follows the closely related work of WIENERS as [Wie1'99, Wie2'99], where also more details can be found. We define the space of stresses S as

$$S \;\; := \;\; H_{\Gamma_N}(\operatorname{div}, \Omega)^{2 \times 2} \; , \qquad (3.50)$$

together with a scalar product

$$(\boldsymbol{\sigma}, \boldsymbol{\tau})_S \;\; := \;\; (\mathcal{C}^{-1} \boldsymbol{\sigma}, \boldsymbol{\tau})_{0,\Omega} \; , \qquad (3.51)$$

and we define a subspace $S_{SSR} \subset S$ via

$$S_{SSR} \;\; := \;\; \{ \boldsymbol{\sigma} \in S : \boldsymbol{\sigma} = \mathcal{C} \, \boldsymbol{\epsilon}(\mathbf{v}) \quad \forall \, \mathbf{v} \in L^2(\Omega)^2 \} \; . \qquad (3.52)$$

Thus, S_{SSR} is the space of such stresses that fulfill the *stress-strain-relationship* (2.2). Furthermore, we define the space $S_{SSR}^{\perp}$ as the orthogonal complement to S_{SSR} with respect to the scalar product $(\,\cdot\,,\,\cdot\,)_S$.

Assuming elastic material behavior there is a stress $\boldsymbol{\sigma}^{el} \in S_{SSR}$ that also fulfills the equilibrium of forces and the symmetry condition in (2.5). From [SH'98, Wie1'99, Wie2'99] we know that there is an affine space $S_{EQ} \subset S$ that contains all stresses that fulfill equilibrium and symmetry simultaneously, i.e.

$$S_{EQ} \;:=\; \left\{\boldsymbol{\sigma} \in S : \operatorname{div}\boldsymbol{\sigma} + \mathbf{f} = 0 \quad \wedge \quad \boldsymbol{\sigma}^T = \boldsymbol{\sigma}\right\} . \tag{3.53}$$

This space can also be described as an affine transformation of $S_{SSR}^{\perp}$ through

$$S_{EQ} \;=\; \boldsymbol{\sigma}_{el} \;+\; S_{SSR}^{\perp} , \tag{3.54}$$

as it is depicted in Figure 3.1.
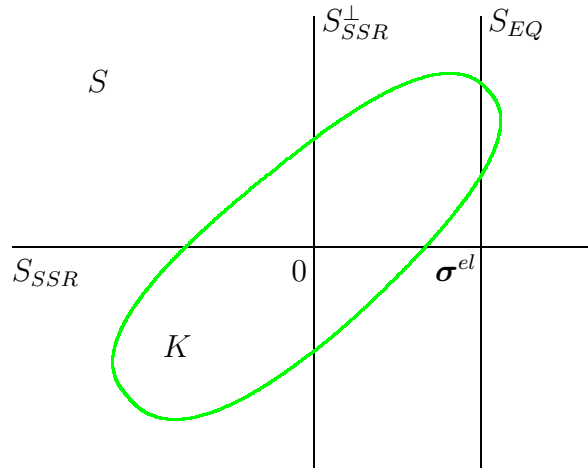
Figure 3.1: *The admissible set K and the stress space S with its subspaces S_{SSR} and $S_{SSR}^{\perp}$ and the affine space S_{EQ}.*

Assuming on the other hand perfect plastic material behavior we have to consider also the convex admissible set K. The solution stress $\boldsymbol{\sigma}^{pl}$ of the plastic problem has to fulfill the following two demands

$$\begin{aligned}(i) & \quad \boldsymbol{\sigma}^{pl} \in K , \\ (ii) & \quad \boldsymbol{\sigma}^{pl} \in S_{EQ} ,\end{aligned} \tag{3.55}$$

but it does not necessarily fulfill the *stress-strain-relationship* any more:

$$\boldsymbol{\sigma}^{pl} \;\neq\; \mathcal{C}\,\boldsymbol{\epsilon}(\mathbf{u}) .$$

This is due to the fact that in the plastic case the strain tensor $\boldsymbol{\epsilon}(\mathbf{u})$ has to be decomposed in an elastic part $\boldsymbol{\epsilon}^e$ and a plastic part $\boldsymbol{\epsilon}^p$

$$\boldsymbol{\epsilon}(\mathbf{u}) \;=\; \boldsymbol{\epsilon}^e(\mathbf{u}) \;+\; \boldsymbol{\epsilon}^p(\mathbf{u}) . \tag{3.56}$$
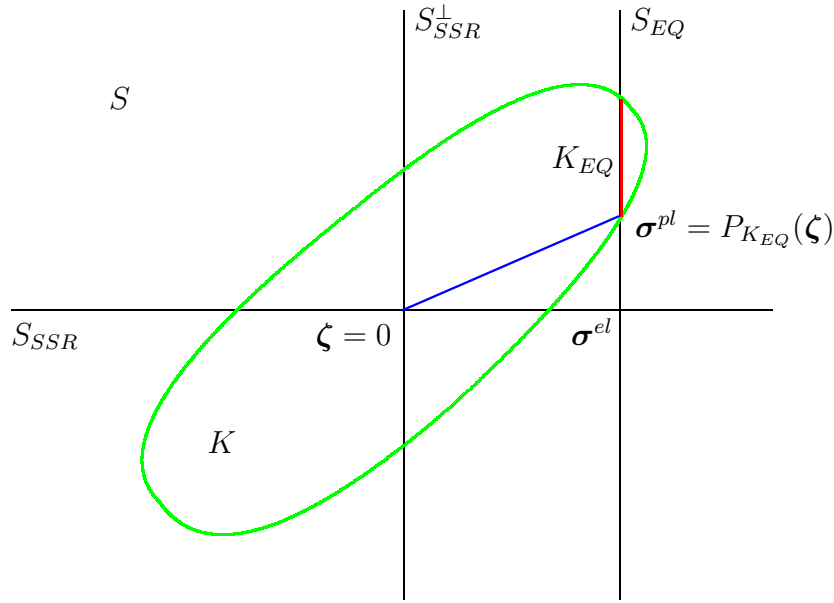
Figure 3.2: *The plastic solution $\boldsymbol{\sigma}^{pl}$ understood as the orthogonal (i.e. closest-point) projection of the zero stress $\boldsymbol{\zeta}$.*

The *stress-strain-relationship* describes an elastic material law and holds thus only true for the elastic strains:

$$\boldsymbol{\sigma}^{pl} = \mathcal{C}\,\boldsymbol{\epsilon}^{e}(\mathbf{u})\;. \tag{3.57}$$

From (3.55) we can deduce that the plastic problem has a solution if we have $K_{EQ} \neq \emptyset$, where we define the set K_{EQ} via

$$K_{EQ} := K \cap S_{EQ}\;.$$

Following the theory and notation of variational inequalities (a topic that we will only touch slightly; for further details we refer to e.g. [DL'76, Gl'84, SH'98]) we can formulate the plastic problem as finding a $\boldsymbol{\sigma}^{pl} \in K_{EQ}$ such that

$$(\boldsymbol{\sigma}^{pl}, \boldsymbol{\tau} - \boldsymbol{\sigma}^{pl})_S \geq 0 \qquad \forall\, \boldsymbol{\tau} \in K_{EQ}\;. \tag{3.58}$$

This problem can be solved by the use of a *closest point projection* $P_{K_{EQ}} : S \longrightarrow K_{EQ}$. Due to the convex nature of K_{EQ} such an orthogonal projection fulfills for $\boldsymbol{\tau} \in K_{EQ}$ and $\boldsymbol{\zeta} \in S$ the inequality (cf. Lemma 1.23)

$$(\boldsymbol{\zeta} - P_{K_{EQ}}(\boldsymbol{\zeta}), \boldsymbol{\tau} - P_{K_{EQ}}(\boldsymbol{\zeta}))_S \leq 0\;. \tag{3.59}$$

Both inequalities (3.58) and (3.59) are simultaneously true for only

$$\boldsymbol{\sigma}^{pl} = P_{K_{EQ}}(\boldsymbol{\zeta}) \quad \wedge \quad \boldsymbol{\zeta} = 0\;,$$

which yields us the stress solution of the plastic problem; this is shown in Figure 3.2.

This solution $\boldsymbol{\sigma}^{pl}$ can also be understood as the result of the orthogonal projection of a *trial stress* $\boldsymbol{\sigma}^{tr} \in S_{SSR}$ onto K as was mentioned several times before (cf. Figure 3.3). In this case we would have to formulate the plastic problem as finding a $\boldsymbol{\sigma}^{tr} \in S_{SSR}$ such that

$$(P_K(\boldsymbol{\sigma}^{tr}), \boldsymbol{\tau})_S \;=\; (\boldsymbol{\sigma}^{el}, \boldsymbol{\tau})_S \qquad \forall\, \boldsymbol{\tau} \in S_{SSR} \;, \tag{3.60}$$

which is of course a nonlinear problem.
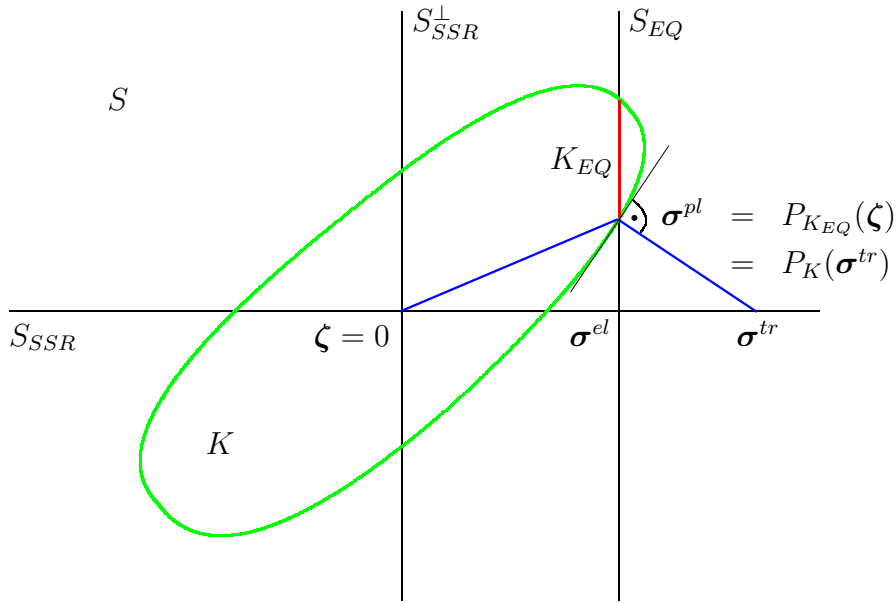
Figure 3.3: *The plastic solution $\boldsymbol{\sigma}^{pl}$ understood as the orthogonal projection of the trial stress $\boldsymbol{\sigma}^{tr}$.*

We will shortly show that the formulations (3.58) and (3.60) of the plastic problem are equivalent. Assuming that a solution $\boldsymbol{\sigma}^{tr}$ to (3.60) exists, we would have $P_K(\boldsymbol{\sigma}^{tr}) \in K$ and $P_K(\boldsymbol{\sigma}^{tr}) \in S_{EQ}$ and thus $P_K(\boldsymbol{\sigma}^{tr}) \in K_{EQ}$. Furthermore, as an orthogonal projection onto a convex set K the projection suffices the inequality (again see Lemma 1.23)

$$(\boldsymbol{\sigma}^{tr} - P_K(\boldsymbol{\sigma}^{tr}), \boldsymbol{\tau} - P_K(\boldsymbol{\sigma}^{tr}))_S \;\leq\; 0 \qquad \forall\, \boldsymbol{\tau} \in K \;. \tag{3.61}$$

Due to $\boldsymbol{\sigma}^{tr} \in S_{SSR}$ and $(\boldsymbol{\tau} - P_K(\boldsymbol{\sigma}^{tr})) \in S_{SSR}^{\perp}$ for $\boldsymbol{\tau} \in K_{EQ}$ we can simplify (3.61) to

$$(-P_K(\boldsymbol{\sigma}^{tr}), \boldsymbol{\tau} - P_K(\boldsymbol{\sigma}^{tr}))_S \;\leq\; 0 \qquad \forall\, \boldsymbol{\tau} \in K_{EQ} \;, \tag{3.62}$$

and finally to

$$(P_K(\boldsymbol{\sigma}^{tr}), \boldsymbol{\tau} - P_K(\boldsymbol{\sigma}^{tr}))_S \;\geq\; 0 \qquad \forall\, \boldsymbol{\tau} \in K_{EQ} \;, \tag{3.63}$$

which has the same form as (3.58). Thus, $P_K(\boldsymbol{\sigma}^{tr})$ is a solution to that variational inequality. On the other hand (3.58) has a unique solution $\boldsymbol{\sigma}^{pl}$ which yields $\boldsymbol{\sigma}^{pl} = P_K(\boldsymbol{\sigma}^{tr})$.

With these considerations we have justified the return mapping approach using an orthogonal projection P_K. The explicit form of P_K as presented in definition (3.49) will not be deduced here; for further details we refer to the literature, e.g. [SH'98, Wie1'99, Wie2'99].

It remains to find a reasonable variational approach for the plastic problem using the *PEERS* method. At this point we will give only a brief sketch of the proposed scheme that will be covered in detail in Section 4.2 where we present an efficient solution algorithm. The main idea of our scheme is depicted in Figure 3.4.
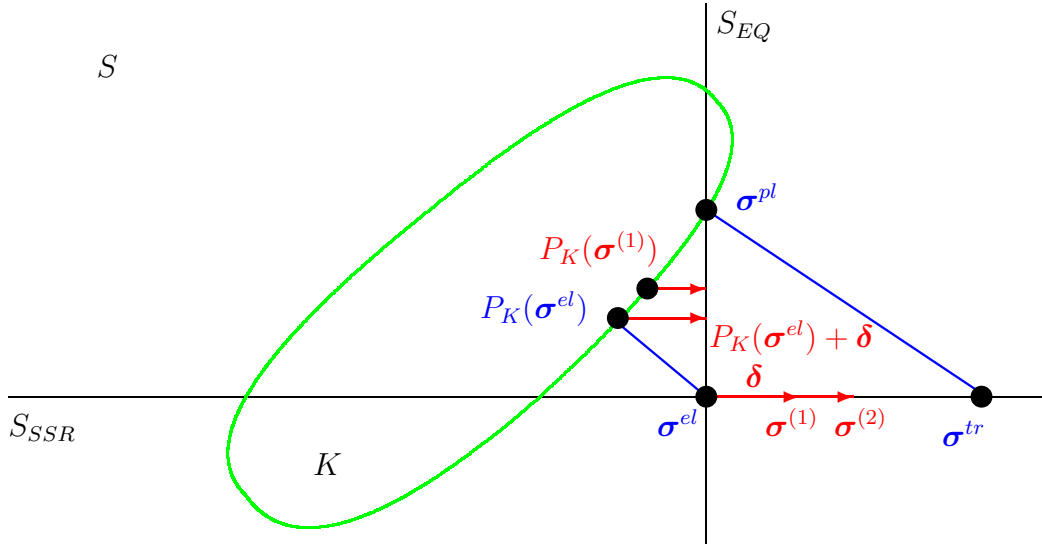

Figure 3.4: *Iterative approximation of the trial stress $\boldsymbol{\sigma}^{tr}$ starting from the solution $\boldsymbol{\sigma}^{el}$ of an assumed elastic problem.*

This approach starts with assumed mere linear elastic material behavior. After computing the stress solution $\boldsymbol{\sigma}^{el}$ of this elastic problem with the *PEERS* method from Section 3.3.3 one applies the projection P_K to $\boldsymbol{\sigma}^{el}$. If we are in the elastic range of the elastoplastic problem the projection is equal to the identity operator and we have solved the problem. Otherwise $P_K(\boldsymbol{\sigma}^{el})$ is an admissible stress but violates the equilibrium condition, e.g. $P_K(\boldsymbol{\sigma}^{el}) \notin S_{EQ}$. To correct this defect of $P_K(\boldsymbol{\sigma}^{el})$ we can solve the following variational problem for the triple $(\boldsymbol{\delta}, \mathbf{w}, \vartheta) \in H_{\Gamma_N}(\mathsf{div}, \Omega)^{2\times 2} \times L^2(\Omega)^2 \times L^2(\Omega)$:

$$(\mathcal{C}^{-1}\boldsymbol{\delta}, \boldsymbol{\tau})_{0,\Omega} \; + \; (\mathbf{w}, \mathsf{div}\,\boldsymbol{\tau})_{0,\Omega} \; + \; (\vartheta, \mathsf{as}\,\boldsymbol{\tau})_{0,\Omega} \;\; = \;\; 0 \qquad \forall\,\boldsymbol{\tau} \in H_{\Gamma_N}(\mathsf{div}, \Omega)^{2\times 2}\ ,$$

$$(\mathsf{div}\,(P_K(\boldsymbol{\sigma}^{el}) + \boldsymbol{\delta}), \mathbf{v})_{0,\Omega} \;\; = \;\; 0 \qquad \forall\,\mathbf{v} \in L^2(\Omega)^2\ , \qquad (3.64)$$

$$(\mathsf{as}\,(P_K(\boldsymbol{\sigma}^{el}) + \boldsymbol{\delta}), \eta)_{0,\Omega} \;\; = \;\; 0 \qquad \forall\,\eta \in L^2(\Omega)\ .$$

Note that we can solve this problem with the *PEERS* approach. Having computed the solution to (3.64) we can correct the solution of the assumed elastic problem $(\boldsymbol{\sigma}^{el}, \mathbf{u}^{el}, \gamma^{el})$

by adding $(\boldsymbol{\delta}, \mathbf{w}, \vartheta)$:

$$
\begin{bmatrix} \boldsymbol{\sigma}^{(1)} \\ \mathbf{u}^{(1)} \\ \gamma^{(1)} \end{bmatrix} = \begin{bmatrix} \boldsymbol{\sigma}^{el} \\ \mathbf{u}^{el} \\ \gamma^{el} \end{bmatrix} + \begin{bmatrix} \boldsymbol{\delta} \\ \mathbf{w} \\ \vartheta \end{bmatrix} , \tag{3.65}
$$

and we see that $\boldsymbol{\sigma}^{(1)}$ and $P_K(\boldsymbol{\sigma}^{(1)})$ are 'better approximations' to $\boldsymbol{\sigma}^{tr}$ and $\boldsymbol{\sigma}^{pl}$ respectively. Setting up an iterative scheme by alternately computing the projection P_K, solving a correction problem like (3.64) and updating $\boldsymbol{\sigma}^{el}$ as in (3.65) we can step by step approximate the *trial stress* and hence also the plastic solution as shown in Figure 3.4. In this way we solve a nonlinear problem by solving a sequence of linear problems with the *PEERS* mixed method and by evaluating an explicitly given projection formula. Note that the correction step via the solution of (3.64) can be understood as another projection onto the affine space S_{EQ}. However, in that projection one is in fact not interested in the solution of the projection but in the vector connecting the projection and the point that is projected.

We assume here a *static* problem of perfect plasticity, which means that we do not have to consider time dependencies that are usually encountered when dealing with plasticity. Instead we only examine the reaction of a material body subjected to a given constant surface traction $\mathbf{g}$. Depending on the scale of $\mathbf{g}$ the material body subjected to that traction reacts elastic or perfectly plastic. A slight modification of the *static* problem is the *quasi-static* one, where we increase the load implied by $\mathbf{g}$ step by step. In this case, there is also no real time dependency. Instead, in each load step increments of the variables have to be added up. A variational formulation of quasi-static perfect plasticity is therefore only an incremental modification of the systems presented in (3.47) and (3.64). Such a formulation will be used in Section 6.3, where we present numerical results for the proposed schemes in the quasi-static case of perfect elastoplasticity.

In the next chapter that will deal with efficient solution algorithms for the presented variational approaches we will also examine the algorithm sketched here in more detail and we will give a proof that in fact it converges to the true solution. However, before we consider these efficient solution procedures we have to make two important remarks. For the first remark we introduce the following definition:

Definition 3.4 (Safe-Load-Assumption) *We say that a plasticity problem satisfies the the 'safe-load assumption' if there exists an $\varepsilon > 0$ and an $\boldsymbol{\varsigma} \in K_{EQ}$ such that*

$$
(\boldsymbol{\varsigma} + \boldsymbol{\tau}) \in K \qquad \forall \, \boldsymbol{\tau} \in S \quad with \quad \| \boldsymbol{\tau} \|_S < \varepsilon \, .
$$

Remark 3.5 *The safe-load assumption guarantees that $K_{EQ} = K \cap S_{EQ}$ is not an empty set and furthermore contains more than one element. Otherwise we could encounter*

plasticity problems that can not be solved with the approach presented above. This fact can be seen best in Figure 3.5, where for S_{EQ}^1 the safe-load assumption is fulfilled while it is violated for S_{EQ}^2 and S_{EQ}^3. Thus, in this thesis we will always assume that the safe-load assumption is fulfilled in order to consider only well-posed problems. This assumption is reasonable and also motivated by the fact that in problems with very large loads we have to consider fracture and fatal damage effects such that the elastoplastic material model is not sufficient any more but has to be substituted by even more elaborate models.
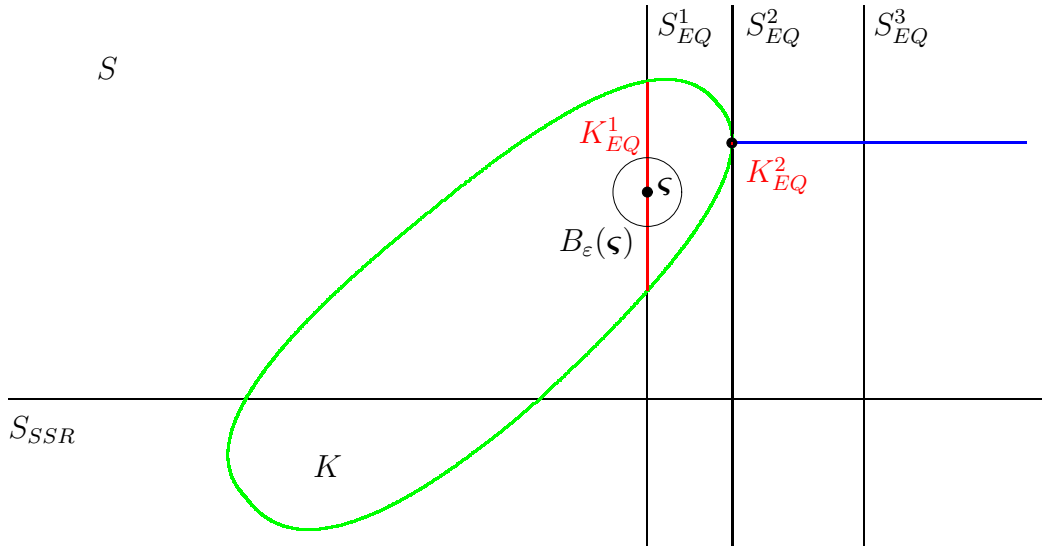
Figure 3.5: *The safe-load assumption is fulfilled for S_{EQ}^1; for S_{EQ}^2 the set K_{EQ}^2 contains only one element and thus the safe-load assumption is violated, while S_{EQ}^3 has no intersection with the admissible set at all.*

Remark 3.6 *Note that in this section the stress tensors were presented for simplicity of notation in a way that neglected the representation of the Neumann boundary conditions via the tensor $\boldsymbol{\sigma}^N \in H(\mathsf{div}, \Omega)^{2\times2}$. All considered stress tensors $\boldsymbol{\sigma} \in S_{SSR}$ have to be understood as $(\boldsymbol{\sigma} + \boldsymbol{\sigma}^N)$ and thus also a projection $P_K(\boldsymbol{\sigma})$ is meant to represent in fact $P_K(\boldsymbol{\sigma} + \boldsymbol{\sigma}^N)$. However, due to the nature of the benchmark problem for plasticity that we want to consider later on in Section 6.3 we can safely assume throughout the rest of this thesis that we have $\boldsymbol{\sigma}^N \equiv 0$ everywhere in the plastic range of the domain Ω and also $\boldsymbol{\sigma}^N \cdot \mathbf{n} \equiv 0$ on all inner and outer edges in the plastic region. This yields $P_K(\boldsymbol{\sigma} + \boldsymbol{\sigma}^N) = P_K(\boldsymbol{\sigma})$ as well as $P_K(\boldsymbol{\sigma} + \boldsymbol{\sigma}^N) \cdot \mathbf{n} = P_K(\boldsymbol{\sigma}) \cdot \mathbf{n}$ in the plastic region and justifies the above presented formulations. We will mention this simplification again in the setup of the benchmark problem.*

Chapter 4

Efficient Solution Methods for the *PEERS* Approach in Elastoplasticity

Finite element methods in general simplify infinite dimensional problems formulated as partial differential equations in the form of approximations given by finite dimensional problems. Those finite problems lead in the end often to 'simple' *linear* systems of equations. The main difficulty that we have to consider in the context of these systems is the fact that they usually consist of a very large number of equations. Problems in engineering science for example can easily have millions or even billions of unknowns and the resulting systems can exceed even the possibilities of today's computers. Furthermore, with growing computer power the scale of the problems we want to address is also growing. Hence it is very important to find efficient and fast solution algorithms for these systems of equations.

We have presented in the last chapter a short overview on some mixed finite element methods suitable for elasticity and even plasticity. We have seen that all these mixed methods are constraint minimization problems and we will see that the resulting linear systems of equations therefore resemble the saddle-point structure of such formulations. Solution algorithms for this kind of problems will have to take that into account in order to be efficient. Furthermore, we will have to address the *nonlinear* nature of the plasticity problem in detail. As presented in Section 3.4 we can formulate plasticity as a series of linear elasticity problems, but the iteration scheme to approximate the plastic solution has to be efficient, too. We will start our considerations as usual with the elastic problem and develop a solution algorithm based on *constraint preconditioning* for the *PEERS* formulation. This *preconditioner* will also be applied to elastic trial problems within a *fixed point iteration* scheme presented afterwards that will yield solutions for plasticity in an efficient way.

4.1   Iterative solvers for elasticity

We recall our discrete variational formulation of linear elasticity in the *PEERS* mixed method. We seek a triple $(\boldsymbol{\sigma}_h, \mathbf{u}_h, \gamma_h)$ in the ansatz space $S_h \times V_h \times Q_h$ as defined in (3.45) such that we have

$$
\begin{aligned}
(\mathcal{C}^{-1}(\boldsymbol{\sigma}^N + \boldsymbol{\sigma}_h), \boldsymbol{\tau}_h)_{0,\Omega} + (\mathbf{u}_h, \mathsf{div}\,\boldsymbol{\tau}_h)_{0,\Omega} + (\gamma_h, \mathsf{as}\,\boldsymbol{\tau}_h)_{0,\Omega} &= 0 \qquad \forall\, \boldsymbol{\tau}_h \in S_h \ , \\
(\mathsf{div}\,(\boldsymbol{\sigma}^N + \boldsymbol{\sigma}_h), \mathbf{v}_h)_{0,\Omega} &= 0 \qquad \forall\, \mathbf{v}_h \in V_h \ , \qquad (4.1) \\
(\mathsf{as}\,(\boldsymbol{\sigma}^N + \boldsymbol{\sigma}_h), \eta_h)_{0,\Omega} &= 0 \qquad \forall\, \eta_h \in Q_h \ .
\end{aligned}
$$

Due to the fact that the representation of the surface tractions $\boldsymbol{\sigma}^N$ is given we recast (4.1) as seeking $(\boldsymbol{\sigma}_h, \mathbf{u}_h, \gamma_h)$ such that

$$
\begin{aligned}
(\mathcal{C}^{-1}\boldsymbol{\sigma}_h, \boldsymbol{\tau}_h)_{0,\Omega} + (\mathbf{u}_h, \mathsf{div}\,\boldsymbol{\tau}_h)_{0,\Omega} + (\gamma_h, \mathsf{as}\,\boldsymbol{\tau}_h)_{0,\Omega} &= -(\mathcal{C}^{-1}\boldsymbol{\sigma}^N, \boldsymbol{\tau}_h)_{0,\Omega} \ , \\
(\mathsf{div}\,\boldsymbol{\sigma}_h, \mathbf{v}_h)_{0,\Omega} &= -(\mathsf{div}\,\boldsymbol{\sigma}^N, \mathbf{v}_h)_{0,\Omega} \ , \qquad (4.2) \\
(\mathsf{as}\,\boldsymbol{\sigma}_h, \eta_h)_{0,\Omega} &= -(\mathsf{as}\,\boldsymbol{\sigma}^N, \eta_h)_{0,\Omega} \ ,
\end{aligned}
$$

holds true for all $(\boldsymbol{\tau}_h, \mathbf{v}_h, \eta_h) \in S_h \times V_h \times Q_h$.

The ansatz functions $(\boldsymbol{\tau}_h, \mathbf{v}_h, \eta_h)$ and the solution functions $(\boldsymbol{\sigma}_h, \mathbf{u}_h, \gamma_h)$ are defined on each triangle T in the triangulation $\mathcal{T}_h$. The degrees of freedom of the solution on each triangle are the coefficients of $(\boldsymbol{\sigma}_h, \mathbf{u}_h, \gamma_h)$ in the related discrete space $S_h \times V_h \times Q_h$ while the ansatz functions are represented via the coefficients of the basis functions in $S_h \times V_h \times Q_h$. In this way we can understand the above equations on each triangle as a small system of linear equations which can as usual be understood as a matrix equation in the form

$$
\mathcal{A}_T \cdot \mathbf{x}_T = \mathbf{b}_T \ ,
$$

where $\mathcal{A}_T$ is the so-called *element stiffness matrix*. All these small linear systems for each element 'overlap' at the degrees of freedom on edges between triangles and thus, they form with an overall *stiffness matrix* $\mathcal{A}$ given by

$$
\mathcal{A} = \sum_{T \in \mathcal{T}_h} \mathcal{A}_T \ ,
$$

the large linear system that describes the whole problem on the domain Ω in the space $S_h \times V_h \times Q_h$:

$$
\mathcal{A} \cdot \mathbf{x} = \mathbf{b} \ . \tag{4.3}
$$

In our problem the structure of the matrix $\mathcal{A}$ resembles the effects of the operators div and as and of the compliance tensor $\mathcal{C}^{-1}$ dominating it, while the right-hand side $\mathbf{b}$ is

only filled with entries originating from the surface tractions represented through $\boldsymbol{\sigma}^N$ as in (4.2). The solution triple $(\boldsymbol{\sigma}_h, \mathbf{u}_h, \gamma_h)$ is of course represented by $\mathbf{x}$. We write equation (4.3) more detailed in the following block matrix form, which we will use later on:

$$\underbrace{\begin{bmatrix} A & B^T & C^T \\ B & 0 & 0 \\ C & 0 & 0 \end{bmatrix}}_{\mathcal{A}} \underbrace{\begin{bmatrix} \boldsymbol{\sigma}_h \\ \mathbf{u}_h \\ \gamma_h \end{bmatrix}}_{\mathbf{x}} = \underbrace{\begin{bmatrix} \mathbf{b}_{\boldsymbol{\sigma}} \\ \mathbf{b}_{\mathbf{u}} \\ \mathbf{b}_{\gamma} \end{bmatrix}}_{\mathbf{b}} . \tag{4.4}$$

In the matrix $\mathcal{A}$ the block $A \in \mathbb{R}^{n \times n}$ is a non-singular symmetric positive definite matrix originating from the compliance tensor $\mathcal{C}^{-1}$ and the ansatz space S_h while the matrices $B \in \mathbb{R}^{m_1 \times n}$ and $C \in R^{m_2 \times n}$ are of full rank and represent the divergence and the antisymmetric operator on the ansatz spaces V_h and Q_h. Note that thus equation (4.4) is obviously an indefinite linear system.

As mentioned in the preface of this chapter linear systems as e.g. (4.4) are usually very large when we consider engineering problems and this is also true for linear elasticity. The linear systems arising from our *PEERS* method will be so large that any *direct solver* (as e.g. the *Gaussian Elimination Algorithm* and its modifications, however efficient they may be) is not competitive any more. Instead of a direct solver we use *iterative solvers* to compute the solution to such linear systems. These methods start with an initial guess of the solution and modify it step by step, thus approximating the true solution to a given tolerance. Generally, we can distinguish between two different kinds of iterative methods: *relaxation methods* and *Krylov subspace methods*. Relaxation methods are based on the following approach: given a system of the form

$$A x = b , \tag{4.5}$$

we decompose the system matrix A

$$A = P - N ,$$

where P has to be non-singular and 'easy-to-invert'. With this notation the iteration scheme is of the form

$$x^{(k+1)} = x^{(k)} + P^{-1} \left(b - A x^{(k)} \right) .$$

Methods of this form are also not the most competitive solution algorithms for very large linear systems due to the fact that they usually need a large number of iteration steps to approximate the solution with reasonable accuracy. However, these methods usually reduce the error $e^{(k)} = \| x - x^{(k)} \|$ very fast in their first two or three iterations before they 'slow down' significantly. This is the reason why these schemes are extensively used in *multilevel approaches* where one is interested in such effects (cf. e.g. [Ge'00]). Krylov

subspace methods on the other hand construct the approximation to the true solution via orthogonal projections onto spaces of the form

$$\mathcal{K}_m(\mathcal{A}, \mathbf{b}) \; := \; \text{span}\{\mathbf{b}, \, \mathcal{A}\,\mathbf{b}, \, \mathcal{A}^2\,\mathbf{b}, \, \dots, \, \mathcal{A}^{m-1}\,\mathbf{b}\} \, ,$$

which is called the *Krylov subspace of order m*. The most common Krylov subspace methods are the method of *conjugate gradients (CG)*, the method of *minimum residuals (MINRES)* and the method of *generalized minimum residuals (GMRES)*, while each of these methods exists in diverse modifications and closely related sub-methods that are especially tuned for one or another class of problems. Generally, the *CG* method is appropriate for symmetric positive definite problems and can be applied to indefinite problems only when modified. *MINRES* on the other hand only requires symmetric problems and deals well with indefinite problems, while *GMRES* does not even require a symmetric nature of the problem. The main advantage of these methods is the fact that the initial guess of the solution is updated through the orthogonal projection in such way that in each iteration step a 'component' of the approximate solution is fitted to the true solution. Therefore, the solution of a system of size n is computed in maximally n iteration steps. However, n iteration steps carried out for very large linear systems requires still too much computational resources and is not efficient, which leads to the technique of *preconditioning*. The idea of this approach is to multiply the system (4.5) with the inverse of an 'easy-to-invert' *preconditioner G* leading to

$$G^{-1}\,A\,x \; = \; G^{-1}\,b \, . \tag{4.6}$$

Here, G should also be some simplified approximation of the matrix A such that the preconditioned matrix $G^{-1}\,A$ has improved spectral properties, i.e. that the eigenvalues of $G^{-1}\,A$ are clustered within only small intervals. This reduces substantially the number of iterations needed in the related Krylov subspace method.

Parallel to the so-called *constraint preconditioner* proposed in the following section another efficient solution method for the *PEERS* formulation of linear elasticity was developed: a block preconditioner that uses multi-level preconditioning techniques for the stress-related block A in the system (4.4). Finally the developed block preconditioner was applied within a *MINRES* scheme to solve the indefinite problem (4.2). For details concerning this method we refer to [KS'04]. Further material about iterative solution methods in general can be found in the literature, e.g. in [Me'99, QSS'02].

4.1.1   Constraint preconditioning

In this section we present a reasonable preconditioner for the saddle-point structured problem (4.4) following an approach proposed in [KGW'00]. This approach uses precon-

ditioners that preserve the general saddle-point pattern of the linear elasticity formulations (4.1) and (4.2) which is due to the constraints represented by the matrices B and C in (4.4). The idea for this method is based on earlier work on *quadratic programming problems* that lead also to indefinite linear systems; this work can be found e.g. in [Co'94, GHN'98, LV'98].

To represent the same structure as in $\mathcal{A}$ from (4.4) we choose a preconditioner $\mathcal{G}$ of the following form

$$\mathcal{G} \;=\; \left[\begin{array}{ccc} G & B^T & C^T \\ B & 0 & 0 \\ C & 0 & 0 \end{array} \right] \;, \tag{4.7}$$

where G has to be an 'easy-to-invert' approximation of the block matrix $A \in \mathbb{R}^{n \times n}$ from (4.4). The preconditioned version of (4.3) now reads

$$\mathcal{G}^{-1} \mathcal{A} \cdot \mathbf{x} \;=\; \mathcal{G}^{-1} \mathbf{b} \;. \tag{4.8}$$

It is useful to keep the matrix blocks $B \in \mathbb{R}^{m_1 \times n}$ and $C \in R^{m_2 \times n}$ unchanged in our preconditioner $\mathcal{G}$. They characterize the constraints and the nature of the ansatz space $S_h \times V_h \times Q_h$ from definition (3.45) yields that $m = m_1 + m_2$ is significantly smaller than n. Thus, the computation of the inverse $\mathcal{G}^{-1}$ which is necessary for (4.8) should not be complicated much by these matrix blocks. Due to the constraint terms that are still present in the preconditioner this approach is called *constraint preconditioning*. In [KGW'00] the eigenvalue and eigenvector properties of the preconditioned matrix $\mathcal{G}^{-1}\mathcal{A}$ are closely examined. The detailed analysis there shows that the method of constraint preconditioning yields a favorable eigenvalue distribution. Furthermore, [KGW'00] yields also convergence results for the *GMRES* method: the iteration scheme will reach the solution (up to a given tolerance) in at most $n - m + 2$ iteration steps. We will skip details of the analysis and the proofs here and refer the interested reader to the paper [KGW'00]. However, we have yet to examine the nature of the 'approximation' G to the block A. The more the matrix G resembles the structure of A the better are eigenvalue distribution of $\mathcal{G}^{-1}\mathcal{A}$ and convergence behavior of the Krylov subspace method but the computation of $\mathcal{G}^{-1}$ will also be much more complex. That is why in this thesis we will consider G to be the main diagonal D of A.

4.1.2 Implementation of a constraint preconditioner

Having decided about the detailed form of the preconditioner $\mathcal{G}$ we can address implementation issues of such a preconditioner. We will give some short notes on this topic

here. For simplicity of notation we join B and C in a matrix $\bar{B}$,

$$\bar{B} := \begin{bmatrix} B \\ C \end{bmatrix} ,$$

and thus, $\mathcal{G}$ is of the form

$$\mathcal{G} = \begin{bmatrix} D & \bar{B}^T \\ \bar{B} & 0 \end{bmatrix} .$$

In this notation we can split $\mathcal{G}$ into the matrix product

$$\begin{bmatrix} D & \bar{B}^T \\ \bar{B} & 0 \end{bmatrix} = \begin{bmatrix} I & 0 \\ \bar{B}D^{-1} & I \end{bmatrix} \cdot \begin{bmatrix} D & 0 \\ 0 & -\bar{B}D^{-1}\bar{B}^T \end{bmatrix} \cdot \begin{bmatrix} I & D^{-1}\bar{B}^T \\ 0 & I \end{bmatrix} , \qquad (4.9)$$

where $\bar{B}D^{-1}\bar{B}^T$ is the so-called *Schur-complement*. For an implementation of an preconditioned iterative solver we need the inverse of $\mathcal{G}$ and thus the inverse to the three matrices on the right-hand side of (4.9). The two triangular matrices,

$$\begin{bmatrix} I & 0 \\ \bar{B}D^{-1} & I \end{bmatrix} ,$$

and its transpose are easy to invert due to their triangular nature. Only the Schur-complement poses problems: direct computation of the inverse of $\bar{B}D^{-1}\bar{B}^T$ would be too costly. A reasonable approach to this problem is the *Cholesky factorization*,

$$R^T R = \bar{B}D^{-1}\bar{B}^T ,$$

of the Schur-complement, where R is an upper triangular matrix. In this step, it is also necessary to reorder the rows and columns in $\bar{B}D^{-1}\bar{B}^T$ to get a sparser Cholesky factor R which significantly reduces the needed processor time and the number of floating point operations used in the Cholesky algorithm. Having finally computed the factorization $R^T R$ we can recast (4.9) as

$$\mathcal{G} = M_1 M_2 := \begin{bmatrix} D & 0 \\ \bar{B} & -R^T \end{bmatrix} \cdot \begin{bmatrix} I & D^{-1}\bar{B}^T \\ 0 & R \end{bmatrix} . \qquad (4.10)$$

Both factors M_1 and M_2 in (4.10) are as triangular matrices quite easy to invert and hence are fulfilling our demands for a reasonable preconditioner. We apply this preconditioner in the *GMRES* method which was the iterative solver of choice for our discretized *PEERS* problem. Numerical data describing in detail the behavior of the preconditioned solver for the elasticity problem can be found in Section 6.2. We conclude this section with the remark that the considerations and results of this section as well as some of the numerical data concerning the solver are already published in [Ge'03].

4.2 A fixed point iteration scheme for plasticity

We presented in the Sections 2.3 and 3.4 the general concept of static and quasi-static perfect plasticity problems and their solution via the return mapping procedure and also a variational approach for this procedure based on an iteration scheme, respectively. In this section we will take a closer look at the return mapping and develop a related solution method based on a *fixed point iteration scheme*. First, we shortly recall some basic formulae. The solution $\boldsymbol{\sigma}^{pl} \in H_{\Gamma_N}(\mathsf{div}, \Omega)^{2\times 2}$ of a static perfect plasticity problem with *von-Mises flow rule* and vanishing volume force $\mathbf{f}$ has to fulfill the following demands:

$$
\begin{aligned}
\mathcal{C}^{-1}(\boldsymbol{\sigma}^{pl} + \boldsymbol{\sigma}^{N}) &= \boldsymbol{\epsilon}^{e}(\mathbf{u}) && \text{on } \Omega \ , \\
\mathsf{div}\,(\boldsymbol{\sigma}^{pl} + \boldsymbol{\sigma}^{N}) &= 0 && \text{on } \Omega \ , \\
\mathsf{as}\,(\boldsymbol{\sigma}^{pl} + \boldsymbol{\sigma}^{N}) &= 0 && \text{on } \Omega \ , \\
\mathbf{u} &= 0 && \text{on } \Gamma_D \ , \\
P_K(\boldsymbol{\sigma}^{N}) \cdot \mathbf{n} &= \mathbf{g} && \text{on } \Gamma_N \ , \\
\boldsymbol{\sigma}^{pl} &\in K && \text{on } \Omega \ .
\end{aligned}
\tag{4.11}
$$

Here, $\boldsymbol{\epsilon}^{e}(\mathbf{u})$ represents the elastic strains from decomposition (3.56) and equation (3.57) while K is the admissible set of all $\boldsymbol{\sigma} \in H_{\Gamma_N}(\mathsf{div}, \Omega)^{2\times 2}$ that fulfill

$$
\| \mathsf{dev}\,\boldsymbol{\sigma} \|_F \ \leq \ \sqrt{\frac{2}{3}}\ \sigma^{\star} \qquad \text{a.e. in } \Omega
\tag{4.12}
$$

with a material dependent yield stress $\sigma^{\star} \in \mathbb{R}$. Note that we still consider a 3D model reduced to a 2D problem by the additional assumption of a plane strain condition (cf. Section 2.2) which means the strain tensor $\boldsymbol{\epsilon}$ is of the form

$$
\boldsymbol{\epsilon} \ = \ \begin{bmatrix} \epsilon_{xx} & \epsilon_{xy} & 0 \\ \epsilon_{yx} & \epsilon_{yy} & 0 \\ 0 & 0 & 0 \end{bmatrix} \ ,
$$

which leads to a stress tensor[1]

$$
\boldsymbol{\sigma} \ = \ \begin{bmatrix} \sigma_{xx} & \sigma_{xy} & 0 \\ \sigma_{yx} & \sigma_{yy} & 0 \\ 0 & 0 & \sigma_{zz} \end{bmatrix} \ .
$$

---

[1] Contrary to equation (2.10) the strain tensor and the stress tensor are written here in a non-symmetric way. This is due to the fact that the symmetry of these tensors is not enforced via the chosen spaces but via the additional equation for the anti-symmetric part which can lead to a non-symmetric $\boldsymbol{\sigma}$ in the variational setting.

The reduction to 2D is possible because in this case σ_{zz} is implicitly given in terms of σ_{xx} and σ_{yy} as

$$\sigma_{zz} \;=\; \nu \left(\sigma_{xx} + \sigma_{yy} \right) . \tag{4.13}$$

Thus, for our purposes it suffices to understand $\boldsymbol{\epsilon}$ and $\boldsymbol{\sigma}$ only as

$$\boldsymbol{\epsilon} \;=\; \begin{bmatrix} \epsilon_{xx} & \epsilon_{xy} \\[4pt] \epsilon_{yx} & \epsilon_{yy} \end{bmatrix} \qquad \text{and} \qquad \boldsymbol{\sigma} \;=\; \begin{bmatrix} \sigma_{xx} & \sigma_{xy} \\[4pt] \sigma_{yx} & \sigma_{yy} \end{bmatrix} .$$

Plastic effects however are a three-dimensional problem as the formula for the deviatoric part of $\boldsymbol{\sigma}$ indicates:

$$\mathsf{dev}\,\boldsymbol{\sigma} \;:=\; \boldsymbol{\sigma} - \frac{1}{3}\,\mathsf{tr}\,\boldsymbol{\sigma}\,\mathcal{I} . \tag{4.14}$$

The deviator depends on the dimension of the problem via the factor with which the trace part is weighted. Due to the fact that $\mathsf{dev}\,\boldsymbol{\sigma}$ is the criterion whether a stress is elastic or plastic we have to compute it in its (3×3)-tensor form:

$$\mathsf{dev}\,\boldsymbol{\sigma} \;=\; \frac{1}{3} \begin{bmatrix} 2\,\sigma_{xx} - \sigma_{yy} - \sigma_{zz} & 3\,\sigma_{xy} & 0 \\[6pt] 3\,\sigma_{yx} & 2\,\sigma_{yy} - \sigma_{xx} - \sigma_{zz} & 0 \\[6pt] 0 & 0 & 2\,\sigma_{zz} - \sigma_{xx} - \sigma_{yy} \end{bmatrix} .$$

With (4.13) we therefore get

$$\mathsf{dev}\,\boldsymbol{\sigma} \;=\; \frac{1}{3} \begin{bmatrix} (2-\nu)\sigma_{xx} - (1+\nu)\sigma_{yy} & 3\,\sigma_{xy} & 0 \\[6pt] 3\,\sigma_{yx} & (2-\nu)\sigma_{yy} - (1+\nu)\sigma_{xx} & 0 \\[6pt] 0 & 0 & (2\,\nu - 1)(\sigma_{xx} + \sigma_{yy}) \end{bmatrix} .$$

Considering the orthogonal projection P_K from Section 3.4 which has the form

$$\boldsymbol{\sigma}^{pl} \;=\; P_K(\boldsymbol{\sigma}^{tr}) \;=\; \boldsymbol{\sigma}^{tr} - \max\{0\,;\, \|\,\mathsf{dev}\,\boldsymbol{\sigma}^{tr}\,\|_F - \sqrt{\tfrac{2}{3}}\,\sigma^\star\}\,\frac{\mathsf{dev}\,\boldsymbol{\sigma}^{tr}}{\|\,\mathsf{dev}\,\boldsymbol{\sigma}^{tr}\,\|_F} \tag{4.15}$$

it is obvious that we have to compute also the zz-component of $\boldsymbol{\sigma}^{pl}$, which is of course still implicitly given by σ_{xx}^{tr} and σ_{yy}^{tr}. Computing $\mathsf{dev}\,\boldsymbol{\sigma}$ as the above (3×3)-tensor and inserting it in (4.15) yields in the plastic case

$$\boldsymbol{\sigma}_{zz}^{pl} \;=\; \frac{1}{3} \left(\sigma_{xx}^{tr} + \sigma_{yy}^{tr} \right)$$

$$\left[\nu + 1 + \sqrt{\frac{((2\,\nu - 1)\,\sigma^\star)^2}{3\,(\boldsymbol{\sigma}_{xy}^{tr})^2 + (1 - \nu + \nu^2)((\sigma_{xx}^{tr})^2 + (\sigma_{yy}^{tr})^2) - (1 - 2\,\nu + 2\,\nu^2)\sigma_{xx}^{tr}\sigma_{yy}^{tr}}} \right] .$$

After considering these formulae that describe the orthogonal projection we can now start a closer examination of the iterative algorithm we have in mind.

4.2.1 The iterative algorithm

The idea to the iterative scheme we want to set up was presented in Section 3.4 and can intuitively be best understood by considering Figure 3.4. In each iterative step k we want to solve the indefinite problem (3.64) that we will recall here in a slightly different form. Given an approximation $(\boldsymbol{\sigma}^{(k-1)}, \mathbf{u}^{(k-1)}, \gamma^{(k-1)})$ to $(\boldsymbol{\sigma}^{pl}, \mathbf{u}^{pl}, \gamma^{pl})$ we seek a triple $(\boldsymbol{\delta}^{(k)}, \mathbf{w}^{(k)}, \vartheta^{(k)}) \in H_{\Gamma_N}(\text{div}, \Omega)^{2\times 2} \times L^2(\Omega)^2 \times L^2(\Omega)$ such that

$$(\mathcal{C}^{-1}\boldsymbol{\delta}^{(k)}, \boldsymbol{\tau})_{0,\Omega} + (\mathbf{w}^{(k)}, \text{div}\,\boldsymbol{\tau})_{0,\Omega} + (\vartheta^{(k)}, \text{as}\,\boldsymbol{\tau})_{0,\Omega} = 0 ,$$
$$(\text{div}\,\boldsymbol{\delta}^{(k)}, \mathbf{v})_{0,\Omega} = -(\text{div}\,P_K(\boldsymbol{\sigma}^{(k-1)}), \mathbf{v})_{0,\Omega} , \quad (4.16)$$
$$(\text{as}\,\boldsymbol{\delta}^{(k)}, \eta)_{0,\Omega} = -(\text{as}\,P_K(\boldsymbol{\sigma}^{(k-1)}), \eta)_{0,\Omega} ,$$

holds true for all triples $(\boldsymbol{\tau}, \mathbf{v}, \eta) \in H_{\Gamma_N}(\text{div}, \Omega)^{2\times 2} \times L^2(\Omega)^2 \times L^2(\Omega)$. The new approximation $(\boldsymbol{\sigma}^{(k)}, \mathbf{u}^{(k)}, \gamma^{(k)})$ is finally computed as

$$\begin{bmatrix} \boldsymbol{\sigma}^{(k)} \\ \mathbf{u}^{(k)} \\ \gamma^{(k)} \end{bmatrix} := \begin{bmatrix} \boldsymbol{\sigma}^{(k-1)} \\ \mathbf{u}^{(k-1)} \\ \gamma^{(k-1)} \end{bmatrix} + \begin{bmatrix} \boldsymbol{\delta}^{(k)} \\ \mathbf{w}^{(k)} \\ \vartheta^{(k)} \end{bmatrix} \quad \text{and} \quad \begin{bmatrix} \boldsymbol{\sigma}^{(0)} \\ \mathbf{u}^{(0)} \\ \gamma^{(0)} \end{bmatrix} := \begin{bmatrix} \boldsymbol{\sigma}^{el} \\ \mathbf{u}^{el} \\ \gamma^{el} \end{bmatrix} , \quad (4.17)$$

where $(\boldsymbol{\sigma}^{el}, \mathbf{u}^{el}, \gamma^{el})$ is the solution of an auxiliary elastic problem in the form of (3.47) that holds true for all $(\boldsymbol{\tau}, \mathbf{v}, \eta) \in H_{\Gamma_N}(\text{div}, \Omega)^{2\times 2} \times L^2(\Omega)^2 \times L^2(\Omega)$:

$$(\mathcal{C}^{-1}(\boldsymbol{\sigma}^N + \boldsymbol{\sigma}^{el}), \boldsymbol{\tau})_{0,\Omega} + (\mathbf{u}^{el}, \text{div}\,\boldsymbol{\tau})_{0,\Omega} + (\gamma^{el}, \text{as}\,\boldsymbol{\tau})_{0,\Omega} = 0 ,$$
$$(\text{div}\,(\boldsymbol{\sigma}^N + \boldsymbol{\sigma}^{el}), \mathbf{v})_{0,\Omega} = 0 , \quad (4.18)$$
$$(\text{as}\,(\boldsymbol{\sigma}^N + \boldsymbol{\sigma}^{el}), \eta)_{0,\Omega} = 0 .$$

Such an iterative approximation scheme is indeed a *fixed point iteration*. This can be seen by rewriting the linear systems above as an iteration rule for the computation of the next iterate $(\boldsymbol{\sigma}^{(k+1)}, \mathbf{u}^{(k+1)}, \gamma^{(k+1)})$. Consequently, we get the equations

$$(\mathcal{C}^{-1}(\boldsymbol{\sigma}^N + \boldsymbol{\sigma}^{(k+1)}), \boldsymbol{\tau})_{0,\Omega} = -(\mathbf{u}^{(k+1)}, \text{div}\,\boldsymbol{\tau})_{0,\Omega} - (\gamma^{(k+1)}, \text{as}\,\boldsymbol{\tau})_{0,\Omega} ,$$
$$(\text{div}\,(\boldsymbol{\sigma}^N + \boldsymbol{\sigma}^{(k+1)}), \mathbf{v})_{0,\Omega} = (\text{div}\,(\boldsymbol{\sigma}^N + \boldsymbol{\sigma}^{(k)}), \mathbf{v})_{0,\Omega} - (\text{div}\,P_K(\boldsymbol{\sigma}^{(k)}), \mathbf{v})_{0,\Omega} , \quad (4.19)$$
$$(\text{as}\,(\boldsymbol{\sigma}^N + \boldsymbol{\sigma}^{(k+1)}), \eta)_{0,\Omega} = (\text{as}\,(\boldsymbol{\sigma}^N + \boldsymbol{\sigma}^{(k)}), \eta)_{0,\Omega} - (\text{as}\,P_K(\boldsymbol{\sigma}^{(k)}), \eta)_{0,\Omega} ,$$

that have to hold true for all $(\boldsymbol{\tau}, \mathbf{v}, \eta) \in H_{\Gamma_N}(\text{div}, \Omega)^{2\times 2} \times L^2(\Omega)^2 \times L^2(\Omega)$. The system (4.19) can be deduced easily from (4.16), (4.17) and (4.18). The first part of (4.19) follows directly from the rule (4.17), the first equation of the system (4.18) and the fact that it is

$$(\mathcal{C}^{-1}\boldsymbol{\delta}^{(k)}, \boldsymbol{\tau})_{0,\Omega} + (\mathbf{w}^{(k)}, \text{div}\,\boldsymbol{\tau})_{0,\Omega} + (\vartheta^{(k)}, \text{as}\,\boldsymbol{\tau})_{0,\Omega} = 0 \qquad \forall\, k \in \mathbb{N} .$$

Analogously, the other two equations are a result of a straightforward application of (4.17) and (4.16). Examining (4.19) we realize that the trial triple $(\boldsymbol{\sigma}^{tr}, \mathbf{u}^{tr}, \gamma^{tr})$ is a fixed point of this iteration – and furthermore the only one – due to

$$
\begin{aligned}
(\operatorname{div} P_K(\boldsymbol{\sigma}^{tr}), \mathbf{v})_{0,\Omega} &= (\operatorname{div} \boldsymbol{\sigma}^{pl}, \mathbf{v})_{0,\Omega} &= 0 \,, \\
(\operatorname{as} P_K(\boldsymbol{\sigma}^{tr}), \eta)_{0,\Omega} &= (\operatorname{as} \boldsymbol{\sigma}^{pl}, \eta)_{0,\Omega} &= 0 \,,
\end{aligned}
\tag{4.20}
$$

and due to the nature of the plastic problem and the orthogonal projection presented in Section 3.4 and depicted e.g. in Figure 3.3.

It remains to prove convergence of the proposed method; this topic will be examined closely in the next section of this chapter. However, before this analysis we have to formulate a discrete version of the presented variational problems and the iteration rule. In this context we also have to discuss the nature of the two terms

$$
(\operatorname{div} P_K(\boldsymbol{\sigma}^{(k)}), \mathbf{v})_{0,\Omega} \qquad \text{and} \qquad (\operatorname{as} P_K(\boldsymbol{\sigma}^{(k)}), \eta)_{0,\Omega} \,.
\tag{4.21}
$$

We begin with the term describing the anti-symmetric part; it is

$$
\begin{aligned}
\operatorname{as} P_K(\boldsymbol{\sigma}^{(k)}) &= \operatorname{as}\left(\boldsymbol{\sigma}^{(k)} - \operatorname{dev} \boldsymbol{\sigma}^{(k)} + \sqrt{\frac{2}{3}}\, \frac{\sigma^\star \operatorname{dev} \boldsymbol{\sigma}^{(k)}}{\| \operatorname{dev} \boldsymbol{\sigma}^{(k)} \|_F} \right) \\
&= \operatorname{as}\left(\sqrt{\frac{2}{3}}\, \frac{\sigma^\star \operatorname{dev} \boldsymbol{\sigma}^{(k)}}{\| \operatorname{dev} \boldsymbol{\sigma}^{(k)} \|_F} \right) \\
&= \sqrt{\frac{2}{3}}\, \frac{\sigma^\star}{\| \operatorname{dev} \boldsymbol{\sigma}^{(k)} \|_F}\, \operatorname{as} \boldsymbol{\sigma}^{(k)} \,.
\end{aligned}
$$

Consequently we get

$$
(\operatorname{as} \boldsymbol{\sigma}^{(k)}, \eta)_{0,\Omega} = 0 \qquad \Longrightarrow \qquad (\operatorname{as} P_K(\boldsymbol{\sigma}^{(k)}), \eta)_{0,\Omega} = 0 \qquad \forall\, \eta \in L^2(\Omega) \,.
\tag{4.22}
$$

The solution of our variational problems yields $(\operatorname{as} \boldsymbol{\sigma}^{(k)}, \eta)_{0,\Omega} = 0$ for all $\eta \in L^2(\Omega)$; hence also $(\operatorname{as} P_K(\boldsymbol{\sigma}^{(k)}), \eta)_{0,\Omega}$ is vanishing for all such η and can be neglected.

The term describing the divergence of $\boldsymbol{\sigma}^{(k)}$ on the other hand is more complicate to deal with. Note that

$$
\boldsymbol{\sigma}^{(k)} \in H_{\Gamma_N}(\operatorname{div}, \Omega)^{2\times 2} \qquad \nRightarrow \qquad P_K(\boldsymbol{\sigma}^{(k)}) \in H_{\Gamma_N}(\operatorname{div}, \Omega)^{2\times 2}
\tag{4.23}
$$

due to the nonlinear form of P_K. Nevertheless, given a triangulation $\mathcal{T}_h$ on Ω we have on each element $T \in \mathcal{T}_h$

$$
P_K(\boldsymbol{\sigma}^{(k)}) \in H(\operatorname{div}, T)^{2\times 2} \,,
$$

and we can compute the divergence of $P_K(\boldsymbol{\sigma}^{(k)})$ locally on each triangle via

$$
\begin{aligned}
(\operatorname{div} P_K(\boldsymbol{\sigma}^{(k)}), \boldsymbol{\chi}_T)_{0,T} &= \int_T \operatorname{div} P_K(\boldsymbol{\sigma}^{(k)})\, dx \\
&= \int_{\partial T} P_K(\boldsymbol{\sigma}^{(k)}) \cdot \mathbf{n}\, dx \\
&= \sum_{E \subset \partial T} P_K(\boldsymbol{\sigma}^{(k)}) \cdot \mathbf{n} \bigg|_{m_E} \cdot h_E \, ,
\end{aligned}
\tag{4.24}
$$

with $\boldsymbol{\chi}_T \in V_h$ being the characteristic function on the element T and m_E being the edge midpoint of E. Obviously, this representation of $P_K(\boldsymbol{\sigma}^{(k)})$ leads to jumps in the normal component of the stress on an edge E if we consider $P_K(\boldsymbol{\sigma}^{(k)})$ first on the left-hand side triangle $T_{E,l}$ of E and then on the right-hand side triangle $T_{E,r}$. We define this jump of $P_K(\boldsymbol{\sigma}^{(k)})$ on a given edge E through

$$
\left[P_K(\boldsymbol{\sigma}^{(k)}) \cdot \mathbf{n} \right] := \left(P_K(\boldsymbol{\sigma}^{(k)})\big|_{T_{E,l}} - P_K(\boldsymbol{\sigma}^{(k)})\big|_{T_{E,r}} \right) \cdot \mathbf{n} \, .
\tag{4.25}
$$

Let $\mathcal{E}_h$ be the set of all edges related to the triangulation $\mathcal{T}_h$. If we assume that we have no jumps in $P_K(\boldsymbol{\sigma}^{(k)})$ at all, i.e.

$$
\left(\left[P_K(\boldsymbol{\sigma}^{(k)}) \cdot \mathbf{n} \right], \mathbf{v} \right)_{0,E} = 0 \qquad \forall\, E \in \mathcal{E}_h \, , \mathbf{v} \in V_h \, ,
\tag{4.26}
$$

we deduce the following important statement that holds for all $\mathbf{v} \in V_h$:

$$
(4.26) \quad \Longrightarrow \quad (\operatorname{div} P_K(\boldsymbol{\sigma}^{(k)}), \mathbf{v})_{0,\Omega} = \sum_{T \in \mathcal{T}_h} (\operatorname{div} P_K(\boldsymbol{\sigma}^{(k)}), \boldsymbol{\chi}_T)_{0,T} \, .
\tag{4.27}
$$

This means in other words that we get $P_K(\boldsymbol{\sigma}^{(k)}) \in H_{\Gamma_N}(\operatorname{div}, \Omega)^{2 \times 2}$ under the assumption of vanishing jump terms. In this case the sum of the locally computed divergence terms of $P_K(\boldsymbol{\sigma}^{(k)})$ is the same as the global divergence of $P_K(\boldsymbol{\sigma}^{(k)})$ on the whole domain that we are looking for. Hence, we have to find a $\boldsymbol{\sigma}^{(k)}$ with vanishing local divergence as well as with vanishing jump terms. Such a $\boldsymbol{\sigma}^{(k)}$ would also have vanishing global divergence on all of Ω. These considerations can be understood as a *consistency criterion* for the iteration process. If we determine $\boldsymbol{\sigma}^{(k)}$ via the fixed point iteration scheme in a way that it is

$$
\begin{aligned}
(\operatorname{div} P_K(\boldsymbol{\sigma}^{(k)}), \mathbf{v})_{0,T} &\approx 0 \qquad \forall\, T \in \mathcal{T}_h \, , \mathbf{v} \in V_h \, , \\
\left(\left[P_K(\boldsymbol{\sigma}^{(k)}) \cdot \mathbf{n} \right], \mathbf{v} \right)_{0,E} &\approx 0 \qquad \forall\, E \in \mathcal{E}_h \, , \mathbf{v} \in V_h \, ,
\end{aligned}
\tag{4.28}
$$

we have established a *consistent* iteration scheme. This can also be seen by examining the mean value of the normal component $P_K(\boldsymbol{\sigma}^{(k)})$ on an edge:

$$
P_K(\boldsymbol{\sigma}^{(k)})\big|_{mean} \cdot \mathbf{n} = \frac{1}{2} \left(P_K(\boldsymbol{\sigma}^{(k)})\big|_{T,l} + P_K(\boldsymbol{\sigma}^{(k)})\big|_{T,r} \right) \cdot \mathbf{n} \, .
$$

If we are given a $\boldsymbol{\sigma}^{(k)}$ that fulfills (4.28) we get for all $\mathbf{v} \in V_h$

$$
\begin{aligned}
0 \quad &\approx \quad \left(\operatorname{div} P_K(\boldsymbol{\sigma}^{(k)}), \mathbf{v}\right)_{0,T} - \frac{1}{2}\left(\left[P_K(\boldsymbol{\sigma}^{(k)}) \cdot \mathbf{n}\right], \mathbf{v}\right)_{0,\partial T} \\[2mm]
&= \quad \left(P_K(\boldsymbol{\sigma}^{(k)})\big|_{T,l} \cdot \mathbf{n}, \mathbf{v}\right)_{0,\partial T} - \frac{1}{2}\left(\left[P_K(\boldsymbol{\sigma}^{(k)}) \cdot \mathbf{n}\right], \mathbf{v}\right)_{0,\partial T} \\[2mm]
&= \quad \left(\frac{1}{2}\left(P_K(\boldsymbol{\sigma}^{(k)})\big|_{T,l} + P_K(\boldsymbol{\sigma}^{(k)})\big|_{T,r}\right) \cdot \mathbf{n}, \mathbf{v}\right)_{0,\partial T} \\[2mm]
&= \quad \left(P_K(\boldsymbol{\sigma}^{(k)})\big|_{mean} \cdot \mathbf{n}, \mathbf{v}\right)_{0,\partial T} .
\end{aligned}
\tag{4.29}
$$

We will come back to this consistency result later on in Section 5.2, when we develop an error estimator for the plastic case.

Remark 4.1 *Note that the boundary condition*

$$
P_K(\boldsymbol{\sigma}^N) \cdot \mathbf{n} = \mathbf{g} \qquad on \; \Gamma_N
\tag{4.30}
$$

can easily be incorporated into this variational formulation and the iteration scheme. If we are in the elastic range the projection P_K is the identity operator. Hence, the demand (4.30) is already fulfilled by assumption (3.46). Otherwise we are in the plastic range where we have $\boldsymbol{\sigma}^N \equiv 0$ and $\boldsymbol{\sigma}^N \cdot \mathbf{n} \equiv 0$ on all inner and outer edges (cf. Remark 3.6). Consequently, (4.30) holds true. The right-hand side triangle contributions of the boundary edges with such homogeneous boundary conditions are incorporated in the projection with the assumption that on such a boundary edge

$$
\left(P_K(\boldsymbol{\sigma}^{(k)})\big|_{T,r}\right) \cdot \mathbf{n} = 0 ,
$$

holds. Without the assumption from Remark 3.6 we would also have to incorporate the inhomogeneous Neumann conditions accordingly.

After these considerations about the nature of the terms in (4.19) that contain the projection P_K we can finally formulate a discrete version of the variational formulations (4.16) and (4.18) as well as a discrete iteration rule similar to (4.19) for the plastic problem.

Let an approximation $(\boldsymbol{\sigma}_h^{(k-1)}, \mathbf{u}_h^{(k-1)}, \gamma_h^{(k-1)}) \in S_h \times V_h \times Q_h$ of the plastic solution $(\boldsymbol{\sigma}_h^{pl}, \mathbf{u}_h^{pl}, \gamma_h^{pl}) \in S_h \times V_h \times Q_h$ be given. We seek a triple $(\boldsymbol{\delta}^{(k)}, \mathbf{w}^{(k)}, \vartheta^{(k)}) \in S_h \times V_h \times Q_h$ such that

$$
(\mathcal{C}^{-1}\boldsymbol{\delta}_h^{(k)}, \boldsymbol{\tau}_h)_{0,\Omega} + (\mathbf{w}_h^{(k)}, \operatorname{div}\boldsymbol{\tau}_h)_{0,\Omega} + (\vartheta_h^{(k)}, \mathsf{as}\,\boldsymbol{\tau}_h)_{0,\Omega} = 0 ,
\tag{4.31}
$$

$$
(\operatorname{div}\boldsymbol{\delta}_h^{(k)}, \mathbf{v}_h)_{0,\Omega} = -\sum_{T \in \mathcal{T}_h}\left((\operatorname{div} P_K(\boldsymbol{\sigma}_h^{(k-1)}), \boldsymbol{\chi}_T)_{0,T} - \frac{1}{2}\left(\left[P_K(\boldsymbol{\sigma}^{(k-1)}) \cdot \mathbf{n}\right], \mathbf{v}_h)_{0,\partial T}\right) ,
$$

$$
(\mathsf{as}\,\boldsymbol{\delta}^{(k)}, \eta_h)_{0,\Omega} = 0 ,
$$

holds true for all triples $(\boldsymbol{\tau}_h, \mathbf{v}_h, \eta_h) \in S_h \times V_h \times Q_h$. Here, $\boldsymbol{\chi}_T$ is again the characteristic function on T. A new approximation $(\boldsymbol{\sigma}_h^{(k)}, \mathbf{u}_h^{(k)}, \gamma_h^{(k)})$ is computed via the following iteration rule

$$
\begin{bmatrix} \boldsymbol{\sigma}_h^{(k)} \\ \mathbf{u}_h^{(k)} \\ \gamma_h^{(k)} \end{bmatrix} := \begin{bmatrix} \boldsymbol{\sigma}_h^{(k-1)} \\ \mathbf{u}_h^{(k-1)} \\ \gamma_h^{(k-1)} \end{bmatrix} + \begin{bmatrix} \boldsymbol{\delta}_h^{(k)} \\ \mathbf{w}_h^{(k)} \\ \vartheta_h^{(k_h)} \end{bmatrix} \quad \text{and} \quad \begin{bmatrix} \boldsymbol{\sigma}_h^{(0)} \\ \mathbf{u}_h^{(0)} \\ \gamma_h^{(0)} \end{bmatrix} := \begin{bmatrix} \boldsymbol{\sigma}_h^{el} \\ \mathbf{u}_h^{el} \\ \gamma_h^{el} \end{bmatrix} . \quad (4.32)
$$

The triple $(\boldsymbol{\sigma}_h^{el}, \mathbf{u}_h^{el}, \gamma_h^{el})$ is the solution of an auxiliary elastic problem in the form of (3.48) holding true for all $(\boldsymbol{\tau}_h, \mathbf{v}_h, \eta_h) \in S_h \times V_h \times Q_h$:

$$
(\mathcal{C}^{-1}(\boldsymbol{\sigma}^N + \boldsymbol{\sigma}_h^{el}), \boldsymbol{\tau}_h)_{0,\Omega} \;+\; (\mathbf{u}_h^{el}, \mathsf{div}\,\boldsymbol{\tau}_h)_{0,\Omega} \;+\; (\gamma_h^{el}, \mathsf{as}\,\boldsymbol{\tau}_h)_{0,\Omega} \;=\; 0 \;,
$$

$$
(\mathsf{div}\,(\boldsymbol{\sigma}^N + \boldsymbol{\sigma}_h^{el}), \mathbf{v}_h)_{0,\Omega} \;=\; 0 \;, \quad (4.33)
$$

$$
(\mathsf{as}\,(\boldsymbol{\sigma}^N + \boldsymbol{\sigma}_h^{el}), \eta_h)_{0,\Omega} \;=\; 0 \;.
$$

Analogously to (4.19) the iteration rule (4.34) can also be formulated as a variational system if we consider the demands for consistency presented in the statements (4.26) to (4.29). We seek $(\boldsymbol{\sigma}_h^{(k+1)}, \mathbf{u}_h^{(k+1)}, \gamma_h^{(k+1)}) \in S_h \times V_h \times Q_h$ such that

$$
(\mathcal{C}^{-1}(\boldsymbol{\sigma}^N + \boldsymbol{\sigma}_h^{(k+1)}), \boldsymbol{\tau}_h)_{0,\Omega} \;=\; -\,(\mathbf{u}_h^{(k+1)}, \mathsf{div}\,\boldsymbol{\tau}_h)_{0,\Omega} \;-\; (\gamma_h^{(k+1)}, \mathsf{as}\,\boldsymbol{\tau}_h)_{0,\Omega} \;,
$$

$$
(\mathsf{div}\,(\boldsymbol{\sigma}^N + \boldsymbol{\sigma}_h^{(k+1)}), \mathbf{v}_h)_{0,\Omega} \;=\; (\mathsf{div}\,(\boldsymbol{\sigma}^N + \boldsymbol{\sigma}_h^{(k)}), \mathbf{v}_h)_{0,\Omega} \quad (4.34)
$$

$$
-\, \sum_{T \in \mathcal{T}_h} \left((\mathsf{div}\, P_K(\boldsymbol{\sigma}_h^{(k)}), \boldsymbol{\chi}_T)_{0,T} \;-\; \frac{1}{2}\,([P_K(\boldsymbol{\sigma}^{(k)}) \cdot \mathbf{n}], \mathbf{v}_h)_{0,\partial T} \right) \;,
$$

$$
(\mathsf{as}\,(\boldsymbol{\sigma}^N + \boldsymbol{\sigma}_h^{(k+1)}), \eta_h)_{0,\Omega} \;=\; 0 \;,
$$

is fulfilled for all $(\boldsymbol{\tau}_h, \mathbf{v}_h, \eta_h) \in S_h \times V_h \times Q_h$. The consistency considerations now guarantee that the discrete iteration rule (4.34) is consistent to the iteration rule (4.19). The convergence of an iteration following this rule will be proved in the next section.

4.3 Convergence of the fixed point iteration scheme

Let $S_h \subset H_{\Gamma_N}(\mathsf{div}, \Omega)^{2\times 2}$ be the usual finite element ansatz space for the stresses. Inserting discrete stresses $\boldsymbol{\sigma}_h \in S_h$ as the old iterate $\boldsymbol{\sigma}^{(k)}$ in the iteration rule (4.19) we can naturally write the fixed point iteration scheme as a mapping $\Lambda : S_h \longrightarrow S_h$ from the ansatz space onto itself through

$$
\Lambda(\boldsymbol{\sigma}_h) \;=\; \mathcal{L}\,\mathcal{Q}\,(\mathsf{id} - P_K)(\boldsymbol{\sigma}_h), \quad (4.35)
$$

for any $\boldsymbol{\sigma}_h \in S_h$. Consequently, $\Lambda(\boldsymbol{\sigma}_h)$ represents the new iterate $\boldsymbol{\sigma}^{(k+1)}$ in (4.19). This yields us that in the formula (4.35) P_K is the well-known orthogonal projection from the

return mapping procedure for perfect plasticity as defined in e.g. (4.15) while id denotes of course the identity operator. Assuming that we are in the plastic case,[2] i.e. $P_K \neq \mathsf{id}$, the operator $(\mathsf{id} - P_K)$ has the form

$$
(\mathsf{id} - P_K)(\boldsymbol{\sigma}_h) \;=\; \left(1 \;-\; \sqrt{\frac{2}{3}} \; \frac{\sigma^\star}{\|\, \mathsf{dev}\, \boldsymbol{\sigma}_h \,\|_F} \right) \; \mathsf{dev}\, \boldsymbol{\sigma}_h \;. \tag{4.36}
$$

The operator $\mathcal{Q}$ on the other hand is an orthogonal projection from $L^2(\Omega)$ back onto S_h which is due to the above mentioned fact that in general we do not have $P_K(\boldsymbol{\sigma}^{(k)}) \in H_{\Gamma_N}(\mathsf{div}, \Omega)^{2\times 2}$ any more; cf. statement (4.23). We only define $\mathcal{Q}$ in general through

$$
\begin{aligned}
\mathcal{Q} \,:\, L^2 &\;\longrightarrow\; S_h \;, \\
\boldsymbol{\tau} &\;\longmapsto\; \mathcal{Q}\boldsymbol{\tau} \;.
\end{aligned}
\tag{4.37}
$$

Finally, we know from (4.19) that $\mathcal{L}$ is a linear operator given through the system

$$
\begin{aligned}
(\mathcal{C}^{-1}(\mathcal{L}\,\boldsymbol{\sigma}_h), \boldsymbol{\tau}_h)_{0,\Omega} \;+\; (\mathbf{u}_h, \mathsf{div}\, \boldsymbol{\tau}_h)_{0,\Omega} \;+\; (\gamma_h, \mathsf{as}\, \boldsymbol{\tau}_h)_{0,\Omega} &\;=\; 0 &&\forall\, \boldsymbol{\tau}_h \in S_h \;, \\
(\mathsf{div}\,(\mathcal{L}\,\boldsymbol{\sigma}_h), \mathbf{v}_h)_{0,\Omega} \;-\; (\mathsf{div}\, \boldsymbol{\sigma}_h, \mathbf{v}_h)_{0,\Omega} &\;=\; 0 &&\forall\, \mathbf{v}_h \in V_h \;, \\
(\mathsf{as}\,(\mathcal{L}\,\boldsymbol{\sigma}_h), \eta_h)_{0,\Omega} &\;=\; 0 &&\forall\, \eta_h \in Q_h \;,
\end{aligned}
\tag{4.38}
$$

where we have $(\boldsymbol{\sigma}_h, \mathbf{u}_h, \gamma_h) \in S_h \times V_h \times Q_h$. In a simplified mixed matrix-operator-expression the system (4.38) can also be written as

$$
\underbrace{\begin{bmatrix} \mathcal{C}^{-1} & \mathsf{div}^* & \mathsf{as}^* \\ \mathsf{div} & 0 & 0 \\ \mathsf{as} & 0 & 0 \end{bmatrix}}_{=:\; \mathcal{A}} \begin{bmatrix} \mathcal{L}\,\boldsymbol{\sigma} \\ \mathbf{u} \\ \gamma \end{bmatrix} \;=\; \begin{bmatrix} 0 \\ \mathsf{div}\, \boldsymbol{\sigma} \\ 0 \end{bmatrix} \;, \tag{4.39}
$$

where we denote by div^* and as^* the adjoint operators (cf. e.g. [AFW'97]) of div and as defined through

$$
\begin{aligned}
\mathsf{div}^* \;:\; V_h \longrightarrow S_h \quad\text{such that}\quad (\mathsf{div}^*\, \mathbf{u}, \boldsymbol{\tau})_{0,\Omega} &\;=\; (\mathbf{u}, \mathsf{div}\, \boldsymbol{\tau}) \quad \forall\, \boldsymbol{\tau} \in S_h \;, \\
\mathsf{as}^* \;:\; Q_h \longrightarrow S_h \quad\text{such that}\quad (\mathsf{as}^*\, \gamma, \boldsymbol{\tau})_{0,\Omega} &\;=\; (\gamma, \mathsf{as}\, \boldsymbol{\tau}) \quad \forall\, \boldsymbol{\tau} \in S_h \;.
\end{aligned}
\tag{4.40}
$$

By multiplying the expression (4.39) from the left-hand side with $\mathcal{A}^{-1}$ and omitting the variable $\boldsymbol{\sigma}$ we get the following representation of $\mathcal{L}$:

$$
\mathcal{L} \;=\; [\, I \;\; 0 \;\; 0 \,] \underbrace{\begin{bmatrix} \mathcal{C}^{-1} & \mathsf{div}^* & \mathsf{as}^* \\ \mathsf{div} & 0 & 0 \\ \mathsf{as} & 0 & 0 \end{bmatrix}^{-1}}_{=\; \mathcal{A}^{-1}} \begin{bmatrix} 0 \\ \mathsf{div} \\ 0 \end{bmatrix} \;, \tag{4.41}
$$

---

[2] Otherwise we would not need the fixed point iteration scheme.

where I denotes the identity block matrix. Using the *Schur complement form* from (4.9) the matrix $\mathcal{A}$ can be split in a matrix product

$$\mathcal{A} = LBL^T , \qquad (4.42)$$

with

$$L = \begin{bmatrix} I & 0 & 0 \\ \mathsf{div}\,\mathcal{C} & I & 0 \\ \mathsf{as}\,\mathcal{C} & 0 & I \end{bmatrix} , \qquad L^T = \begin{bmatrix} I & \mathcal{C}\,\mathsf{div}^* & \mathcal{C}\,\mathsf{as}^* \\ 0 & I & 0 \\ 0 & 0 & I \end{bmatrix} ,$$

and

$$B = \begin{bmatrix} \mathcal{C}^{-1} & 0 & 0 \\ 0 & -\,\mathsf{div}\,\mathcal{C}\,\mathsf{div}^* & -\,\mathsf{div}\,\mathcal{C}\,\mathsf{as}^* \\ 0 & -\,\mathsf{as}\,\mathcal{C}\,\mathsf{div}^* & -\,\mathsf{as}\,\mathcal{C}\,\mathsf{as}^* \end{bmatrix} .$$

Hence, we can write $\mathcal{A}^{-1}$ as

$$\mathcal{A}^{-1} = (L^T)^{-1} B^{-1} L^{-1} , \qquad (4.43)$$

with

$$(L^T)^{-1} = \begin{bmatrix} I & -\,\mathcal{C}\,\mathsf{div}^* & -\,\mathcal{C}\,\mathsf{as}^* \\ 0 & I & 0 \\ 0 & 0 & I \end{bmatrix} , \qquad L^{-1} = \begin{bmatrix} I & 0 & 0 \\ -\,\mathsf{div}\,\mathcal{C} & I & 0 \\ -\,\mathsf{as}\,\mathcal{C} & 0 & I \end{bmatrix} ,$$

and

$$B^{-1} = \begin{bmatrix} \mathcal{C} & 0 & 0 \\ 0 & & \\ 0 & -\left(\begin{matrix} \mathsf{div}\,\mathcal{C}\,\mathsf{div}^* & \mathsf{div}\,\mathcal{C}\,\mathsf{as}^* \\ \mathsf{as}\,\mathcal{C}\,\mathsf{div}^* & \mathsf{as}\,\mathcal{C}\,\mathsf{as}^* \end{matrix}\right)^{-1} \end{bmatrix} .$$

Inserting (4.43) in (4.41) yields finally a reduced expression for $\mathcal{L}$ in the form

$$\mathcal{L} = \mathcal{C}\,[\,\mathsf{div}^* \quad \mathsf{as}^*\,] \begin{bmatrix} \mathsf{div}\,\mathcal{C}\,\mathsf{div}^* & \mathsf{div}\,\mathcal{C}\,\mathsf{as}^* \\ \mathsf{as}\,\mathcal{C}\,\mathsf{div}^* & \mathsf{as}\,\mathcal{C}\,\mathsf{as}^* \end{bmatrix}^{-1} \begin{bmatrix} \mathsf{div} \\ 0 \end{bmatrix} , \qquad (4.44)$$

owing to the fact that with the factor $[\,I \quad 0 \quad 0\,]$ we need to consider only the first component of $\mathcal{A}^{-1}\,[\,0 \quad \mathsf{div} \quad 0\,]^T$.

With these notations we have described our fixed point iteration scheme represented by the mapping Λ in terms of the operators $\mathcal{L}$, $\mathcal{Q}$ and $(\mathsf{id} - P_K)$. Remember from (4.19) and (4.20) that the iteration scheme has only one fixed point $\boldsymbol{\sigma}_h^{tr}$. For a proof of convergence we therefore have to show that Λ is a contraction, i.e.

$$\|\Lambda\,\boldsymbol{\sigma}_h\| \leq L\,\|\boldsymbol{\sigma}_h\| \qquad \forall\,\boldsymbol{\sigma}_h \in S_h , \qquad (4.45)$$

with a constant $0 < L < 1$ and an appropriate norm $\|\cdot\|$. We will first define this norm and proof afterwards for each operator $\mathcal{L}$, $\mathcal{Q}$ and $(\mathsf{id} - P_K)$ certain results that yield convergence for Λ if combined.

Definition 4.2 (Inner product in $H(\mathsf{div}, \Omega)^{2\times 2}$) *For any $\boldsymbol{\sigma}$ and any $\boldsymbol{\tau}$ in $H(\mathsf{div}, \Omega)^{2\times 2}$ we define an inner product on this space via*

$$(\boldsymbol{\sigma}, \boldsymbol{\tau})_{\mathcal{C}^{-1},\mathsf{div}} \; := \; (\mathsf{div}\,\boldsymbol{\sigma}, \mathsf{div}\,\boldsymbol{\tau})_{0,\Omega} \; + \; (\mathcal{C}^{-1}\,\boldsymbol{\sigma}, \boldsymbol{\tau})_{0,\Omega} \; .$$

This inner product induces as usual a norm which is given by

$$\|\,\boldsymbol{\sigma}\,\|_{\mathcal{C}^{-1},\mathsf{div}} \; := \; \left(\|\,\mathsf{div}\,\boldsymbol{\sigma}\,\|^2_{0,\Omega} \; + \; \|\,\mathcal{C}^{-\frac{1}{2}}\,\boldsymbol{\sigma}\,\|^2_{0,\Omega} \right)^{\frac{1}{2}} \; .$$

Lemma 4.3 *With the operator $\mathcal{L}$ from (4.44) the following inequality holds:*

$$\|\,\mathcal{L}\,\boldsymbol{\sigma}_h\,\|_{\mathcal{C}^{-1},\mathsf{div}} \; \leq \; \|\,\boldsymbol{\sigma}_h\,\|_{\mathcal{C}^{-1},\mathsf{div}} \qquad\qquad \forall\,\boldsymbol{\sigma}_h \in S_h \; . \tag{4.46}$$

Proof: *To prove Lemma 4.3 we have to use a Helmholtz decomposition of the space $S_h \subset H_{\Gamma_N}(\mathsf{div}, \Omega)^{2\times 2}$. This decomposition will also be of importance in the next chapter, when we derive an a posteriori error estimator (cf. Theorem 5.1). For further details we refer to the literature; the general theory concerning this decomposition can be found in [WH'99] while the Helmholtz decomposition for linear elasticity used here is analyzed in [CS'03]. For the purposes of this proof it suffices to state that we can decompose any tensor $\boldsymbol{\sigma}_h \in S_h$ orthogonally into*

$$\boldsymbol{\sigma}_h \; = \; \nabla^\perp \boldsymbol{\varphi}_h \; \oplus \; \mathcal{C}\,\nabla\,\mathbf{q}_h \; , \tag{4.47}$$

where we have $\boldsymbol{\varphi}_h \in H^1_{\Gamma_N}(\Omega)^2$ and $\mathbf{q}_h \in H^1_{\Gamma_D}(\Omega)^2$. Due to (4.44) and $\mathsf{div}\,\nabla^\perp\boldsymbol{\varphi}_h = 0$ we have evidently $\mathcal{L}\,(\nabla^\perp\boldsymbol{\varphi}_h) = 0$. Therefore the expression

$$\mathcal{L}\,(\mathcal{C}\,\nabla\,\mathbf{q}_h) \; = \; \mathcal{C}\,\left[\,\mathsf{div}^* \;\; \mathsf{as}^*\,\right] \begin{bmatrix} \mathsf{div}\,\mathcal{C}\,\mathsf{div}^* & \mathsf{div}\,\mathcal{C}\,\mathsf{as}^* \\ \mathsf{as}\,\mathcal{C}\,\mathsf{div}^* & \mathsf{as}\,\mathcal{C}\,\mathsf{as}^* \end{bmatrix}^{-1} \begin{bmatrix} \mathsf{div}\,\mathcal{C}\,\nabla\,\mathbf{q}_h \\ 0 \end{bmatrix} \tag{4.48}$$

remains to be examined. With the two properties

$$\|\,\mathcal{C}^{-\frac{1}{2}}\,\mathcal{L}\,(\mathcal{C}\,\nabla\,\mathbf{q}_h)\,\|_{0,\Omega} \; \leq \; \|\,\mathcal{C}^{\frac{1}{2}}\,\nabla\,\mathbf{q}_h\,\|_{0,\Omega} \; , \tag{4.49}$$

$$\|\,\mathsf{div}\,\mathcal{L}\,(\mathcal{C}\,\nabla\,\mathbf{q}_h)\,\|_{0,\Omega} \; \leq \; \|\,\mathsf{div}\,\mathcal{C}\,\nabla\,\mathbf{q}_h\,\|_{0,\Omega} \; , \tag{4.50}$$

we have

$$
\begin{aligned}
\|\,\mathcal{L}\,\boldsymbol{\sigma}_h\,\|^2_{\mathcal{C}^{-1},\mathsf{div}} \; &= \; \|\,\mathsf{div}\,\mathcal{L}\,\boldsymbol{\sigma}_h\,\|^2_{0,\Omega} \; + \; \|\,\mathcal{C}^{-\frac{1}{2}}\,\mathcal{L}\,\boldsymbol{\sigma}_h\,\|^2_{0,\Omega} \\[2mm]
&= \; \|\,\mathsf{div}\,\mathcal{L}\,(\mathcal{C}\,\nabla\,\mathbf{q}_h)\,\|^2_{0,\Omega} \; + \; \|\,\mathcal{C}^{-\frac{1}{2}}\,\mathcal{L}\,(\mathcal{C}\,\nabla\,\mathbf{q}_h)\,\|^2_{0,\Omega} \\[2mm]
&\leq \; \|\,\mathsf{div}\,\mathcal{C}\,\nabla\,\mathbf{q}_h\,\|_{0,\Omega} \; + \; \|\,\mathcal{C}^{\frac{1}{2}}\,\nabla\,\mathbf{q}_h\,\|_{0,\Omega} \\[2mm]
&= \; \|\,\mathsf{div}\,\mathcal{C}\,\nabla\,\mathbf{q}_h\,\|_{0,\Omega} \; + \; \|\,\mathcal{C}^{-\frac{1}{2}}\,\mathcal{C}\,\nabla\,\mathbf{q}_h\,\|_{0,\Omega} \\[2mm]
&= \; \|\,\mathcal{C}\,\nabla\,\mathbf{q}_h\,\|^2_{\mathcal{C}^{-1},\mathsf{div}} \\[2mm]
&\leq \; \|\,\boldsymbol{\sigma}_h\,\|^2_{\mathcal{C}^{-1},\mathsf{div}} \; ,
\end{aligned}
$$

*and thus, Lemma 4.3 would be proven. Therefore, we have to show the inequalities (4.49)
and (4.50). We start with the first property; obviously it is*

$$\| \mathcal{C}^{-\frac{1}{2}} \mathcal{L} (\mathcal{C} \nabla \mathbf{q}_h) \|_{0,\Omega}^2 \;=\; \left(\mathcal{C}^{-1} \mathcal{L} (\mathcal{C} \nabla \mathbf{q}_h), \mathcal{L} (\mathcal{C} \nabla \mathbf{q}_h) \right)$$

*By using the explicit form of $\mathcal{L}$ from (4.44) and adjoint techniques we get for the left side
of the scalar product the term*

$$\begin{bmatrix} \mathrm{div}\,\mathcal{C}\,\mathrm{div}^* & \mathrm{div}\,\mathcal{C}\,\mathrm{as}^* \\ \mathrm{as}\,\mathcal{C}\,\mathrm{div}^* & \mathrm{as}\,\mathcal{C}\,\mathrm{as}^* \end{bmatrix}^{-1} \begin{bmatrix} \mathrm{div}\,\mathcal{C}\,\nabla\,\mathbf{q}_h \\ 0 \end{bmatrix},$$

while the right side is of the form

$$\begin{bmatrix} \mathrm{div} \\ \mathrm{as} \end{bmatrix} \mathcal{C} \begin{bmatrix} \mathrm{div}^* & \mathrm{as}^* \end{bmatrix} \begin{bmatrix} \mathrm{div}\,\mathcal{C}\,\mathrm{div}^* & \mathrm{div}\,\mathcal{C}\,\mathrm{as}^* \\ \mathrm{as}\,\mathcal{C}\,\mathrm{div}^* & \mathrm{as}\,\mathcal{C}\,\mathrm{as}^* \end{bmatrix}^{-1} \begin{bmatrix} \mathrm{div}\,\mathcal{C}\,\nabla\,\mathbf{q}_h \\ 0 \end{bmatrix} = \begin{bmatrix} \mathrm{div}\,\mathcal{C}\,\nabla\,\mathbf{q}_h \\ 0 \end{bmatrix}.$$

Together, this results in

$$\| \mathcal{C}^{-\frac{1}{2}} \mathcal{L} (\mathcal{C} \nabla \mathbf{q}_h) \|_{0,\Omega}^2$$

$$= \left(\begin{bmatrix} \mathrm{div}\,\mathcal{C}\,\mathrm{div}^* & \mathrm{div}\,\mathcal{C}\,\mathrm{as}^* \\ \mathrm{as}\,\mathcal{C}\,\mathrm{div}^* & \mathrm{as}\,\mathcal{C}\,\mathrm{as}^* \end{bmatrix}^{-1} \begin{bmatrix} \mathrm{div}\,\mathcal{C}\,\nabla\,\mathbf{q}_h \\ 0 \end{bmatrix}, \begin{bmatrix} \mathrm{div}\,\mathcal{C}\,\nabla\,\mathbf{q}_h \\ 0 \end{bmatrix} \right)_{0,\Omega}.$$

*At this point we want to replace the block matrix $\begin{bmatrix} \mathrm{div}\,\mathcal{C}\,\nabla\,\mathbf{q}_h & 0 \end{bmatrix}^T$ and consider therefore
the following indisputable equation:*

$$\begin{bmatrix} \mathrm{div}\,\mathcal{C}\,\nabla\,\mathbf{q}_h \\ 0 \end{bmatrix} = \begin{bmatrix} (\mathrm{div}\,\mathcal{C}\,\nabla)^{-\frac{1}{2}} & 0 \\ 0 & (\mathrm{div}\,\mathcal{C}\,\nabla)^{-\frac{1}{2}} \end{bmatrix}^{-1} \begin{bmatrix} (\mathrm{div}\,\mathcal{C}\,\nabla)^{\frac{1}{2}}\,\mathbf{q}_h \\ 0 \end{bmatrix}.$$

*Abbreviating $\mathcal{D}^- := (\mathrm{div}\,\mathcal{C}\,\nabla)^{-\frac{1}{2}}$ and $\mathcal{D}^+ := (\mathrm{div}\,\mathcal{C}\,\nabla)^{\frac{1}{2}}$ and using adjoint techniques once
more we finally have*

$$\| \mathcal{C}^{-\frac{1}{2}} \mathcal{L} (\mathcal{C} \nabla \mathbf{q}_h) \|_{0,\Omega}^2$$

$$= \left(\underbrace{\begin{bmatrix} I & \mathcal{D}^- (\mathrm{div}\,\mathcal{C}\,\mathrm{as}^*)\,\mathcal{D}^- \\ \mathcal{D}^- (\mathrm{as}\,\mathcal{C}\,\mathrm{div}^*)\,\mathcal{D}^- & \mathcal{D}^- (\mathrm{as}\,\mathcal{C}\,\mathrm{as}^*)\,\mathcal{D}^- \end{bmatrix}^{-1}}_{=:\,\mathcal{Y}^{-1}} \begin{bmatrix} \mathcal{D}^+\,\mathbf{q}_h \\ 0 \end{bmatrix}, \begin{bmatrix} \mathcal{D}^+\,\mathbf{q}_h \\ 0 \end{bmatrix} \right)_{0,\Omega}.$$

$$= \left(I\,\mathcal{D}^+\,\mathbf{q}_h, \mathcal{D}^+\,\mathbf{q}_h \right)_{0,\Omega} + \underbrace{\left((\mathcal{X}_1\,\mathrm{as}\,\mathcal{X}_2 + \mathcal{X}_3\,\mathrm{as}^*\,\mathcal{X}_4)\,\mathbf{q}_h, \mathcal{D}^+\,\mathbf{q}_h \right)_{0,\Omega}}_{=:\,\mathbf{z}},$$

with operators $\mathcal{X}_i$, $i = 1, \ldots, 4$ depending on entries of the matrix $\mathcal{Y}^{-1}$. Note that for any $\boldsymbol{\sigma}_h \in S_h$ we consider in our fixed point iteration scheme it is $(\mathsf{as}\,\boldsymbol{\sigma}_h, \eta)_{0,\Omega} = 0$ for all $\eta \in L^2(\Omega)$. This yields $(\mathsf{as}\,\mathbf{q}_h, \eta)_{0,\Omega} = 0$ and also $(\mathsf{as}^*\,\mathbf{q}_h, \eta)_{0,\Omega} = 0$ for all $\eta \in L^2(\Omega)$. Therefore the scalar product $\mathbf{z}$ is vanishing and we get

$$
\begin{aligned}
\| \mathcal{C}^{-\frac{1}{2}} \mathcal{L} \left(\mathcal{C} \nabla \mathbf{q}_h \right) \|_{0,\Omega}^2 &= \left((\mathsf{div}\,\mathcal{C}\,\nabla)^{\frac{1}{2}} \mathbf{q}_h \,, (\mathsf{div}\,\mathcal{C}\,\nabla)^{\frac{1}{2}} \mathbf{q}_h \right)_{0,\Omega} \\
&= \left(\mathsf{div}\,\mathcal{C}\,\nabla\,\mathbf{q}_h \,, \mathbf{q}_h \right)_{0,\Omega} \\
&= \left(\mathcal{C}\,\nabla\,\mathbf{q}_h \,, \nabla\,\mathbf{q}_h \right)_{0,\Omega} \\
&= \left(\mathcal{C}^{\frac{1}{2}} \nabla\,\mathbf{q}_h \,, \mathcal{C}^{\frac{1}{2}} \nabla\,\mathbf{q}_h \right)_{0,\Omega} \\
&= \| \mathcal{C}^{\frac{1}{2}} \nabla\,\mathbf{q}_h \|_{0,\Omega}^2 \ .
\end{aligned}
$$

Thus, property (4.49) is proven. Due to the above considerations concerning the operator as we have

$$
\begin{aligned}
\| \mathsf{div}\,\mathcal{L}\left(\mathcal{C}\,\nabla\,\mathbf{q}_h \right) \|_{0,\Omega}^2 &= \left\| \begin{bmatrix} \mathsf{div} \\ \mathsf{as} \end{bmatrix} \mathcal{L}\left(\mathcal{C}\,\nabla\,\mathbf{q}_h \right) \right\|_{0,\Omega}^2 \\
&= \left(\begin{bmatrix} \mathsf{div} \\ \mathsf{as} \end{bmatrix} \mathcal{L}\left(\mathcal{C}\,\nabla\,\mathbf{q}_h \right) , \begin{bmatrix} \mathsf{div} \\ \mathsf{as} \end{bmatrix} \mathcal{L}\left(\mathcal{C}\,\nabla\,\mathbf{q}_h \right) \right)_{0,\Omega} .
\end{aligned}
$$

Considering again the explicit form of $\mathcal{L}$ from (4.44) each side of the above scalar product is of the form

$$
\begin{bmatrix} \mathsf{div} \\ \mathsf{as} \end{bmatrix} \mathcal{C} \begin{bmatrix} \mathsf{div}^* & \mathsf{as}^* \end{bmatrix} \begin{bmatrix} \mathsf{div}\,\mathcal{C}\,\mathsf{div}^* & \mathsf{div}\,\mathcal{C}\,\mathsf{as}^* \\ \mathsf{as}\,\mathcal{C}\,\mathsf{div}^* & \mathsf{as}\,\mathcal{C}\,\mathsf{as}^* \end{bmatrix}^{-1} \begin{bmatrix} \mathsf{div}\,\mathcal{C}\,\nabla\,\mathbf{q}_h \\ 0 \end{bmatrix} = \begin{bmatrix} \mathsf{div}\,\mathcal{C}\,\nabla\,\mathbf{q}_h \\ 0 \end{bmatrix} ,
$$

which results in

$$
\| \mathsf{div}\,\mathcal{L}\left(\mathcal{C}\,\nabla\,\mathbf{q}_h \right) \|_{0,\Omega}^2 = \| \mathsf{div}\,\mathcal{C}\,\nabla\,\mathbf{q}_h \|_{0,\Omega}^2 \ .
$$

With this equality property (4.50) and therefore also Lemma 4.3 are proven. $\square$

In the next Lemma we will state a result concerning the projection $\mathcal{Q}$. However, this result depends on an assumption that we will verify only later on while considering the properties of the operator $\mathsf{id} - P_K$.

Lemma 4.4 With a given subset $R \subset S_h$ and a given constant $0 < L_1 < 1$ such that it is

$$
\| \left(\mathsf{id} - P_K \right) \boldsymbol{\sigma}_h \|_{0,\Omega} \ \leq \ L_1 \, \| \boldsymbol{\sigma}_h \|_{0,\Omega} \qquad \forall\, \boldsymbol{\sigma}_h \in R \ , \tag{4.51}
$$

there exists a projection $\mathcal{Q} : L^2 \longrightarrow S_h$ as in (4.37) and a constant $0 < L_2 < 1$ such that the following inequality holds:

$$\| \mathcal{Q} \, (\mathsf{id} - P_K) \, \boldsymbol{\sigma}_h \|_{\mathcal{C}^{-1},\mathsf{div}} \quad \leq \quad L_2 \, \| \boldsymbol{\sigma}_h \|_{\mathcal{C}^{-1},\mathsf{div}} \qquad \forall \, \boldsymbol{\sigma}_h \in R \, . \qquad (4.52)$$

Proof: *The obvious fact that it is $R \subset S_h \subset H_{\Gamma_N}(\mathsf{div}, \Omega)^{2\times2}$ and $H_{\Gamma_N}(\mathsf{div}, \Omega)^{2\times2}$ being a dense subspace of L^2 together with (4.51) yield us the existence of a projection $\mathcal{Q}$ as postulated in (4.52).* $\qquad\qquad\square$

With the results from the two Lemmata 4.3 and 4.4 it remains to examine the operator $(\mathsf{id} - P_K)$ before we can formulate a theorem on the convergence of the operator Λ that describes the fixed point iteration.

Lemma 4.5 *Let the operator $(\mathsf{id} - P_K)$ from equation (4.36) and $\boldsymbol{\sigma}_h, \boldsymbol{\tau}_h \in S_h$ be given. In that case the following two properties hold true:*

(i) If $\boldsymbol{\sigma}_h$ and $\boldsymbol{\tau}_h$ are collinear and have different signs, i.e.

$$\boldsymbol{\sigma}_h \parallel \boldsymbol{\tau}_h \qquad and \qquad \boldsymbol{\sigma}_h = -c\,\boldsymbol{\tau}_h \qquad with \qquad 0 < c \in \mathbb{R} \, , \qquad (4.53)$$

we have

$$\| (\mathsf{id} - P_K) \, \boldsymbol{\sigma}_h \ - \ (\mathsf{id} - P_K) \, \boldsymbol{\tau}_h \|_{0,\Omega} \quad = \quad \| \boldsymbol{\sigma}_h \ - \ \boldsymbol{\tau}_h \|_{0,\Omega} \ . \qquad (4.54)$$

(ii) Otherwise there exists a constant $0 < L < 1$ such that

$$\| (\mathsf{id} - P_K) \, \boldsymbol{\sigma}_h \ - \ (\mathsf{id} - P_K) \, \boldsymbol{\tau}_h \|_{0,\Omega} \quad \leq \quad L \, \| \boldsymbol{\sigma}_h \ - \ \boldsymbol{\tau}_h \|_{0,\Omega} \ . \qquad (4.55)$$

Proof: *Due to the form of $(\mathsf{id} - P_K)$ from equation (4.36) we have*

$$(\mathsf{id} - P_K) \, \boldsymbol{\sigma}_h \ = \ \rho \, (\boldsymbol{\sigma}_h) \, \mathsf{dev} \, \boldsymbol{\sigma}_h \, ,$$

with a function ρ

$$\rho \, (\boldsymbol{\sigma}_h) \ := \ 1 \ - \ \sqrt{\frac{2}{3}} \ \frac{\sigma^\star}{\| \, \mathsf{dev} \, \boldsymbol{\sigma}_h \, \|_F} \ .$$

Here, it is $\| \, \mathsf{dev} \, \boldsymbol{\sigma}_h \, \|_F > \sqrt{\frac{2}{3}} \, \sigma^\star$ owing to the fact that we are in the plastic case. Thus, similar to the function ρ we define another function $\hat{\rho}$ via

$$\hat{\rho} \, (x) \ := \ 1 \ - \ \frac{1}{| \, x \, |} \qquad\qquad with \qquad | \, x \, | > 1 \, .$$

Without any loss of generality it suffices for the prove of property (4.55) to show that the inequality

$$| \hat{\rho}(x)\, x \; + \; \hat{\rho}(y)\, y | \;\; \leq \;\; L \, | x \; + \; y | \qquad\qquad (4.56)$$

holds true with $x, y \in \mathbb{R}^n$, $|x| > 1$, $|y| > 1$, $x \neq -c\,y$ and constants L and c as in (4.55) and (4.53). Inequality (4.56) is equivalent to

$$\left| x \; - \; \frac{x}{|x|} \; + \; y \; - \; \frac{y}{|y|} \right| \;\; \leq \;\; L \, | x \; + \; y | \,, \qquad\qquad (4.57)$$

and obviously we have

$$x \; - \; \frac{x}{|x|} \;\; = \;\; l_1\, x \qquad and \qquad y \; - \; \frac{y}{|y|} \;\; = \;\; l_2\, y \,,$$

with $0 < l_1 < 1$ and $0 < l_2 < 1$. Recalling $x \neq -c\,y$, this yields

$$\left| x \; - \; \frac{x}{|x|} \; + \; y \; - \; \frac{y}{|y|} \right| \;\; = \;\; | l_1\, x \; + \; l_2\, y | \;\; \leq \;\; \max\{l_1, l_2\} \, | x \; + \; y | \,,$$

proving the statement of inequality (4.57) with a constant $L := \max\{l_1, l_2\}$. If on the other hand it is $x = -c\,y$ straightforward calculations show that (4.57) becomes an equality with $L = 1$, therefore supplying us with property (4.54). $\qquad\qquad\square$

Remark 4.6 *Note that in the proposed fixed point iteration scheme for each two iterates $\boldsymbol{\sigma}_h^{(k_i)} \in S_h$ and $\boldsymbol{\sigma}_h^{(k_j)} \in S_h$ with $i \neq j$ and a constant $0 < c \in \mathbb{R}$ the following inequality holds true:*

$$\boldsymbol{\sigma}_h^{(k_i)} \;\; \neq \;\; -c\,\boldsymbol{\sigma}_h^{(k_j)} \;\; . \qquad\qquad (4.58)$$

In other words, the angle between any two iterates $\boldsymbol{\sigma}_h^{(k_i)}$ and $-\boldsymbol{\sigma}_h^{(k_i)}$ in S_h is bounded away from zero, i.e.

$$\sphericalangle\,(\boldsymbol{\sigma}_h^{(k_i)}, \, -\boldsymbol{\sigma}_h^{(k_j)}) \;\; \geq \;\; \theta \;\; > \;\; 0 \,.$$

Thus, Lemma 4.5 states that $(\mathsf{id} - P_K)$ is a contraction for all $\boldsymbol{\sigma}_h \in S_h$ relevant in the fixed point iteration scheme.

Together, the three Lemmata 4.3, 4.4 and 4.5 and the Remark 4.6 guarantee the convergence of the proposed fixed point iteration scheme as we state in the following theorem:

Theorem 4.7 (Convergence of the fixed point iteration scheme) *The operator* Λ *from (4.35) that is induced by the fixed point iteration scheme from (4.19) is a contraction, i.e. we have for all* $\boldsymbol{\sigma}_h \in S_h$

$$\| \Lambda \, \boldsymbol{\sigma}_h \|_{\mathcal{C}^{-1},\mathsf{div}} \;\; = \;\; \| \mathcal{L} \, \mathcal{Q} \, (\mathsf{id} - P_K) \, \boldsymbol{\sigma}_h \|_{\mathcal{C}^{-1},\mathsf{div}} \;\; \leq \;\; L \, \| \, \boldsymbol{\sigma}_h \, \|_{\mathcal{C}^{-1},\mathsf{div}} \;\; , \tag{4.59}$$

with a constant $0 < L < 1$.

Proof: *The Lemmata 4.3, 4.4 and 4.5 and the Remark 4.6 yield the desired result.* □

Chapter 5

An *a posteriori* Error Estimator in Elastoplasticity

After presenting in the last chapter an efficient solution method for the considered elastoplastic problem we now focus on the setup of an efficient adaptive finite element scheme in elastoplasticity. That means that we want to derive an algorithm that can

- solve our model problem for any given finite element grid,

- easily compute a quantity that gives a 'good' global estimate[1] of the error of the approximate solution on that grid,

- easily determine large local contributions to that global quantity, and

- refine the given grid with respect to that large local contributions.

This quantity that we look for is called an *a posteriori error estimator* because it is computed in the post-processing (a posteriori). Different from an *a priori error estimator* which can derived within the analysis of a given finite element scheme (in the 'pre-processing') it does not give a general upper bound for the discretization error depending on the 'variables' mesh width and polynomial order of the ansatz functions. Instead it gives a quality measure for an already computed approximation on a given mesh. Altogether this makes an *a priori error estimate* a guideline for the decision what finite element spaces one wants to use and an *a posteriori error estimate* a tool to verify whether a given method behaves as the *a priori error estimate* predicts. Finite element

---

[1] We will shortly discuss later what we mean by a 'good' estimator. For now it is sufficient that an estimator has to bound the error globally from above (which is called *reliability*) and locally from below (which is called *efficiency*).

schemes using these error estimation techniques are of paramount importance in engineer-
ing sciences and applications because due to the enormous amount of degrees of freedom
in today's computations it is necessary to keep algorithms efficient (cf. Chapter 4). Even
the fast advancing computer hardware technology can not compensate fully the growing
needs for large-scale computations in industry and science. Thus, engineers and mathe-
maticians have to handle degrees of freedom carefully and spend them only in that regions
of a problem in consideration where the extra amount of computer resources pays off in
a better approximation of the sought solution. That is why a posteriori error estimation
was an important topic throughout the last decades and why it will stay that way in the
future.

As in the other chapters of this thesis we will first focus on the elastic problem and
present an error estimator for the *PEERS* finite element method in linear elasticity. In a
second section we extend this method to the more complex elastoplastic case using the
fixed point iteration scheme presented in the last chapter.

5.1   Error estimation in linear elasticity

Our approach for an adaptive *PEERS* finite element method for linear elasticity is based
on a residual error estimator. Assuming that we have given a PDE system with some
known differential operator $\mathcal{A}$ and known right-hand side $\mathbf{b}$

$$\mathcal{A}\mathbf{x} \;=\; \mathbf{b}\;,$$

and assuming furthermore that we have computed an approximation $\mathbf{x}_h$ of the sought
solution $\mathbf{x}$ we are interested in the quantity $\mathbf{e}_h = \mathbf{x} - \mathbf{x}_h$. In general we can not compute
$\mathbf{e}_h$ or a bound for it because we do not know $\mathbf{x}$. However, we can compute the residuum

$$\mathbf{r}_h \;=\; \mathcal{A}\,\mathbf{e}_h \;=\; \mathcal{A}\,(\mathbf{x} - \mathbf{x}_h) \;=\; \mathbf{b} - \mathcal{A}\,\mathbf{x}_h\;,$$

which can give us a quite good indication about the quality of the approximation for a
broad variety of problems. Thus, in this section we want to derive such a residual estimator
and show that it is *reliable* and *efficient*. The terminus *reliability* means that the estimator
is an upper bound on the global error on the whole discretized domain Ω. Such an upper
bound on the global error is of course a quantity of high interest in any application. If
possible it has to be controlled and minimized up to a given accuracy to achieve a good
approximation of the true solution. *Efficiency* on the other hand provides a lower bound
on the local contributions of the global error. Therefore, large local contributions to the
estimator mean also large local contributions to the overall error which yields a reasonable

refinement criterion, i.e. that we refine only such elements that have error contributions higher than a certain threshold value.

5.1.1 Residual error representation

First we have to find a way to express the error in the different variables of our *PEERS* method in terms of the residual quantities that we can compute. Recalling our simplified *PEERS* problem with vanishing volume force and a suitable extension of the inhomogeneous Neumann boundary conditions via a function $\boldsymbol{\sigma}^N \in H(\text{div}, \Omega)^{2\times 2}$ that fulfills

$$\boldsymbol{\sigma}^N \cdot \mathbf{n} = \mathbf{g} \qquad \text{on } \Gamma_N \,,$$

we have to seek a triple $(\boldsymbol{\sigma}, \mathbf{u}, \gamma) \in H_{\Gamma_N}(\text{div}, \Omega)^{2\times 2} \times L^2(\Omega)^2 \times L^2(\Omega)$ such that the system

$$(\mathcal{C}^{-1}(\boldsymbol{\sigma}^N + \boldsymbol{\sigma}), \boldsymbol{\tau})_{0,\Omega} + (\mathbf{u}, \text{div}\,\boldsymbol{\tau})_{0,\Omega} + (\gamma, \text{as}\,\boldsymbol{\tau})_{0,\Omega} = 0 \,,$$
$$(\text{div}\,(\boldsymbol{\sigma}^N + \boldsymbol{\sigma}), \mathbf{v})_{0,\Omega} = 0 \,, \qquad (5.1)$$
$$(\text{as}\,(\boldsymbol{\sigma}^N + \boldsymbol{\sigma}), \eta)_{0,\Omega} = 0 \,,$$

holds for all triples $(\boldsymbol{\tau}, \mathbf{v}, \eta) \in H_{\Gamma_N}(\text{div}, \Omega)^{2\times 2} \times L^2(\Omega)^2 \times L^2(\Omega)$. To do so we discretized the problem seeking for an approximating triple $(\boldsymbol{\sigma}_h, \mathbf{u}_h, \gamma_h) \in S_h \times V_h \times Q_h$ to $(\boldsymbol{\sigma}, \mathbf{u}, \gamma)$ where S_h, V_h and Q_h are subspaces of the related Sobolev spaces. We have chosen Q_h to contain continuous, piecewise linear ansatz functions and V_h to be the space of componentwise piecewise constant functions while S_h was defined as Raviart-Thomas space of lowest order enriched by rotations of cubic bubble functions (to fulfill the *inf-sup-condition*). This leads to the system

$$(\mathcal{C}^{-1}(\boldsymbol{\sigma}^N + \boldsymbol{\sigma}_h), \boldsymbol{\tau}_h)_{0,\Omega} + (\mathbf{u}_h, \text{div}\,\boldsymbol{\tau}_h)_{0,\Omega} + (\gamma_h, \text{as}\,\boldsymbol{\tau}_h)_{0,\Omega} = 0 \,,$$
$$(\text{div}\,(\boldsymbol{\sigma}^N + \boldsymbol{\sigma}_h), \mathbf{v}_h)_{0,\Omega} = 0 \,, \qquad (5.2)$$
$$(\text{as}\,(\boldsymbol{\sigma}^N + \boldsymbol{\sigma}_h), \eta_h)_{0,\Omega} = 0 \,,$$

where we aim to find the triple $(\boldsymbol{\sigma}_h, \mathbf{u}_h, \gamma_h)$ such that the system is fulfilled for every $(\boldsymbol{\tau}_h, \mathbf{v}_h, \eta_h) \in S_h \times V_h \times Q_h$.

Defining the error terms in each variable via

$$\boldsymbol{\sigma}_e := \boldsymbol{\sigma} - \boldsymbol{\sigma}_h \,,$$
$$\mathbf{u}_e := \mathbf{u} - \mathbf{u}_h \,,$$
$$\gamma_e := \gamma - \gamma_h \,,$$

we can write the system (5.1) also as

$$(\mathcal{C}^{-1}(\boldsymbol{\sigma}^N + \boldsymbol{\sigma}_h + \boldsymbol{\sigma}_e), \boldsymbol{\tau})_{0,\Omega} + (\mathbf{u}_h + \mathbf{u}_e, \text{div}\,\boldsymbol{\tau})_{0,\Omega} + (\gamma_h + \gamma_e, \text{as}\,\boldsymbol{\tau})_{0,\Omega} = 0 \ ,$$

$$(\text{div}\,(\boldsymbol{\sigma}^N + \boldsymbol{\sigma}_h + \boldsymbol{\sigma}_e), \mathbf{v})_{0,\Omega} = 0 \ , \qquad (5.3)$$

$$(\text{as}\,(\boldsymbol{\sigma}^N + \boldsymbol{\sigma}_h + \boldsymbol{\sigma}_e), \eta)_{0,\Omega} = 0 \ ,$$

which has to hold for all $(\boldsymbol{\tau}, \mathbf{v}, \eta) \in H_{\Gamma_N}(\text{div}, \Omega)^{2\times2} \times L^2(\Omega)^2 \times L^2(\Omega)$. This system now consists only of error terms and residual terms. To make this clear we define

$$
\begin{aligned}
r_1(\boldsymbol{\tau}) &:= -(\mathcal{C}^{-1}(\boldsymbol{\sigma}^N + \boldsymbol{\sigma}_h), \boldsymbol{\tau})_{0,\Omega} - (\mathbf{u}_h, \text{div}\,\boldsymbol{\tau})_{0,\Omega} - (\gamma_h, \text{as}\,\boldsymbol{\tau})_{0,\Omega} \ , \\
r_2(\mathbf{v}) &:= -(\text{div}\,(\boldsymbol{\sigma}^N + \boldsymbol{\sigma}_h), \mathbf{v})_{0,\Omega} \ , \\
r_3(\eta) &:= -(\text{as}\,(\boldsymbol{\sigma}^N + \boldsymbol{\sigma}_h), \eta)_{0,\Omega} \ ,
\end{aligned}
\qquad (5.4)
$$

and rewrite system (5.3) in the form

$$
\begin{aligned}
(\mathcal{C}^{-1}\boldsymbol{\sigma}_e, \boldsymbol{\tau})_{0,\Omega} + (\mathbf{u}_e, \text{div}\,\boldsymbol{\tau})_{0,\Omega} + (\gamma_e, \text{as}\,\boldsymbol{\tau})_{0,\Omega} &= r_1(\boldsymbol{\tau}) \ , \\
(\text{div}\,\boldsymbol{\sigma}_e, \mathbf{v})_{0,\Omega} &= r_2(\mathbf{v}) \ , \\
(\text{as}\,\boldsymbol{\sigma}_e, \eta)_{0,\Omega} &= r_3(\eta) \ ,
\end{aligned}
\qquad (5.5)
$$

such that the error terms $(\boldsymbol{\sigma}_e, \mathbf{u}_e, \gamma_e)$ and the discrete approximations $(\boldsymbol{\sigma}_h, \mathbf{u}_h, \gamma_h)$ fulfill this system for all $(\boldsymbol{\tau}, \mathbf{v}, \eta) \in H_{\Gamma_N}(\text{div}, \Omega)^{2\times2} \times L^2(\Omega)^2 \times L^2(\Omega)$.

In the following we will assume that the Neumann boundary conditions $\boldsymbol{\sigma}^N \cdot \mathbf{n}$ are given as piecewise constant tractions on Γ_N and thus, we have $\boldsymbol{\sigma}^N \in S_h$. With this we have the additional result that $(\boldsymbol{\sigma}^N + \boldsymbol{\sigma}_h)$ is an element of S_h which yields – due to the nature of S_h – that $\text{div}\,(\boldsymbol{\sigma}^N + \boldsymbol{\sigma}_h)$ is itself piecewise constant. At the same time we know from (5.2) that $(\text{div}\,(\boldsymbol{\sigma}^N + \boldsymbol{\sigma}_h), \mathbf{v}_h)_{0,\Omega}$ equals zero for all $\mathbf{v}_h \in V_h$ and that the functions $\mathbf{v}_h$ are also piecewise constant. That means that the L^2 inner product of a piecewise constant function with all other piecewise constants is zero thus leading us to the conclusion that $\text{div}\,(\boldsymbol{\sigma}^N + \boldsymbol{\sigma}_h)$ itself equals zero everywhere on Ω which implies that

$$
\begin{aligned}
(i) \qquad & \text{div}\,\boldsymbol{\sigma}_e \equiv 0 \ , \\
(ii) \quad r_2(\mathbf{v}) = {}& (\text{div}\,\boldsymbol{\sigma}_e, \mathbf{v})_{0,\Omega} = 0 \qquad \forall\,\mathbf{v} \in V_h \ .
\end{aligned}
\qquad (5.6)
$$

Therefore, the assumption that the surface tractions are given as piecewise constant functions on the boundary simplifies the residual error expression by one equation. For a broad variety of problems this simplified approach seems to be reasonable and will thus be used throughout the rest of this thesis. However, if one wants to deal with problems where this assumption is not applicable one could include the residual r_2 in the error

analysis which leads to additional error contributions in the final estimator; we refer to e.g. [Lo'02, LoV'04] for further details on this topic.

To derive a residuum-based error estimator from the two residuals r_1 and r_3 that contain contributions in $H(\text{div}, \Omega)$ we have to apply a *Helmholtz decomposition* on the functions of $H(\text{div}, \Omega)$. The general theory concerning this topic can be found in an extensive paper by WOHLMUTH and HOPPE ([WH'99]), while an appropriate decomposition for the problem of linear elasticity together with a proof can be found in the recent paper of CAI and STARKE ([CS'03]); this *Helmholtz decomposition* will also be used here and is thus shortly presented in the following theorem. Recall that in Section 4.3 we already applied a discrete version of this decomposition.

Theorem 5.1 (Helmholtz Decomposition for Linear Elasticity) *Any given tensor $\boldsymbol{\tau} \in H_{\Gamma_N}(\text{div}, \Omega)^{2\times 2}$ can be decomposed orthogonally*

$$\boldsymbol{\tau} = \nabla^{\perp}\boldsymbol{\varphi} \oplus \mathcal{C}\,\nabla\mathbf{q} \, ,$$

where we have $\boldsymbol{\varphi} \in H^1_{\Gamma_N}(\Omega)^2$ and $\mathbf{q} \in H^1_{\Gamma_D}(\Omega)^2$.

Applying this decomposition on elements $\boldsymbol{\tau} \in H_{\Gamma_N}(\text{div}, \Omega)^{2\times 2}$ we make use of the special inner product on $H(\text{div}, \Omega)^{2\times 2}$ from Definition 4.2 which will be shortly recalled here:

$$(\boldsymbol{\sigma}, \boldsymbol{\tau})_{\mathcal{C}^{-1},\text{div}} := (\text{div}\,\boldsymbol{\sigma}, \text{div}\,\boldsymbol{\tau})_{0,\Omega} + (\mathcal{C}^{-1}\,\boldsymbol{\sigma}, \boldsymbol{\tau})_{0,\Omega} \, .$$

With the *Helmholtz decomposition* and the $(\,\cdot\,, \cdot\,)_{\mathcal{C}^{-1},\text{div}}$ inner product we can decompose $\boldsymbol{\sigma}_e$, leading to

$$\boldsymbol{\sigma}_e = \boldsymbol{\sigma}_e^0 \oplus \boldsymbol{\sigma}_e^{0,\perp} \, .$$

Here $\boldsymbol{\sigma}_e^0$ is the divergence-free part of $\boldsymbol{\sigma}_e$ and $\boldsymbol{\sigma}_e^{0,\perp}$ its orthogonal complement with respect to $(\,\cdot\,, \cdot\,)_{\mathcal{C}^{-1},\text{div}}$, i.e.

$$(\mathcal{C}^{-1}\,\boldsymbol{\sigma}_e^0, \boldsymbol{\sigma}_e^{0,\perp})_{0,\Omega} = 0 \, .$$

With respect to the fact that $\boldsymbol{\sigma}_e$ itself is divergence-free – cf. equation (5.6) – we have $\boldsymbol{\sigma}_e = \boldsymbol{\sigma}_e^0$. Therefore it suffices to fulfill system (5.5) only for such $\boldsymbol{\tau} \in H_{\Gamma_N}(\text{div}, \Omega)^{2\times 2}$ that belong to the subspace of the first orthogonal component $\nabla^{\perp}\boldsymbol{\varphi}$. This results also in the fact that the terms

$$(\mathbf{u}_e, \text{div}\,\nabla^{\perp}\boldsymbol{\varphi})_{0,\Omega} \quad ,$$

$$(\mathbf{u}_h, \text{div}\,\nabla^{\perp}\boldsymbol{\varphi})_{0,\Omega}$$

are canceled out and what remains is the system

$$(\mathcal{C}^{-1}\boldsymbol{\sigma}_e, \nabla^{\perp}\boldsymbol{\varphi})_{0,\Omega} + (\gamma_e, \text{as}\,\nabla^{\perp}\boldsymbol{\varphi})_{0,\Omega} = r_1(\nabla^{\perp}\boldsymbol{\varphi}) \, ,$$

$$(\text{as}\,\boldsymbol{\sigma}_e, \eta)_{0,\Omega} = r_3(\eta) \tag{5.7}$$

that has to hold true for all $(\boldsymbol{\varphi}, \eta) \in H^1_{\Gamma_N}(\Omega)^2 \times L^2(\Omega)$. For clarity we define the reduced residual r_1 once again and more precisely via:

$$r_1(\nabla^\perp \boldsymbol{\varphi}) := - (\mathcal{C}^{-1}(\boldsymbol{\sigma}^N + \boldsymbol{\sigma}_h), \nabla^\perp \boldsymbol{\varphi})_{0,\Omega} - (\gamma_h, \mathsf{as}\, \nabla^\perp \boldsymbol{\varphi})_{0,\Omega} . \tag{5.8}$$

5.1.2   Error estimation: reliability

From the error expression in terms of residual quantities in (5.7) we have to derive an easily computable quantity that bounds the error from above and below within a small range. The most important goal is of course the *reliability* of the estimator which is implied through a global error bound from above. Therefore, we will start deriving such an global upper bound in this subsection. Nevertheless, we will state a central theorem that also guarantees *efficiency* of the estimator, which means that there are local lower bounds for the error on each triangle and that these lower bounds consist of the same local quantities that also form the global upper bound for the error. The *efficiency* of the estimator will be proven in the subsection 5.1.3 following the central theorem. To prove *reliability* we will first give a stability estimate that bounds the error in $\boldsymbol{\sigma}$ and γ in their associated norms in terms of the residuals r_1 and r_3 and proceed by estimating these residuals through computable quantities.

Lemma 5.2 *The error $\boldsymbol{\sigma}_e$ in the stress tensor measured in the $(\,\cdot\,,\,\cdot\,)_{\mathcal{C}^{-1},\mathsf{div}}$-norm and the error γ_e in the Lagrangian parameter measured in the L^2-norm can be estimated independently of the mesh width h and the Lamé constants λ and μ via*

$$\|\boldsymbol{\sigma}_e\|^2_{\mathcal{C}^{-1},\mathsf{div}} + \|\gamma_e\|^2_{0,\Omega} \lesssim \sup_{\boldsymbol{\varphi}} \frac{[r_1(\nabla^\perp \boldsymbol{\varphi})]^2}{\|\mathcal{C}^{-1/2}\nabla^\perp \boldsymbol{\varphi}\|^2_{0,\Omega}} + \sup_\eta \frac{[r_3(\eta)]^2}{\|\eta\|^2_{0,\Omega}} . \tag{5.9}$$

Proof: *Lemma 5.2 is a consequence of the fact that the inf-sup condition is fulfilled for the PEERS formulation (cf. Section 3.3.3). Hence, we know from Section 3.2.1 that the system (5.7) defines a bounded linear mapping $\mathcal{L}$ from $H_{\Gamma_N}(\mathsf{div},\Omega)^2 \times L^2(\Omega)$ onto its dual space. Furthermore, $\mathcal{L}$ is an isomorphism and thus there exists also a bounded linear mapping $\mathcal{L}^{-1}$ from the dual space back onto the space $H_{\Gamma_N}(\mathsf{div},\Omega)^2 \times L^2(\Omega)$. The isomorphism $\mathcal{L}$ finally guarantees the stability estimate (5.9); for further details we refer to [Bz'74, BF'91, Br'97, KS'04].* □

Remark 5.3 *Note that by applying the general theory of [Bz'74, BF'91] the inequality (5.9) had to be put formally as*

$$\|\boldsymbol{\sigma}_e\|^2_{\mathcal{C}^{-1},\mathsf{div}} + \|\mathbf{u}_e\|^2_{0,\Omega} + \|\gamma_e\|^2_{0,\Omega} \lesssim \sup_{\boldsymbol{\varphi}} \frac{[r_1(\nabla^\perp \boldsymbol{\varphi})]^2}{\|\mathcal{C}^{-1/2}\nabla^\perp \boldsymbol{\varphi}\|^2_{0,\Omega}} + \sup_{\mathbf{v}} \frac{[r_2(\mathbf{v})]^2}{\|\mathbf{v}\|^2_{0,\Omega}} + \sup_\eta \frac{[r_3(\eta)]^2}{\|\eta\|^2_{0,\Omega}} .$$

Due to the fact that for all $\mathbf{v} \in V$ we have $r_2(\mathbf{v}) = 0$ (cf. equation (5.6)) this inequality reduces to

$$\|\boldsymbol{\sigma}_e\|_{\mathcal{C}^{-1},\mathrm{div}}^2 + \|\mathbf{u}_e\|_{0,\Omega}^2 + \|\gamma_e\|_{0,\Omega}^2 \;\lesssim\; \sup_{\boldsymbol{\varphi}} \frac{[r_1(\nabla^\perp \boldsymbol{\varphi})]^2}{\|\mathcal{C}^{-1/2}\nabla^\perp \boldsymbol{\varphi}\|_{0,\Omega}^2} + \sup_{\eta} \frac{[r_3(\eta)]^2}{\|\eta\|_{0,\Omega}^2} \;,$$

which also implies (5.9).

For the further derivation of our error estimator we need two more Lemmata. The first one is a standard result concerning the *Clément interpolation operator* that maps a function from the Sobolev space H^1 to an associated finite element ansatz space. Interpolation operators such as *Cléments operator* are used to gain estimates for a piecewise polynomial approximation. The general approximation theorem gives us error estimates depending on the global norm of the function we want to approximate. In general this theorem does not hold true for H^1-functions but only for H^2-functions or H^1-functions that are at least continuous over Ω while the *Clément operator* guarantees estimates for all kinds of H^1-functions in a quasi-local norm, e.g. a norm on a patch of elements that have a least one common point. For further details concerning this topic we reference [Br'97, Ve'99], where the interested reader can find a definition for the operator and proofs for the approximation results.

Lemma 5.4 *There exists a projection $\mathcal{I}_h : H_{\Gamma_N}^1(\Omega)^2 \longrightarrow (\mathcal{M}_{0,h}^1 \cap H_{\Gamma_N}^1(\Omega))^2$ such that for any $\boldsymbol{\varphi} \in H_{\Gamma_N}^1(\Omega)^2$ we have*

$$
\begin{aligned}
\|\boldsymbol{\varphi} - \mathcal{I}_h\boldsymbol{\varphi}\|_{0,T} &\;\lesssim\; h_T \|\boldsymbol{\varphi}\|_{1,\Omega_T} \;, \\
\|\boldsymbol{\varphi} - \mathcal{I}_h\boldsymbol{\varphi}\|_{0,E} &\;\lesssim\; h_E^{\frac{1}{2}} \|\boldsymbol{\varphi}\|_{1,\Omega_E} \;.
\end{aligned}
\tag{5.10}
$$

Here, the domains Ω_T and Ω_E are given as the union of elements having at least one point in common with a triangle T or an edge E, respectively. The operator $\mathcal{I}_h$ can be chosen componentwise to be the standard Clément operator mentioned above.

Proof: *With $\mathcal{I}_h$ chosen as the Clément operator the above Lemma is an immediate consequence of the results presented in [Ve'99].* $\qquad\square$

The second Lemma will give bounds for the patch-norms $\| \cdot \|_{1,\Omega_T}$ and $\| \cdot \|_{1,\Omega_E}$ in terms of the global norm $\| \cdot \|_{0,\Omega}$.

Lemma 5.5 *Assuming that we have given a triangulation $\mathcal{T}_h$ and that Γ_N is a non-empty subset of $\partial\Omega$ the following inequalities hold true for all $\boldsymbol{\varphi} \in H_{\Gamma_N}^1(\Omega)^2$:*

$$
\begin{aligned}
\sum_{T \in \mathcal{T}_h} \|\boldsymbol{\varphi}\|_{1,\Omega_T}^2 &\;\lesssim\; \|\mathcal{C}^{-1/2}\nabla^\perp \boldsymbol{\varphi}\|_{0,\Omega}^2 \;, \\
\sum_{T \in \mathcal{T}_h} \|\boldsymbol{\varphi}\|_{1,\Omega_E}^2 &\;\lesssim\; \|\mathcal{C}^{-1/2}\nabla^\perp \boldsymbol{\varphi}\|_{0,\Omega}^2 \;.
\end{aligned}
\tag{5.11}
$$

Proof: *The patches Ω_T and Ω_E contain only a limited number of elements and are thus bounded. Furthermore, the sum of these patch norms over all triangles is obviously bounded and it follows that we have for all $\boldsymbol{\varphi} \in H^1_{\Gamma_N}(\Omega)^2$*

$$\sum_{T \in \mathcal{T}_h} \|\boldsymbol{\varphi}\|^2_{1,\Omega_T} \;\lesssim\; \|\boldsymbol{\varphi}\|^2_{1,\Omega} \;,$$

$$\sum_{T \in \mathcal{T}_h} \|\boldsymbol{\varphi}\|^2_{1,\Omega_E} \;\lesssim\; \|\boldsymbol{\varphi}\|^2_{1,\Omega} \;.$$

With (2.4) and (2.9) we can write the inner product $(\mathcal{C}^{-1} \cdot\,,\,\cdot\,)_{0,\Omega}$ also as

$$(\mathcal{C}^{-1}\boldsymbol{\sigma}, \boldsymbol{\tau})_{0,\Omega} \;=\; \frac{1}{2\,\mu}\,(\operatorname{dev}\boldsymbol{\sigma}, \operatorname{dev}\boldsymbol{\tau})_{0,\Omega} \;+\; \frac{1}{4\,(\lambda + \mu)}\,(\operatorname{tr}\boldsymbol{\sigma}, \operatorname{tr}\boldsymbol{\tau})_{0,\Omega} \;, \tag{5.12}$$

which expresses the orthogonal nature of the decomposition of a stress $\boldsymbol{\sigma}$ into its deviatoric and its volumetric part (cf. Section 2.1). This leads to the estimate

$$
\begin{aligned}
\|\mathcal{C}^{-1/2}\nabla^{\perp}\boldsymbol{\varphi}\|^2_{0,\Omega} \;&=\; (\mathcal{C}^{-1}\nabla^{\perp}\boldsymbol{\varphi}, \nabla^{\perp}\boldsymbol{\varphi})_{0,\Omega} \\[2mm]
&=\; \frac{1}{2\,\mu}\,\|\operatorname{dev}\nabla^{\perp}\boldsymbol{\varphi}\|^2_{0,\Omega} \;+\; \frac{1}{4\,(\lambda + \mu)}\,\|\operatorname{tr}\nabla^{\perp}\boldsymbol{\varphi}\|^2_{0,\Omega} \\[2mm]
&\geq\; \frac{1}{2\,\mu}\,\|\operatorname{dev}\nabla^{\perp}\boldsymbol{\varphi}\|^2_{0,\Omega} \\[2mm]
&=\; \frac{1}{2\,\mu}\,\left\| \begin{bmatrix} \frac{1}{2}(\partial_2\varphi_1 + \partial_1\varphi_2) & -\partial_1\varphi_1 \\ \partial_2\varphi_2 & -\frac{1}{2}(\partial_2\varphi_1 + \partial_1\varphi_2) \end{bmatrix} \right\|^2_{0,\Omega} \\[2mm]
&=\; \frac{1}{2\,\mu}\,\left\| \begin{bmatrix} \frac{1}{2}(\partial_2\varphi_1 + \partial_1\varphi_2) & \partial_1\varphi_1 \\ \partial_2\varphi_2 & \frac{1}{2}(\partial_2\varphi_1 + \partial_1\varphi_2) \end{bmatrix} \right\|^2_{0,\Omega} \\[2mm]
&=\; \frac{1}{2\,\mu}\,\left\| \frac{1}{2}\,(\nabla\boldsymbol{\varphi} + \nabla\boldsymbol{\varphi}^T) \right\|^2_{0,\Omega} \;,
\end{aligned}
$$

for all $\boldsymbol{\varphi} \in H^1_{\Gamma_N}(\Omega)^2$. Finally, using the assumption that the Neumann boundary Γ_N is a non-empty subset of the whole boundary of Ω we obtain with Korn's second inequality that

$$\|\boldsymbol{\varphi}\|_{1,\Omega} \;\lesssim\; \|\tfrac{1}{2}\,(\nabla\boldsymbol{\varphi} + \nabla\boldsymbol{\varphi}^T)\|_{0,\Omega} \qquad \forall\,\boldsymbol{\varphi} \in H^1_{\Gamma_N}(\Omega)^2 \;.$$

Thus, we have for all $\boldsymbol{\varphi} \in H^1_{\Gamma_N}(\Omega)^2$

$$\sum_{T \in \mathcal{T}_h} \|\boldsymbol{\varphi}\|^2_{1,\Omega_T} \;\lesssim\; \|\boldsymbol{\varphi}\|^2_{1,\Omega} \;\lesssim\; \|\tfrac{1}{2}\,(\nabla\boldsymbol{\varphi} + \nabla\boldsymbol{\varphi}^T)\|^2_{0,\Omega} \;\lesssim\; \|\mathcal{C}^{-1/2}\nabla^{\perp}\boldsymbol{\varphi}\|^2_{0,\Omega}$$

and the same holds true respectively for the norm $\|\boldsymbol{\varphi}\|_{1,\Omega_E}$ which finishes the proof. $\square$

Combining the results of the above three Lemmata we can now derive some computable estimate. Note that the first equation of the discretized system (5.2) together with the

definition of the residuum r_1 in (5.4) implies that

$$r_1(\boldsymbol{\tau}_h) \;=\; 0 \qquad \forall\, \boldsymbol{\tau}_h \in S_h \;.$$

By applying the interpolation operator $\mathcal{I}_h$ to the addend $\nabla^\perp \boldsymbol{\varphi}$ from the *Helmholtz decomposition* we note furthermore that we have $\nabla^\perp(\mathcal{I}_h\boldsymbol{\varphi}) \in S_h$ and thus[2]

$$r_1(\nabla^\perp(\mathcal{I}_h\boldsymbol{\varphi})) \;=\; 0 \qquad \forall\, \boldsymbol{\varphi} \in H^1_{\Gamma_N}(\Omega)^2 \;.$$

Using this result we can expand and rewrite $r_1(\nabla^\perp\boldsymbol{\varphi})$:

$$
\begin{aligned}
r_1(\nabla^\perp\boldsymbol{\varphi}) \;&=\; r_1(\nabla^\perp\boldsymbol{\varphi}) \,-\, r_1(\nabla^\perp(\mathcal{I}_h\boldsymbol{\varphi})) \\[2mm]
&=\; r_1(\nabla^\perp(\boldsymbol{\varphi}-\mathcal{I}_h\boldsymbol{\varphi})) \\[2mm]
&=\; -\,(\mathcal{C}^{-1}(\boldsymbol{\sigma}^N + \boldsymbol{\sigma}_h), \nabla^\perp(\boldsymbol{\varphi}-\mathcal{I}_h\boldsymbol{\varphi}))_{0,\Omega} \,-\, (\gamma_h, \mathsf{as}\,\nabla^\perp(\boldsymbol{\varphi}-\mathcal{I}_h\boldsymbol{\varphi}))_{0,\Omega} \;.
\end{aligned}
\tag{5.13}
$$

This expression of integrals over Ω can of course be split up in a sum of element integrals over elements T in the triangulation $\mathcal{T}_h$ and we get

$$
\begin{aligned}
R \;&:=\; (\mathcal{C}^{-1}(\boldsymbol{\sigma}^N + \boldsymbol{\sigma}_h), \nabla^\perp(\boldsymbol{\varphi}-\mathcal{I}_h\boldsymbol{\varphi}))_{0,\Omega} \,+\, (\gamma_h, \mathsf{as}\,\nabla^\perp(\boldsymbol{\varphi}-\mathcal{I}_h\boldsymbol{\varphi}))_{0,\Omega} \\[2mm]
&=\; \sum_{T \in \mathcal{T}_h} \Big[(\mathcal{C}^{-1}(\boldsymbol{\sigma}^N + \boldsymbol{\sigma}_h), \nabla^\perp(\boldsymbol{\varphi}-\mathcal{I}_h\boldsymbol{\varphi}))_{0,T} \,+\, (\gamma_h, \mathsf{as}\,\nabla^\perp(\boldsymbol{\varphi}-\mathcal{I}_h\boldsymbol{\varphi}))_{0,T} \Big] \\[2mm]
&=\; \sum_{T \in \mathcal{T}_h} \Big[(\mathcal{C}^{-1}(\boldsymbol{\sigma}^N + \boldsymbol{\sigma}_h), \nabla^\perp(\boldsymbol{\varphi}-\mathcal{I}_h\boldsymbol{\varphi}))_{0,T} \,+\, (\gamma_h, \mathsf{div}\,(\boldsymbol{\varphi}-\mathcal{I}_h\boldsymbol{\varphi}))_{0,T} \Big] \;,
\end{aligned}
\tag{5.14}
$$

where the last equality sign is a consequence of the identity

$$
\mathsf{as}\,\nabla^\perp\mathbf{v} \;=\; \mathsf{as}\,
\begin{bmatrix}
\dfrac{\partial v_1}{\partial x_2} & -\dfrac{\partial v_1}{\partial x_1} \\[3mm]
\dfrac{\partial v_2}{\partial x_2} & -\dfrac{\partial v_2}{\partial x_1}
\end{bmatrix}
\;=\; \dfrac{\partial v_2}{\partial x_2} \,-\, \Big(-\dfrac{\partial v_1}{\partial x_1}\Big) \;=\; \mathsf{div}\,\mathbf{v} \qquad \forall\, \mathbf{v} \in H^1(\Omega) \;.
$$

With the div-operator in use we can apply *Green's Formula* to the second part in the last line of (5.14). Employing also partial integration onto the first part of the sum we have

$$
\begin{aligned}
R \;=\; \sum_{T \in \mathcal{T}_h} \Big[&(\mathcal{C}^{-1}(\boldsymbol{\sigma}^N + \boldsymbol{\sigma}_h)\cdot\mathbf{t}, \boldsymbol{\varphi}-\mathcal{I}_h\boldsymbol{\varphi})_{0,\partial T} \,+\, \mathsf{curl}\,(\mathcal{C}^{-1}(\boldsymbol{\sigma}^N + \boldsymbol{\sigma}_h), \boldsymbol{\varphi}-\mathcal{I}_h\boldsymbol{\varphi})_{0,T} \\[2mm]
&+\, (\gamma_h, \mathbf{n}\cdot(\boldsymbol{\varphi}-\mathcal{I}_h\boldsymbol{\varphi}))_{0,\partial T} \,-\, (\nabla\gamma_h, \boldsymbol{\varphi}-\mathcal{I}_h\boldsymbol{\varphi})_{0,T} \Big] \;,
\end{aligned}
$$

---

[2] The *Clément operator* yields $\mathcal{I}_h\boldsymbol{\varphi} \in (\mathcal{M}^1_{0,h})^2$ such that $\nabla^\perp(\mathcal{I}_h\boldsymbol{\varphi})$ is an element of either $(\mathcal{RT}^0_h)^2$ or $(\mathsf{curl}\,\mathcal{B}^3_{0,h})^2$ and therefore of S_h.

where by $\mathbf{v} \cdot \mathbf{t}$ we denote the tangential component of a vector $\mathbf{v}$ on a triangle edge E. Combining the edge integrals and the element integrals in two distinct sums results in

$$
\begin{aligned}
R \;=\; & \sum_{T \in \mathcal{T}_h} (\operatorname{curl} \mathcal{C}^{-1}(\boldsymbol{\sigma}^N + \boldsymbol{\sigma}_h) \;-\; \nabla \gamma_h, \boldsymbol{\varphi} - \mathcal{I}_h \boldsymbol{\varphi})_{0,T} \\
& + \sum_{T \in \mathcal{T}_h} \big[(\mathcal{C}^{-1}(\boldsymbol{\sigma}^N + \boldsymbol{\sigma}_h) \cdot \mathbf{t}, \boldsymbol{\varphi} - \mathcal{I}_h \boldsymbol{\varphi})_{0,\partial T} \;+\; (\gamma_h, \mathbf{n} \cdot (\boldsymbol{\varphi} - \mathcal{I}_h \boldsymbol{\varphi}))_{0,\partial T} \big] \;.
\end{aligned}
$$

We note that due to the scalar nature of γ_h it is

$$
(\gamma_h, \mathbf{n} \cdot (\boldsymbol{\varphi} - \mathcal{I}_h \boldsymbol{\varphi}))_{0,\partial T} \;=\; (\gamma_h \, \mathbf{n}, (\boldsymbol{\varphi} - \mathcal{I}_h \boldsymbol{\varphi}))_{0,\partial T} \;,
$$

and we therefore get

$$
\begin{aligned}
R \;=\; & \sum_{T \in \mathcal{T}_h} (\operatorname{curl} \mathcal{C}^{-1}(\boldsymbol{\sigma}^N + \boldsymbol{\sigma}_h) \;-\; \nabla \gamma_h, \boldsymbol{\varphi} - \mathcal{I}_h \boldsymbol{\varphi})_{0,T} \\
& + \sum_{T \in \mathcal{T}_h} (\mathcal{C}^{-1}(\boldsymbol{\sigma}^N + \boldsymbol{\sigma}_h) \cdot \mathbf{t} \;+\; \gamma_h \, \mathbf{n}, \boldsymbol{\varphi} - \mathcal{I}_h \boldsymbol{\varphi})_{0,\partial T} \;.
\end{aligned}
$$

Focusing on the sum of edge integrals we realize that it can also be written as a sum over edges. We know that on all inner edges $E \not\subseteq \partial\Omega$ we have two integral contributions – one from each neighbor element – while on the boundary edges $E \subset \partial\Omega$ we have to take into account only one integral. Furthermore, realize that

$$
\sum_{E \subset \Gamma_N} (\mathcal{C}^{-1}(\boldsymbol{\sigma}^N + \boldsymbol{\sigma}_h) \cdot \mathbf{t} \;+\; \gamma_h \, \mathbf{n}, \boldsymbol{\varphi} - \mathcal{I}_h \boldsymbol{\varphi})_{0,E} \;=\; 0 \;,
$$

because we have $\boldsymbol{\varphi} \in H^1_{\Gamma_N}(\Omega)^2$ and thus $\boldsymbol{\varphi} = 0$ on Γ_N. From the boundary edges we therefore have to consider only the Dirichlet edges while on inner edges we have to compute the jumps in the quantity $\mathcal{C}^{-1}(\boldsymbol{\sigma}^N + \boldsymbol{\sigma}_h) \cdot \mathbf{t}$ on an edge E denoted by the term $j_E(\mathcal{C}^{-1}(\boldsymbol{\sigma}^N + \boldsymbol{\sigma}_h) \cdot \mathbf{t})$. The quantity $\gamma_h \, \mathbf{n}$ will cancel itself out on each inner edge due to the different orientation of the normal component and the fact that γ_h is a quantity computed on each vertex. Finally we end up with

$$
\begin{aligned}
R \;=\; & \sum_{T \in \mathcal{T}_h} (\operatorname{curl} \mathcal{C}^{-1}(\boldsymbol{\sigma}^N + \boldsymbol{\sigma}_h) \;-\; \nabla \gamma_h, \boldsymbol{\varphi} - \mathcal{I}_h \boldsymbol{\varphi})_{0,T} \\
& + \sum_{E \not\subseteq \partial\Omega} (j_E(\mathcal{C}^{-1}(\boldsymbol{\sigma}^N + \boldsymbol{\sigma}_h) \cdot \mathbf{t}), \boldsymbol{\varphi} - \mathcal{I}_h \boldsymbol{\varphi})_{0,E} \qquad\qquad (5.15) \\
& + \sum_{E \subset \Gamma_D} (\mathcal{C}^{-1}(\boldsymbol{\sigma}^N + \boldsymbol{\sigma}_h) \cdot \mathbf{t} \;+\; \gamma_h \, \mathbf{n}, \boldsymbol{\varphi} - \mathcal{I}_h \boldsymbol{\varphi})_{0,E} \;.
\end{aligned}
$$

To simplify the residuum R a little bit we will use the jump term j_E more generally in the further equations as expressed in the following definition:

Definition 5.6 *Let E be an edge in a triangulation $\mathcal{T}_h$ on a domain Ω. E is either part of the boundary of the domain therefore belonging only to one triangle T or part of the*

inner domain therefore belonging to two triangles $T_{E,r}$ and $T_{E,l}$. Quantities that are defined discretely on each triangle may differ on an inner edge. Such quantities are denoted with the symbols $|_{T_{E,r}}$ or $|_{T_{E,l}}$ respectively, indicating to which triangle they belong. With these notations we define

$$j_E(\mathcal{C}^{-1}(\boldsymbol{\sigma}^N + \boldsymbol{\sigma}_h) \cdot \mathbf{t}) := \begin{cases} (\mathcal{C}^{-1}(\boldsymbol{\sigma}^N + \boldsymbol{\sigma}_h) \cdot \mathbf{t})|_{T_{E,r}} \\ \quad - (\mathcal{C}^{-1}(\boldsymbol{\sigma}^N + \boldsymbol{\sigma}_h) \cdot \mathbf{t})|_{T_{E,l}} & \text{if } E \not\subseteq \partial\Omega \\ \mathcal{C}^{-1}(\boldsymbol{\sigma}^N + \boldsymbol{\sigma}_h) \cdot \mathbf{t} + \gamma_h \mathbf{n} & \text{if } E \subset \Gamma_D \\ 0 & \text{if } E \subset \Gamma_N . \end{cases}$$

Combining the results from the equations (5.13), (5.14) and (5.15) we get with the *Cauchy Schwarz inequality* and the above definition of j_E

$$r_1(\nabla^\perp \boldsymbol{\varphi})^2 \;\lesssim\; \sum_{T \in \mathcal{T}_h} \| (\text{curl}\, \mathcal{C}^{-1}(\boldsymbol{\sigma}^N + \boldsymbol{\sigma}_h) - \nabla\gamma_h \|^2_{0,T} \; \| \boldsymbol{\varphi} - \mathcal{I}_h\boldsymbol{\varphi} \|^2_{0,T}$$
$$+ \sum_{E \subset \bar{\Omega}} \| j_E(\mathcal{C}^{-1}(\boldsymbol{\sigma}^N + \boldsymbol{\sigma}_h) \cdot \mathbf{t}) \|^2_{0,E} \; \| \boldsymbol{\varphi} - \mathcal{I}_h\boldsymbol{\varphi} \|^2_{0,E} .$$

Now applying the two Lemmata 5.4 and 5.5 we can estimate the residuum r_1 through

$$r_1(\nabla^\perp \boldsymbol{\varphi})^2 \;\lesssim\; \sum_{T \in \mathcal{T}_h} h_T^2 \| (\text{curl}\, \mathcal{C}^{-1}(\boldsymbol{\sigma}^N + \boldsymbol{\sigma}_h) - \nabla\gamma_h \|^2_{0,T} \; \| \boldsymbol{\varphi} \|^2_{1,\Omega_T}$$
$$+ \sum_{E \subset \bar{\Omega}} h_E \| j_E(\mathcal{C}^{-1}(\boldsymbol{\sigma}^N + \boldsymbol{\sigma}_h) \cdot \mathbf{t}) \|^2_{0,E} \; \| \boldsymbol{\varphi} \|^2_{1,\Omega_E}$$
$$\lesssim\; \sum_{T \in \mathcal{T}_h} h_T^2 \| (\text{curl}\, \mathcal{C}^{-1}(\boldsymbol{\sigma}^N + \boldsymbol{\sigma}_h) - \nabla\gamma_h \|^2_{0,T} \sum_{T \in \mathcal{T}_h} \| \boldsymbol{\varphi} \|^2_{1,\Omega_T}$$
$$+ \sum_{E \subset \bar{\Omega}} h_E \| j_E(\mathcal{C}^{-1}(\boldsymbol{\sigma}^N + \boldsymbol{\sigma}_h) \cdot \mathbf{t}) \|^2_{0,E} \sum_{T \in \mathcal{T}_h} \| \boldsymbol{\varphi} \|^2_{1,\Omega_E} ,$$

and finally by

$$r_1(\nabla^\perp \boldsymbol{\varphi})^2 \;\lesssim\; \sum_{T \in \mathcal{T}_h} h_T^2 \| (\text{curl}\, \mathcal{C}^{-1}(\boldsymbol{\sigma}^N + \boldsymbol{\sigma}_h) - \nabla\gamma_h \|^2_{0,T} \; \| \mathcal{C}^{-1/2}\nabla^\perp \boldsymbol{\varphi} \|^2_{0,\Omega}$$
$$+ \sum_{E \subset \bar{\Omega}} h_E \| j_E(\mathcal{C}^{-1}(\boldsymbol{\sigma}^N + \boldsymbol{\sigma}_h) \cdot \mathbf{t}) \|^2_{0,E} \; \| \mathcal{C}^{-1/2}\nabla^\perp \boldsymbol{\varphi} \|^2_{0,\Omega} . \qquad (5.16)$$

With the result from inequality (5.16) and obtaining a similar and more obvious fact[3] for the residuum r_3, namely

$$\sup_\eta \frac{[r_3(\eta)]^2}{\|\eta\|^2_{0,\Omega}} \;=\; \sup_\eta \frac{(\text{as}\,(\boldsymbol{\sigma}^N + \boldsymbol{\sigma}_h), \boldsymbol{\eta})^2_{0,\Omega}}{\|\eta\|^2_{0,\Omega}} \;=\; \sum_{T \in \mathcal{T}_h} \| \text{as}\,(\boldsymbol{\sigma}^N + \boldsymbol{\sigma}_h) \|^2_{0,T} , \qquad (5.17)$$

---

[3] The second expression in (5.17) is truly an equation again due to the fact that $\text{as}\,(\boldsymbol{\sigma}^N + \boldsymbol{\sigma}_h)$ and η are scalar quantities.

we can estimate the error in the stress tensor from Lemma 5.2 by

$$\|\boldsymbol{\sigma}_e\|^2_{\mathcal{C}^{-1},\text{div}} + \|\gamma_e\|^2_{0,\Omega} \;\lesssim\; \sum_{T\in\mathcal{T}_h} h^2_T \|\,\text{curl}\,\mathcal{C}^{-1}(\boldsymbol{\sigma}^N + \boldsymbol{\sigma}_h) - \nabla\gamma_h\,\|^2_{0,T}$$

$$+ \sum_{E\subset\bar{\Omega}} h_E \|\,j_E(\mathcal{C}^{-1}(\boldsymbol{\sigma}^N + \boldsymbol{\sigma}_h)\cdot\mathbf{t})\,\|^2_{0,E}$$

$$+ \sum_{T\in\mathcal{T}_h} \|\,\text{as}\,(\boldsymbol{\sigma}^N + \boldsymbol{\sigma}_h)\,\|^2_{0,T}\;.$$

With the derivation of this computable estimate we can finally define our residual a posteriori error estimator:

Definition 5.7 *We define three local error contributions for each triangle T through*

$$\eta_{T,1} \;:=\; h_T \,\|\,\text{curl}\,\mathcal{C}^{-1}(\boldsymbol{\sigma}^N + \boldsymbol{\sigma}_h) - \nabla\gamma_h\,\|_{0,T}\;,$$

$$\eta_{T,2} \;:=\; \sum_{E\subset\partial T} h^{\frac{1}{2}}_E \,\|\,j_E(\mathcal{C}^{-1}(\boldsymbol{\sigma}^N + \boldsymbol{\sigma}_h)\cdot\mathbf{t})\,\|_{0,E}\;,$$

$$\eta_{T,3} \;:=\; \|\,\text{as}\,(\boldsymbol{\sigma}^N + \boldsymbol{\sigma}_h)\,\|_{0,T}\;,$$

which together represent the error contribution of each triangle,

$$\eta_T \;:=\; \left(\eta^2_{T,1} + \eta^2_{T,2} + \eta^2_{T,3}\right)^{\frac{1}{2}}\;.$$

The global error estimate η is given by

$$\eta \;:=\; \left(\sum_{T\in\mathcal{T}_h} \eta^2_T\right)^{\frac{1}{2}}\;.$$

With this definition of the error estimator we formulate the following theorem:

Theorem 5.8 *Let Ω be a bounded Lipschitz domain and let the triples $(\boldsymbol{\sigma}, \mathbf{u}, \gamma)$ and $(\boldsymbol{\sigma}_h, \mathbf{u}_h, \gamma_h)$ be solutions of the two linear systems (5.1) and (5.2) on the domain Ω. Given this, the quantity η defined in 5.7 is a robust, reliable and efficient error estimator, e.g. the inequalities*

$$\|\boldsymbol{\sigma}_e\|^2_{\mathcal{C}^{-1},\text{div}} + \|\gamma_e\|^2_{0,\Omega} \;\lesssim\; \eta^2 \tag{5.18}$$

$$\eta^2_T \;\lesssim\; \|\boldsymbol{\sigma}_e\|^2_{\mathcal{C}^{-1},\text{div},\Omega_T} + \|\gamma_e\|^2_{0,\Omega_T} \tag{5.19}$$

hold true independently from the mesh width parameter h as well as from the Lamé constants λ and μ. In this notation we localized the inner product $(\,\cdot\,,\,\cdot\,)_{\mathcal{C}^{-1},\text{div}}$ on an element patch Ω_T (a patch that contains the triangle T and all triangles adjacent to it) by defining

$$\|\boldsymbol{\sigma}_e\|^2_{\mathcal{C}^{-1},\text{div},\Omega_T} \;:=\; (\text{div}\,\boldsymbol{\sigma},\text{div}\,\boldsymbol{\sigma})_{0,\Omega_T} + (\mathcal{C}^{-1}\boldsymbol{\sigma},\boldsymbol{\sigma})_{0,\Omega_T}\;.$$

Proof: *The first inequality follows from the Lemmata 5.2, 5.4 and 5.5 and was shown extensively above within the derivation process of the estimator. The second inequality that states the efficiency of the estimator requires some more work and will be proved in the course of the next subsection.* □

5.1.3 Error estimation: efficiency

To prove inequality (5.19) we first of all need some special form functions ψ_T and ψ_E that can be defined best via barycentric coordinates.

Definition 5.9 *Let T be an element of the triangulation $\mathcal{T}_h$ and let $\lambda_{1,T}$, $\lambda_{2,T}$ and $\lambda_{3,T}$ be the barycentric coordinates of the three vertices of T that fulfill a kind of partition of unity*

$$\sum_{i=1}^{3} \lambda_{i,T} = 1 .$$

With these $\lambda_{i,T}$ we define the bubble function $\psi_T \in \mathcal{B}_0^3$ with $\operatorname{supp} \psi_T = T$ through

$$\psi_T := \prod_{i=1}^{3} \lambda_{i,T} .$$

Furthermore, let $\lambda_{1,E}$ and $\lambda_{2,E}$ be the barycentric coordinates of the two vertices at each end of an edge. Similar to the above definition we can now also define functions $\psi_E \in \mathcal{M}_0^2$ by

$$\psi_E := \prod_{i=1}^{2} \lambda_{i,E} .$$

The support of ψ_E is chosen to be the two triangles $T_{E,r}$ and $T_{E,l}$ adjacent to the edge E. Note that we have $\lambda_{i,T} \geq 0$ and $\lambda_{i,E} \geq 0$ due to the support of ψ_T and ψ_E and thus it is $0 \leq \psi_T \leq 1$ and $0 \leq \psi_E \leq 1$.

Using the form functions ψ_T and ψ_E yields some important estimates we need later on to prove the local lower bound (5.19). We present these estimates in the following lemma and refer for a proof to [Ve'96]; further details concerning the general framework can also be found in [Br'97].

Lemma 5.10 *For a given element $T \in \mathcal{T}_h$ and a given edge E of the triangulation $\mathcal{T}_h$ the following inequalities hold true for all $\boldsymbol{\tau}_h \in S_h$:*

$$\| \operatorname{curl} \boldsymbol{\tau}_h \|_{0,T}^2 \ \lesssim \ (\operatorname{curl} \boldsymbol{\tau}_h, \psi_T \operatorname{curl} \boldsymbol{\tau}_h)_{0,T} \ \lesssim \ \| \operatorname{curl} \boldsymbol{\tau}_h \|_{0,T}^2 \ , \tag{5.20}$$

$$\| \boldsymbol{\tau}_h \cdot \mathbf{t} \|_{0,E}^2 \ \lesssim \ (\boldsymbol{\tau}_h \cdot \mathbf{t}, \psi_T \boldsymbol{\tau}_h \cdot \mathbf{t})_{0,E} \ \lesssim \ \| \boldsymbol{\tau}_h \cdot \mathbf{t} \|_{0,E}^2 \ , \tag{5.21}$$

and

$$\| \operatorname{curl} (\psi_T \operatorname{curl} \boldsymbol{\tau}_h) \|_{0,T} \ \lesssim \ h_T^{-1} \| \psi_T \operatorname{curl} \boldsymbol{\tau}_h \|_{0,T} \ , \tag{5.22}$$

$$\| \operatorname{curl} (\psi_E \boldsymbol{\tau}_h \cdot \mathbf{t}) \|_{0,T} \ \lesssim \ h_T^{-1} \| \psi_E \boldsymbol{\tau}_h \cdot \mathbf{t} \|_{0,T} \ , \tag{5.23}$$

$$\| \psi_E \boldsymbol{\tau}_h \cdot \mathbf{t} \|_{0,T} \ \lesssim \ h_E^{\frac{1}{2}} \| \psi_E \boldsymbol{\tau}_h \cdot \mathbf{t} \|_{0,E} \ . \tag{5.24}$$

Proof: *The inequalities (5.20) and (5.21) are obvious because we know that it is $0 \le \psi_T \le 1$. For the rest of the proof we cite [Ve'96].*   □

With these results we will estimate each addend $\eta_{T,1}$, $\eta_{T,2}$ and $\eta_{T,3}$ of the local quantity η_T in terms of the error. We start with the first component $\eta_{T,1}$ and define a function ρ_T via

$$\rho_T \ := \ \psi_T \operatorname{curl} (\mathcal{C}^{-1}(\boldsymbol{\sigma}^N + \boldsymbol{\sigma}_h) + \gamma_h)$$

to simplify the following notation. With the first part of (5.20) we can estimate

$$\| \operatorname{curl} \mathcal{C}^{-1}(\boldsymbol{\sigma}^N + \boldsymbol{\sigma}_h) - \nabla \gamma_h \|_{0,T}^2 \ = \ \| \operatorname{curl} (\mathcal{C}^{-1}(\boldsymbol{\sigma}^N + \boldsymbol{\sigma}_h) + \gamma_h) \|_{0,T}^2$$

$$\lesssim \ (\operatorname{curl} (\mathcal{C}^{-1}(\boldsymbol{\sigma}^N + \boldsymbol{\sigma}_h) + \gamma_h), \rho_T)_{0,T} \ .$$

Applying partial integration (cf. Lemma 1.22) we shift the curl-operator from one component to the other and we make use of the fact that we have $\psi_T|_{\partial T} = 0 = \rho_T|_{\partial T}$. This is due to the fact that for every point on ∂T at least one barycentric coordinate equals zero. Thus, we get

$$\| \operatorname{curl} \mathcal{C}^{-1}(\boldsymbol{\sigma}^N + \boldsymbol{\sigma}_h) - \nabla \gamma_h \|_{0,T}^2 \ \lesssim \ (\operatorname{curl} (\mathcal{C}^{-1}(\boldsymbol{\sigma}^N + \boldsymbol{\sigma}_h) + \gamma_h), \rho_T)_{0,T}$$

$$= \ (\mathcal{C}^{-1}(\boldsymbol{\sigma}^N + \boldsymbol{\sigma}_h) + \gamma_h, \operatorname{curl} \rho_T)_{0,T}$$

$$= \ (\mathcal{C}^{-1}(\boldsymbol{\sigma}^N + \boldsymbol{\sigma}_h), \operatorname{curl} \rho_T)_{0,T} + (\gamma_h, \operatorname{curl} \rho_T)_{0,T}$$

$$\lesssim \ \| \boldsymbol{\sigma}_e \|_{\mathcal{C}^{-1}, \operatorname{div}, T} \| \operatorname{curl} \rho_T \|_{0,T} + \| \gamma_e \|_{0,T} \| \operatorname{curl} \rho_T \|_{0,T}$$

$$\lesssim \ \| \operatorname{curl} \rho_T \|_{0,T} \left(\| \boldsymbol{\sigma}_e \|_{\mathcal{C}^{-1}, \operatorname{div}, T}^2 + \| \gamma_e \|_{0,T}^2 \right)^{\frac{1}{2}} \ .$$

The term $\| \operatorname{curl} \rho_T \|_{0,T}$ can be estimated via inequality (5.22) and afterwards we can omit one ψ_T term and make use of the second inequality in (5.20). Therefore we have

$$
\begin{aligned}
\| \operatorname{curl} \mathcal{C}^{-1}(\boldsymbol{\sigma}^N + \boldsymbol{\sigma}_h) - \nabla\gamma_h \|_{0,T}^2 \quad &\lesssim \quad \| \operatorname{curl} \rho_T \|_{0,T} \left(\| \boldsymbol{\sigma}_e \|_{\mathcal{C}^{-1},\operatorname{div},T}^2 + \| \gamma_e \|_{0,T}^2 \right)^{\frac{1}{2}} \\
&\lesssim \quad h_T^{-1} \| \rho_T \|_{0,T} \left(\| \boldsymbol{\sigma}_e \|_{\mathcal{C}^{-1},\operatorname{div},T}^2 + \| \gamma_e \|_{0,T}^2 \right)^{\frac{1}{2}} \\
&\lesssim \quad h_T^{-1} \| \operatorname{curl}\left(\mathcal{C}^{-1}(\boldsymbol{\sigma}^N + \boldsymbol{\sigma}_h) + \gamma_h\right) \|_{0,T} \\
&\qquad\qquad \left(\| \boldsymbol{\sigma}_e \|_{\mathcal{C}^{-1},\operatorname{div},T}^2 + \| \gamma_e \|_{0,T}^2 \right)^{\frac{1}{2}} \\
&= \quad h_T^{-1} \| \operatorname{curl} \mathcal{C}^{-1}(\boldsymbol{\sigma}^N + \boldsymbol{\sigma}_h) - \nabla\gamma_h \|_{0,T} \\
&\qquad\qquad \left(\| \boldsymbol{\sigma}_e \|_{\mathcal{C}^{-1},\operatorname{div},T}^2 + \| \gamma_e \|_{0,T}^2 \right)^{\frac{1}{2}} .
\end{aligned}
$$

Now, dividing both sides of this inequality by $h_T^{-1} \| \operatorname{curl} \mathcal{C}^{-1}(\boldsymbol{\sigma}^N + \boldsymbol{\sigma}_h) - \nabla\gamma_h \|_{0,T}$ we finally get

$$
\eta_{T,1} \quad \lesssim \quad \left(\| \boldsymbol{\sigma}_e \|_{\mathcal{C}^{-1},\operatorname{div},T}^2 + \| \gamma_e \|_{0,T}^2 \right)^{\frac{1}{2}} \quad \lesssim \quad \left(\| \boldsymbol{\sigma}_e \|_{\mathcal{C}^{-1},\operatorname{div},\Omega_T}^2 + \| \gamma_e \|_{0,\Omega_T}^2 \right)^{\frac{1}{2}} . \qquad (5.25)
$$

For the second component $\eta_{T,2}$ we will take a similar approach as for $\eta_{T,1}$ and define a function ρ_E:

$$
\rho_E \quad := \quad \psi_E \, j_E(\mathcal{C}^{-1}(\boldsymbol{\sigma}^N + \boldsymbol{\sigma}_h) \cdot \mathbf{t}) .
$$

With inequality (5.21) we have

$$
\| j_E(\mathcal{C}^{-1}(\boldsymbol{\sigma}^N + \boldsymbol{\sigma}_h) \cdot \mathbf{t}) \|_{0,E}^2 \quad \lesssim \quad (j_E(\mathcal{C}^{-1}(\boldsymbol{\sigma}^N + \boldsymbol{\sigma}_h) \cdot \mathbf{t}), \rho_E)_{0,E} .
$$

Recalling the rather complicate definition of $j_E(\cdot)$ from 5.6 we reintroduce on the inner edges the term $\gamma_h \, \mathbf{n}$ that cancels itself out in the quantity j_E due to the fact that it has a different orientation on the two triangles $T_{E,r}$ and $T_{E,l}$. Applying again the partial integration of Lemma 1.22 we get (similarly to the estimation of $\eta_{T,1}$)

$$
\begin{aligned}
\| j_E(\mathcal{C}^{-1}(\boldsymbol{\sigma}^N + \boldsymbol{\sigma}_h) \cdot \mathbf{t}) \|_{0,E}^2 \quad &\lesssim \quad \sum_{T \in T_{E,r} \cup T_{E,l}} \Big((\operatorname{curl}(\mathcal{C}^{-1}(\boldsymbol{\sigma}^N + \boldsymbol{\sigma}_h) + \gamma_h), \rho_E)_{0,T} \\
&\qquad\qquad\qquad - (\mathcal{C}^{-1}(\boldsymbol{\sigma}^N + \boldsymbol{\sigma}_h) + \gamma_h, \operatorname{curl} \rho_E)_{0,T} \Big) \\
&\lesssim \quad \sum_{T \in T_{E,r} \cup T_{E,l}} \Big(\| \operatorname{curl}(\mathcal{C}^{-1}(\boldsymbol{\sigma}^N + \boldsymbol{\sigma}_h) + \gamma_h) \|_{0,T} \| \rho_E \|_{0,T} \\
&\qquad\qquad\qquad + \| \operatorname{curl} \rho_E \|_{0,T} \left(\| \boldsymbol{\sigma}_e \|_{\mathcal{C}^{-1},\operatorname{div},T}^2 + \| \gamma_e \|_{0,T}^2 \right)^{\frac{1}{2}} \Big) \\
&= \quad \sum_{T \in T_{E,r} \cup T_{E,l}} \Big(\| \operatorname{curl} \mathcal{C}^{-1}(\boldsymbol{\sigma}^N + \boldsymbol{\sigma}_h) - \nabla\gamma_h \|_{0,T} \| \rho_E \|_{0,T} \\
&\qquad\qquad\qquad + \| \operatorname{curl} \rho_E \|_{0,T} \left(\| \boldsymbol{\sigma}_e \|_{\mathcal{C}^{-1},\operatorname{div},T}^2 + \| \gamma_e \|_{0,T}^2 \right)^{\frac{1}{2}} \Big) .
\end{aligned}
$$

To estimate this further we will use the result (5.25) and we therefore have

$$\| j_E(\mathcal{C}^{-1}(\boldsymbol{\sigma}^N + \boldsymbol{\sigma}_h) \cdot \mathbf{t}) \|_{0,E}^2 \;\lesssim\; \sum_{T \in T_{E,r} \cup T_{E,l}} \left(h_T^{-1} \| \rho_E \|_{0,T} \;+\; \| \operatorname{curl} \rho_E \|_{0,T} \right.$$
$$\left. \left(\| \boldsymbol{\sigma}_e \|_{\mathcal{C}^{-1},\mathrm{div},T}^2 + \| \gamma_e \|_{0,T}^2 \right)^{\frac{1}{2}} \right) .$$

The norm $\| \operatorname{curl} \rho_E \|_{0,T}$ can be estimated via inequality (5.23) and we are left with the norm $\| \rho_E \|_{0,T}$ that can be estimated via inequality (5.24). Furthermore we note that in this context we can identify h_T with h_E. Omitting ψ_E we end up with

$$\| j_E(\mathcal{C}^{-1}(\boldsymbol{\sigma}^N + \boldsymbol{\sigma}_h) \cdot \mathbf{t}) \|_{0,E}^2 \;\lesssim\; \sum_{T \in T_{E,r} \cup T_{E,l}} \left(h_T^{-1} \| \rho_E \|_{0,T} \right.$$
$$\left. \left(\| \boldsymbol{\sigma}_e \|_{\mathcal{C}^{-1},\mathrm{div},T}^2 + \| \gamma_e \|_{0,T}^2 \right)^{\frac{1}{2}} \right)$$
$$\lesssim\; \sum_{T \in T_{E,r} \cup T_{E,l}} \left(h_E^{-\frac{1}{2}} \| \rho_E \|_{0,E} \right.$$
$$\left. \left(\| \boldsymbol{\sigma}_e \|_{\mathcal{C}^{-1},\mathrm{div},T}^2 + \| \gamma_e \|_{0,T}^2 \right)^{\frac{1}{2}} \right)$$
$$\lesssim\; \sum_{T \in T_{E,r} \cup T_{E,l}} \left(h_E^{-\frac{1}{2}} \| j_E(\mathcal{C}^{-1}(\boldsymbol{\sigma}^N + \boldsymbol{\sigma}_h) \cdot \mathbf{t}) \|_{0,E} \right.$$
$$\left. \left(\| \boldsymbol{\sigma}_e \|_{\mathcal{C}^{-1},\mathrm{div},T}^2 + \| \gamma_e \|_{0,T}^2 \right)^{\frac{1}{2}} \right) .$$

The last inequality provides the desired estimation result for $\eta_{T,2}$ by dividing both sides by $h_E^{-\frac{1}{2}} \| j_E(\mathcal{C}^{-1}(\boldsymbol{\sigma}^N + \boldsymbol{\sigma}_h) \cdot \mathbf{t}) \|_{0,E}$ and summing up the contributions from each edge of the triangle T:

$$\eta_{T,2} \;\lesssim\; \sum_{T \in T_{E,r} \cup T_{E,l}} \left(\| \boldsymbol{\sigma}_e \|_{\mathcal{C}^{-1},\mathrm{div},T}^2 + \| \gamma_e \|_{0,T}^2 \right)^{\frac{1}{2}} \;\lesssim\; \left(\| \boldsymbol{\sigma}_e \|_{\mathcal{C}^{-1},\mathrm{div},\Omega_T}^2 + \| \gamma_e \|_{0,\Omega_T}^2 \right)^{\frac{1}{2}} .$$
$$(5.26)$$

Finally we have to examine the component $\eta_{T,3}$ and get

$$\begin{aligned}
\eta_{T,3}^2 &= \| \operatorname{as}(\boldsymbol{\sigma}^N + \boldsymbol{\sigma}_h) \|_{0,T}^2 \\
&= \| \operatorname{as}(\boldsymbol{\sigma}^N + \boldsymbol{\sigma}) - \operatorname{as}(\boldsymbol{\sigma}^N + \boldsymbol{\sigma}_h) \|_{0,T}^2 \\
&= \| \operatorname{as} \boldsymbol{\sigma}_e \|_{0,T}^2 \\
&\lesssim \| \boldsymbol{\sigma}_e \|_{0,T}^2 \\
&\lesssim \| \boldsymbol{\sigma}_e \|_{\mathcal{C}^{-1},\mathrm{div},T}^2 .
\end{aligned} \qquad (5.27)$$

Combining the results from the estimates (5.25), (5.26) and (5.27) the second inequality of Theorem 5.8 is proven which provides efficiency of the proposed error estimator for the *PEERS* approach in linear elasticity.

5.2 Error estimation in elastoplasticity

In this section we want to extend our residual error estimator derived for the case of linear elasticity to elastoplastic problems. We recall from the Sections 3.4 and 4.2.1 that the solution algorithm for the elastoplastic case required the solution of a series of linear elastic problems. We started this algorithm by computing the solution $(\boldsymbol{\sigma}_h^{el}, \mathbf{u}_h^{el}, \gamma_h^{el})$ of an auxiliary elastic problem on the domain Ω and determined afterwards which part of the domain reacts elastic and which part reacts perfectly plastic. At this point we decompose Ω in the following way:

$$\Omega = \Omega_P \cup \Omega_E , \tag{5.28}$$

where we denote by the plastic region Ω_P the union of all those triangles T in out triangulation $\mathcal{T}_h$ that have plastic material behavior, i.e. where

$$\| \operatorname{dev} \boldsymbol{\sigma}_h^{el} \|_F > \sqrt{\frac{2}{3}} \, \sigma^\star . \tag{5.29}$$

The elastic region Ω_E is therefore given as $\Omega_E = \Omega \setminus \Omega_P$ and on Ω_E the auxiliary elastic solution $(\boldsymbol{\sigma}_h^{el}, \mathbf{u}_h^{el}, \gamma_h^{el})$ is equal to $(\boldsymbol{\sigma}_h^{pl}, \mathbf{u}_h^{pl}, \gamma_h^{pl})$, the solution of the elastoplastic problem. Therefore also the error estimator for the elastic case applied to $(\boldsymbol{\sigma}_h^{el}, \mathbf{u}_h^{el}, \gamma_h^{el})$ is reliant and efficient in the elastic region. In the plastic region however we have to compute the elastic trial solution $(\boldsymbol{\sigma}_h^{tr}, \mathbf{u}_h^{tr}, \gamma_h^{tr})$ which yields via the explicitly given orthogonal projection P_K the plastic stress:

$$\boldsymbol{\sigma}_h^{pl} = P_K(\boldsymbol{\sigma}_h^{tr}) = \boldsymbol{\sigma}_h^{tr} - \operatorname{dev} \boldsymbol{\sigma}_h^{tr} + \sqrt{\frac{2}{3}} \, \frac{\sigma^\star \operatorname{dev} \boldsymbol{\sigma}_h^{tr}}{\| \operatorname{dev} \boldsymbol{\sigma}_h^{tr} \|_F} . \tag{5.30}$$

Note that the displacement in the elastoplastic case $\mathbf{u}_h^{pl}$ is given by $\mathbf{u}_h^{tr}$. The computation of $(\boldsymbol{\sigma}_h^{tr}, \mathbf{u}_h^{tr}, \gamma_h^{tr})$ on the other hand is done via our fixed point iteration scheme from (4.34) where in each iteration step k we compute the solution of the elastic help problem (4.31) that we recall here shortly. We seek the triple $(\boldsymbol{\delta}^{(k)}, \mathbf{w}^{(k)}, \vartheta^{(k)}) \in S_h \times V_h \times Q_h$ such that

$$(\mathcal{C}^{-1}\boldsymbol{\delta}_h^{(k)}, \boldsymbol{\tau}_h)_{0,\Omega} + (\mathbf{w}_h^{(k)}, \operatorname{div} \boldsymbol{\tau}_h)_{0,\Omega} + (\vartheta_h^{(k)}, \operatorname{as} \boldsymbol{\tau}_h)_{0,\Omega} = 0 ,$$

$$(\operatorname{div} \boldsymbol{\delta}_h^{(k)}, \mathbf{v}_h)_{0,\Omega} = -\sum_{T \in \mathcal{T}_h} \Bigg((\operatorname{div} P_K(\boldsymbol{\sigma}_h^{(k-1)}), \mathbf{v}_h)_{0,T}$$

$$-\frac{1}{2} \left(\left[P_K(\boldsymbol{\sigma}^{(k-1)}) \cdot \mathbf{n} \right], \mathbf{v}_h \right)_{0,\partial T} \Bigg) , \tag{5.31}$$

$$(\operatorname{as} \boldsymbol{\delta}^{(k)}, \eta_h)_{0,\Omega} = 0 ,$$

holds true for all triples $(\boldsymbol{\tau}_h, \mathbf{v}_h, \eta_h) \in S_h \times V_h \times Q_h$. From Section 4.3 we know that the fixed point iteration scheme is convergent. Furthermore, the iteration is also consistent if

we have

$$
\begin{aligned}
(\operatorname{div} P_K(\boldsymbol{\sigma}^{(k)}), \mathbf{v}_h)_{0,T} &\approx 0 \qquad \forall\, T \in \mathcal{T}_h \ , \mathbf{v}_h \in V_h \ , \\
\left(\left[P_K(\boldsymbol{\sigma}^{(k)}) \cdot \mathbf{n}\right], \mathbf{v}_h\right)_{0,E} &\approx 0 \qquad \forall\, E \in \mathcal{E}_h \ , \mathbf{v}_h \in V_h \ ,
\end{aligned}
\tag{5.32}
$$

as the consistency considerations from Section 4.2.1 show; cf. the formulae (4.26) to (4.29) concerning the proposed iteration scheme. Together convergence and consistency yield that the two measures

$$
\eta_{T,4} \;:=\; h_T \, \| \operatorname{div} P_K(\boldsymbol{\sigma}^{(k)}) \|_{0,T} \ ,
\tag{5.33}
$$

$$
\eta_{T,5} \;:=\; \sum_{E \subset \partial T} h_E^{\frac{1}{2}} \, \big\| \left[P_K(\boldsymbol{\sigma}^{(k)}) \cdot \mathbf{n}\right] \big\|_{0,E} \ ,
\tag{5.34}
$$

are natural quantities to determine the error of an iterate in the fixed point iteration scheme. Therefore it is reasonable to incorporate these quantities in an adaptive scheme for the plastic case combined with the error estimator for elasticity for the auxiliary elastic problem. This combination is necessary because the auxiliary elastic problem yields the starting iterate $(\boldsymbol{\sigma}_h^{el}, \mathbf{u}_h^{el}, \gamma_h^{el})$ for the fixed point iteration scheme. Large errors in $(\boldsymbol{\sigma}_h^{el}, \mathbf{u}_h^{el}, \gamma_h^{el})$ could thus influence the convergence of the iteration scheme.

A possible algorithm for error estimation in elastoplasticity would therefore be of the form as presented in Algorithm 5.11. Numerical results computed with this method can be found in Section 6.3 for a common benchmark problem.

Algorithm 5.11 (Error estimation for elastoplasticity)

```
Step 1. Compute solution of the auxiliary elastic problem on given
          finite element mesh.

Step 2. Compute error estimate for the auxiliary elastic problem.

Step 3. Determine triangles to be refined on the basis of local error
          contributions for the auxiliary elastic problem.

Step 4. Determine plastic region.

Step 5. Perform given number of iterations of the iteration scheme
          in the plastic region.
```

Step 6. Compute error estimate for the approximation of the solution
        in the plastic region.

Step 7. Determine additional triangles to be refined on the basis of
        local error contributions for the plastic problem.

Step 8. Refine the finite element mesh and restart the algorithm at
        Step 1. until given accuracy is reached.

Chapter 6

Numerical Tests and Results

This chapter finally presents numerical results that will show the efficiency of the methods proposed in this thesis for the elastic as well as the elastoplastic case. We begin with a short introduction of a common benchmark problem that will be examined in all numerical tests. This benchmark for elastoplasticity was extensively analyzed within a major research grant of the *Deutsche Forschungsgemeinschaft (DFG)*[1] only some years ago. The project yields numerous reference data and is therefore very appropriate for evaluating new numerical methods dealing with the topic of elastoplasticity. Furthermore the project is very well documented, cf. [S+'02].

The numerical results in the following sections are always based on a *MATLAB* implementation of the methods proposed in the chapters before.[2]

6.1 The benchmark problem

The benchmark problem is introduced and examined in [S+'02] within a full 3D model but also within a reduced 2D model (under the assumption of the plane strain condition, cf. Section 2.2). However, we will present the benchmark only in the reduced model which we have examined in all our considerations throughout this thesis.

We assume that we have given a square plate of metal with a side length of 20 cm, a negligible thickness and a circular hole of radius 1 cm in its middle occupying the domain $\Omega^\star \subset \mathbb{R}^2$ with $\Omega^\star = (\,[-10, 10] \times [-10, 10]\,) \,\setminus\, B_1(0)\,$. This metal plate is subjected to

---

[1] German Research Foundation

[2] *MATLAB* is a commercial software tool for mathematical computations and also a registered trademark of *The MathWorks, Inc.* .

two opposite and outward surface tractions **g** applied to the specimen from above and below. These tractions have to be incorporated in the problem via Neumann boundary conditions. On the other boundaries, i.e on the left-hand side, on the right-hand side and around the hole we also assume Neumann boundary conditions via zero tractions: $\boldsymbol{\sigma} \cdot \mathbf{n} = 0$. The whole setup is depicted in Figure 6.1.
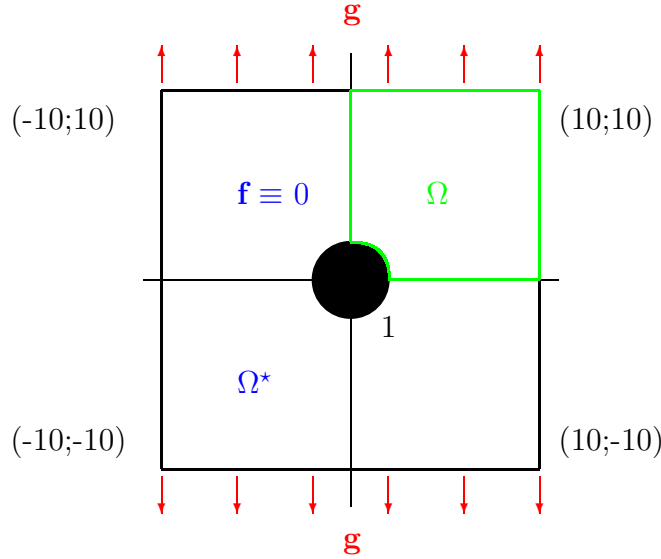

Figure 6.1: *The benchmark problem: a metal square plate with a center hole depicted in the 2D reduced model state with vanishing volume force $\mathbf{f}$ and surface tractions $\mathbf{g}$; only the subdomain $\Omega \subset \Omega^\star$ will be discretized due to symmetry.*

For the metal specimen we assume furthermore the following material parameters:

$$
\begin{aligned}
E &= 206\,900 \text{ MPa} , \\
\nu &= 0.29 , \\
\sigma^\star &= 450 \text{ MPa} .
\end{aligned}
\tag{6.1}
$$

Owing to the symmetric nature of the problem it suffices to study and discretize only a quarter of the whole domain $\Omega^\star$, e.g. $\Omega = ([0, 10] \times [0, 10]) \setminus B_1(0)$ as also shown in Figure 6.1. With this simplification we have to adjust the boundary conditions to the domain Ω. On the top edge of the computational domain we still have $\boldsymbol{\sigma} \cdot \mathbf{n} = \mathbf{g}$ as well as it is $\boldsymbol{\sigma} \cdot \mathbf{n} = 0$ on the edge at the right-hand side and on the edge around the hole. The other two edges have to be addressed differently with respect to the symmetry of the related displacement and stress. The nature of the problem requires that on the bottom edge there are no displacements in the y-direction and vanishing normal components of the stresses in x-direction, i.e. we have split boundary conditions with Neumann conditions for one stress component, $(\sigma_{xx}, \sigma_{xy}) \cdot \mathbf{n} = 0$, and Dirichlet conditions for one displacement component, $u_y = 0$. Analogously we have on the bottom edge $u_x = 0$ and

$(\sigma_{yx}, \sigma_{yy}) \cdot \mathbf{n} = 0$. This is shown together with a possible (and very coarse) initial grid in Figure 6.2. Note that a refinement sequence starting with such an initial grid will also model the curve around the hole better and better with each additional refinement level.
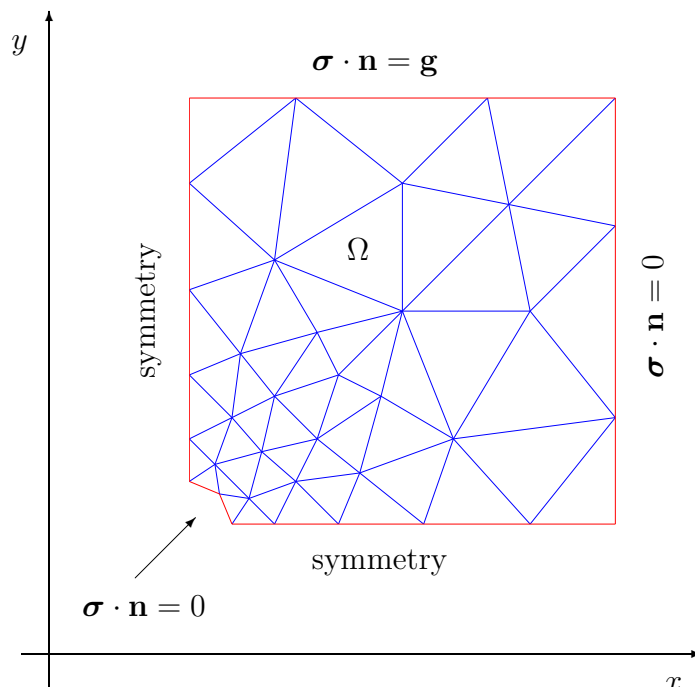

Figure 6.2: *Discretized quarter Ω of the benchmark domain $\Omega^\star$ depicted with the related boundary conditions and an initial grid.*

After this short introduction we will present and discuss in the following two sections the numerical data concerning this model problem. We start with the benchmark that considers elastic material behavior.

6.2   Elastic material behavior

The numerical results presented in this section were computed with a *MATLAB* implementation of the *PEERS* finite element method for elasticity. Due to the fact that we consider here only purely elastic material behavior we ignore in all examples and computations in this section the material parameter $\sigma^\star$ from (6.1).

We start with an examination of the iterative solver that we apply to the linear system of equations arising from the discrete variational formulation of the *PEERS* method. In the Sections 4.1.1 and 4.1.2 we analyzed the topic of such iterative solvers and developed a preconditioned *GMRES* scheme based on a so-called constraint preconditioner, that will

be considered here. We know from [KGW'00] that such a preconditioned *GMRES* method converges to the exact solution in at most $n - m + 2$ iteration steps, where n and m are the number of rows of the matrix blocks in e.g. equation (4.7). Defining n_t as the number of triangles in a discretization and n_e and n_p accordingly as the number of edges and the number of points we can determine the size of n and m and therefore also the maximally needed number of iteration steps. The parameter n describes the size of the matrix block corresponding to the stress variables which is in our discrete *PEERS* formulation equal to approximately $2(n_t + n_e)$. Analogously we can determine the size of m via the number of constraint equations describing displacement and antisymmetric part. Finally we get

$$n - m + 2 = 2(n_t + n_e) - (2n_t + n_p) + 2 \ .$$

With the general relation $n_e = n_t + np - 1$ this yields

$$n - m + 2 = 2n_t + n_p \ ,$$

which is still a quite large maximal number of iterations. However, the results of [KGW'00] show also that usually – depending on the constraints – the iteration numbers for the *GMRES* scheme are significantly smaller than $n - m + 2$, which is due to a favorable eigenvalue distribution of the preconditioned matrix. We experienced such a behavior also in our practical tests as documented in the following two figures and via the table on the next page. The corresponding computations were performed with an assumed surface traction $\mathbf{g} = 450$ MPa on a series of uniformly refined meshes without any adaptive algorithm involved while the tolerance for the norm of the relative residual in the *GMRES* algorithm was chosen to be 1e-10.
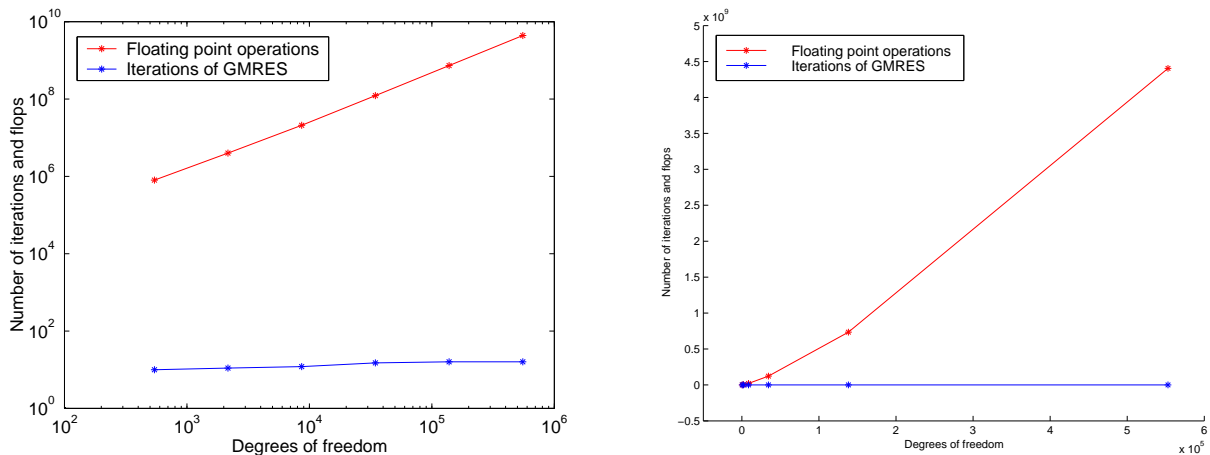

Figure 6.3: *Number of iterations and number of floating point operations depicted on a log-log scale (left) and on a normal scale (right).*

l	degrees of freedom	preconditioned GMRES		$\boldsymbol{\sigma}_{22}(1,0)$
		floating point operations	iterates	
0	543	0.8 Mio	10	921.3
1	2165	4.0 Mio	11	1146.4
2	8649	21.2 Mio	12	1263.9
3	34577	123.6 Mio	15	1319.7
4	138273	733.8 Mio	16	1350.1
5	553025	4405.4 Mio	16	1362.4

Table 6.4: *The preconditioned GMRES scheme with a tolerance of 1e-10 for the norm of the relative residual yields nearly constant iteration numbers and a linearly growing number of floating point operations dependent on the number of degrees of freedom. Furthermore, the stress $\boldsymbol{\sigma}_{22}(1,0)$ at the hole converges slowly to the reference solution of 1388.7 MPa.*

Table 6.4 shows that the preconditioned *GMRES* scheme yields even for a system with more than half a million degrees of freedom about the same number of iterations as for only 543 degrees of freedom. Furthermore, the computer resources needed by the proposed solver (here documented in terms of floating point operations) grow nearly linearly in relation to the mesh size as depicted more clearly in Figure 6.3. Finally, we can see in Table 6.4 that the reference stress $\boldsymbol{\sigma}_{22}(1,0)$ is slowly approximated.

With respect to the solution algorithm for a mere elasticity problem on uniformly refined meshes it remains to analyze the condition numbers of the initial system matrix $\mathcal{A}$ from equation (4.4) and of the preconditioned one $\mathcal{G}^{-1}\mathcal{A}$ from (4.8). Comparing the condition numbers $\kappa_2(\mathcal{A})$ and $\kappa_2(\mathcal{G}^{-1}\mathcal{A})$ in the Euklidian norm,

$$\kappa_2(X) \quad := \quad \|X\|_2 \, \|X^{-1}\|_2 \quad = \quad \frac{\lambda_{max}(X)}{\lambda_{min}(X)} \,,$$

we notice an expected development: the condition number of the preconditioned system is significantly (about fifty times) smaller than $\kappa_2(\mathcal{A})$ and it ranges between 40 and 100 depending on the refinement level. A further reduction of $\kappa_2(\mathcal{G}^{-1}\mathcal{A})$ could probably be obtained by applying other preconditioners G for the matrix block A than its diagonal D; cf. Section 4.1.

Better approximation results than those presented in Table 6.4 for e.g. $\boldsymbol{\sigma}_{22}(1,0)$ can be reached by applying the residual *a posteriori error estimator* developed and examined in Section 5.1. Numerical data for an adaptive *PEERS* method for elasticity can be found in Table 6.5 and a comparison of the error reduction on uniformly and adaptively

l	degrees of freedom	η_1	η_2	η_3	η	$\boldsymbol{\sigma}_{22}(1,0)$
0	663	1.24e00	5.28e00	1.37e00	7.98e00	958.9 MPa
1	1197	5.65e-1	3.02e00	8.44e-1	4.52e00	1131.7 MPa
2	2614	5.08e-1	2.13e00	5.59e-1	3.33e00	1245.4 MPa
3	5413	3.36e-1	1.55e00	4.02e-1	2.35e00	1315.2 MPa
4	11158	2.36e-1	1.11e00	2.83e-1	1.64e00	1346.1 MPa
5	22140	1.66e-1	8.08e-1	2.06e-1	1.10e00	1344.8 MPa
6	43573	1.16e-1	5.87e-1	1.50e-1	8.62e-1	1365.8 MPa
7	83398	8.19e-2	4.33e-1	1.11e-1	5.33e-1	1365.9 MPa
8	158997	5.90e-2	3.17e-1	8.13e-2	4.59e-1	1377.1 MPa
9	295860	4.29e-2	2.35e-1	6.02e-2	3.39e-1	1377.1 MPa

Table 6.5: *Behavior of the adaptive scheme for elasticity: a better approximation with fewer degrees of freedom compared to the results displayed in Table 6.4.*
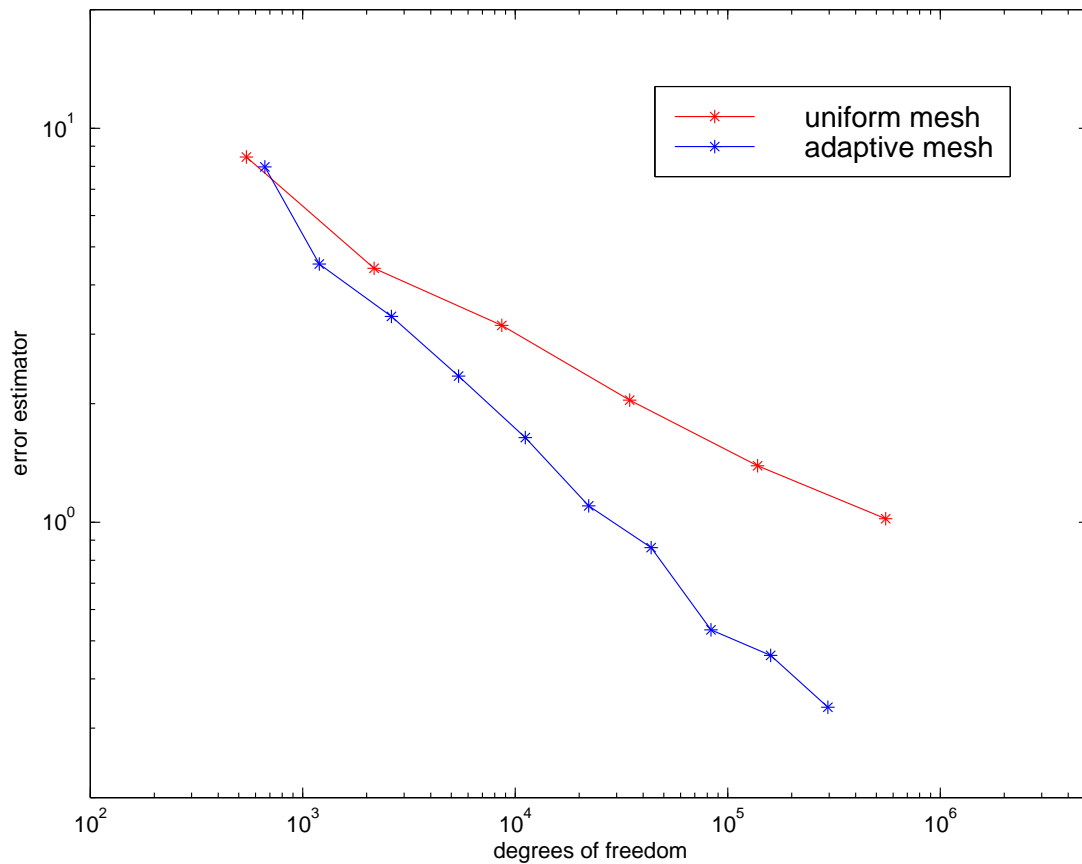

Figure 6.6: *Graphical comparison of the error reduction for uniformly and adaptively refined meshes based on data presented in Table 6.4 and Table 6.5.*

refined meshes is displayed in Figure 6.6. Note that the difference to the reference solution 1388.7 MPa in the point $\boldsymbol{\sigma}_{22}(1,0)$ seems to be quite large. Nevertheless the results for the *PEERS* approach are quite good compared to other solutions presented in [S+'02] and we also have to take into account that the reference solution was computed with a *p*-finite element method, i.e. a method that approximates the solution on a coarse grid with ansatz functions of high polynomial order. In this reference the polynomial degree was of order 19 yielding of course very good approximation results. Incidentally, the application of higher order elements, e.g. Raviart-Thomas elements of order two for the stresses in a *Least-Squares-Approach* leads to significantly better results for a similar number of degrees of freedom, cf. [CKS'04]. However, an implementation and discussion of this method is not the topic of this thesis.

In the context of the adaptive scheme for the elastic problem we also performed numerical tests with nearly incompressible material by setting the material parameter ν from (6.1) equal to 0.49, i.e. close to the incompressible limit of $\nu = 0.5$. This test is not directly motivated from an application and it is uncertain whether there is a material with *Young's modulus $E = 206\,900$* MPa and such a Poisson ratio ν. Nevertheless, the test is of numerical interest and as it is expected the *PEERS* method performs well in this case with a reasonable error reduction from mesh to mesh (cf. Table 6.7).

l	degrees of freedom	η_1	η_2	η_3	η
0	663	1.30e00	4.53e00	1.31e00	4.89e00
1	1197	5.70e-1	2.61e00	8.05e-1	2.79e00
2	2622	4.66e-1	1.81e00	5.15e-1	1.94e00
3	5488	2.99e-1	1.33e00	3.81e-1	1.41e00
4	11193	2.08e-1	9.60e-1	2.71e-1	1.02e00
5	22410	1.46e-1	7.10e-1	2.03e-1	7.52e-1
6	44492	1.03e-1	5.13e-1	1.45e-1	5.43e-1
7	84992	7.02e-2	3.76e-1	1.07e-1	3.97e-1
8	164417	5.16e-2	2.74e-1	7.74e-2	2.89e-1
9	308797	3.61e-2	2.01e-1	5.70e-2	2.12e-1

Table 6.7: *Behavior of the adaptive scheme for elasticity for some nearly incompressible material* $(\nu = 0.49)$.

We conclude this section with some pictures that show the displacement and the stress solution in the elastic case for a surface load of $\mathbf{g} = 200$ MPa on once more uniformly

refined meshes (cf. Figure 6.8). The stress solution is depicted here on a quite coarse mesh to clarify the kind of stresses that will occur in this problem.
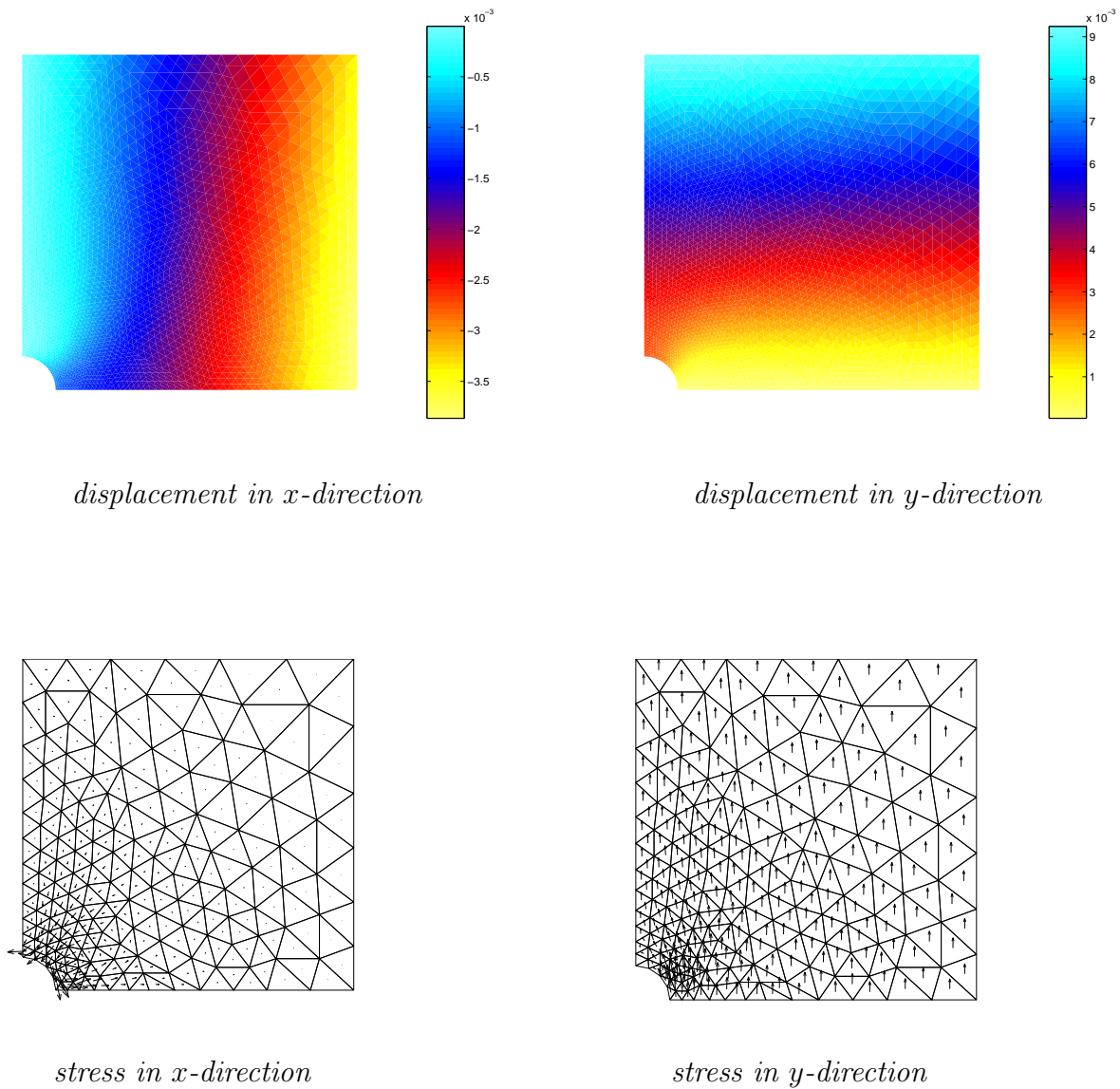

displacement in x-direction

displacement in y-direction

stress in x-direction

stress in y-direction

Figure 6.8: *The two pictures above show the displacement solution in x- and y-direction while the other pictures depict the solution stresses in x- and y-direction.*

In Figure 6.9 we finally show the elastic solution of the stress in a load problem with an applied surface traction of $\mathbf{g} = 450$ MPa on a uniformly refined mesh with approximately 250,000 degrees of freedom. Here, the stress solution is depicted as the total stress in MPa measured in the Frobenius norm.
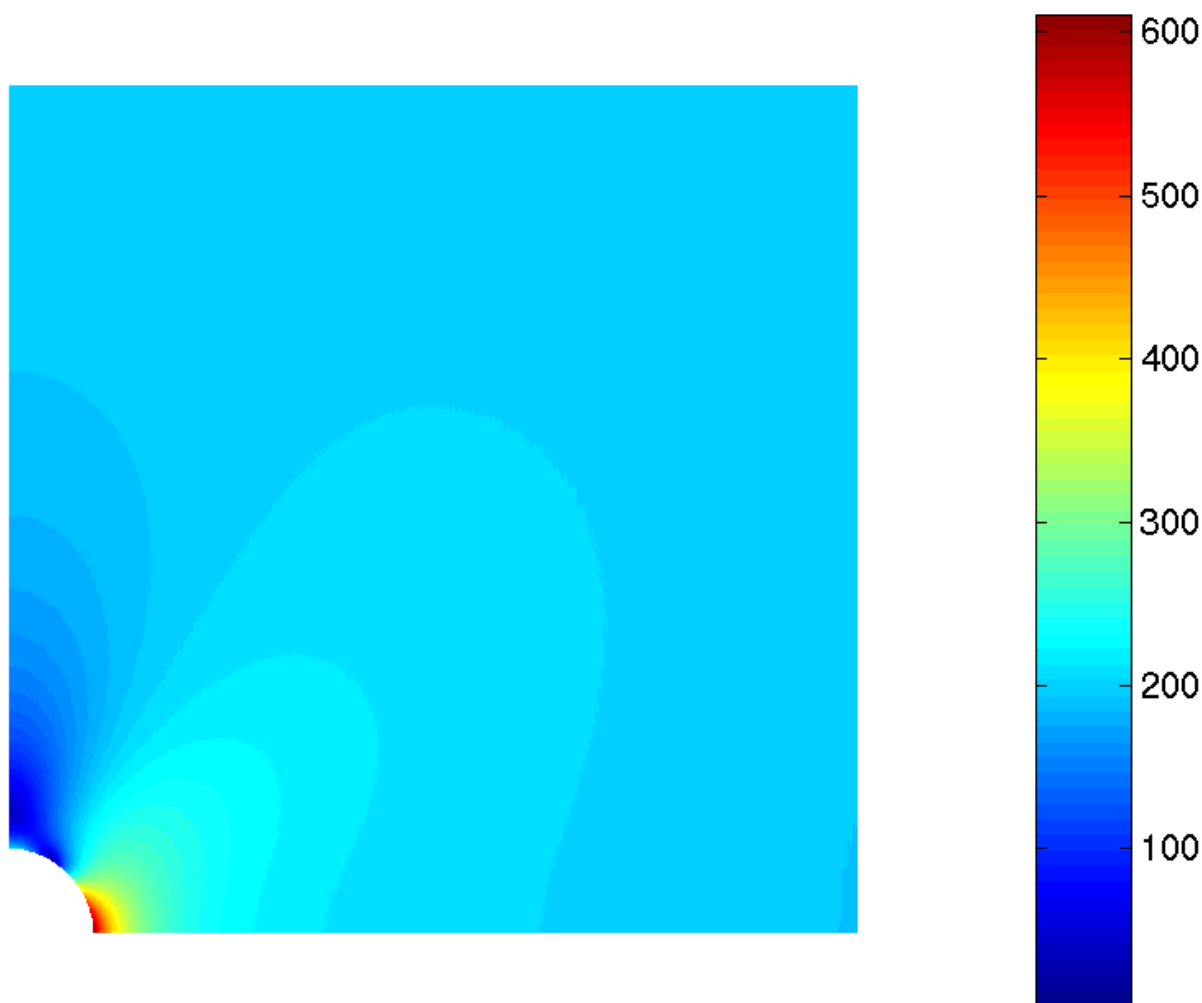
Figure 6.9: *This figure displays the total stress in MPa in the Frobenius norm.*

6.3 Elastoplastic material behavior

In this section we present a comparison between our proposed adaptive solution method from the Sections 3.4 and 4.2 for the elastoplastic problem and the reference data from [S+'02]. Again, all numerical results are based on a *MATLAB* implementation of the related algorithms.

The elastoplastic problem is characterized of course by the yield stress parameter $\sigma^\star$ from (6.1). In the benchmark setup for static and quasi-static perfect plasticity we examine the reactions of the metal plate specimen for various increasing loads **g** . It is known from experimental tests that the critical load of the metal specimen is reached at approximately **g** $= 476$ MPa; any increased load would lead to the failure of the material which can not

g	degrees of freedom	$\sigma^p_{22}(1,0)$	reference	$\sigma^p_{11}(3.8, 3.8)$	reference
100.0	31337	299.1	307.9	- 3.8	- 4.0
175.0	31337	506.6	507.5	- 6.8	- 7.0
200.0	31490	511.9	511.8	- 7.9	- 8.1
225.0	31912	515.6	515.0	- 8.9	- 9.2
250.0	32527	518.7	517.1	- 10.5	- 10.4
275.0	33106	521.0	518.4	- 11.4	- 11.7
300.0	34231	524.4	519.1	- 12.8	- 13.1
325.0	36481	526.8	519.6	- 14.7	- 14.7
350.0	39167	529.5	519.8	- 16.5	- 16.4
400.0	55825	533.4	520.0	- 26.2	- 25.7
412.5	62224	535.1	520.0	- 34.1	- 32.8
425.0	69752	536.6	520.0	- 60.7	- 51.5
437.5	80375	535.2	520.0	- 66.2	- 54.2
450.0	92912	536.1	520.0	- 68.4	- 52.5

Table 6.10: *Behavior of the adaptive scheme for elastoplasticity for two stresses of interest in comparison with the reference solution.*

be modeled in the examined setting. We therefore consider only surface tractions on the upper boundary up to 450 MPa.

As in [S+'02] we observe the first plastic reaction in the material around an applied load of **g** = 168 MPa. Furthermore, the benchmark results show that the two stresses $\sigma_{22}(1,0)$ and $\sigma_{11}(3.8, 3.8)$ are very difficult to approximate correctly. Therefore, we will also examine the related stress values within our solution method. Table 6.10 and Figure 6.11 display a comparison between the reference solution from [S+'02] and the stress solution at these two points after five adaptive refinement cycles for various load parameters **g** computed with the fixed point iteration scheme proposed in this thesis. The numerical results are quite good if we keep in mind that we only employed a *PEERS* finite element method of lowest order. Higher order elements can be expected to yield more accurate results. Moreover, we did not formulate the elastoplastic problem as an incremental loading process with a slowly growing **g** but applied only different values of the surface traction to the initial configuration of the benchmark, which may slightly affect the resulting data, too.

We also present a short examination of the global error estimate in the plastic case for a given **g** = 425 MPa on different refinement levels in Table 6.12. We notice that the
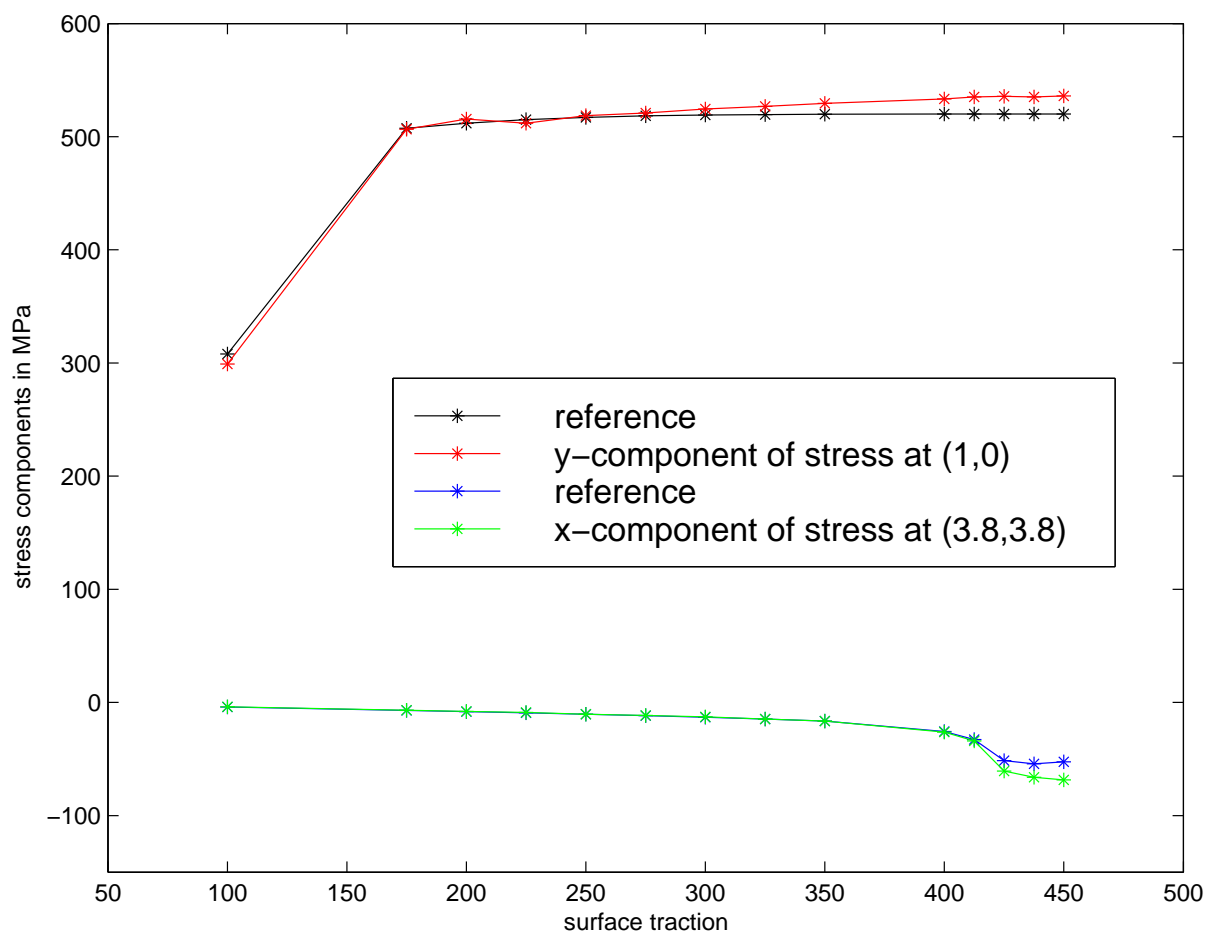
Figure 6.11: *Graphical display of the results presented in Table 6.10.*

l	degrees of freedom	η_e	η_4	η_5
0	663	7.238e00	8.477e00	4.189e01
1	1945	3.834e00	7.254e00	3.578e01
2	4867	2.721e00	6.611e00	3.201e01
3	12173	1.493e00	6.045e00	2.865e01
4	31658	1.010e00	5.563e00	2.267e01
5	80222	6.414e-1	5.278e00	1.996e01

Table 6.12: *Behavior of the adaptive scheme for elastoplasticity for* $\mathbf{g} = 425$ *MPa.*

elastic error estimator η_e as well as the natural error measures for plasticity η_4 and η_5 are reduced nicely. For the adaptive algorithm we utilized the fixed point iteration scheme from Section 4.2 according to Algorithm 5.11. To do so we performed on each adaptive

refinement level at least two steps of the fixed point iteration while on the finest level we iterated until a tolerance of 1e-05 was reached. This algorithm yielded eight iterative steps at most and usually terminated after three or four steps, therefore providing efficient and fast results.

We finally conclude this chapter with two figures. The first one shows an adaptively refined mesh after four refinements for the benchmark problem with $\mathbf{g} = 350$ MPa while the second one displays the plastic region for various loads $\mathbf{g}$.
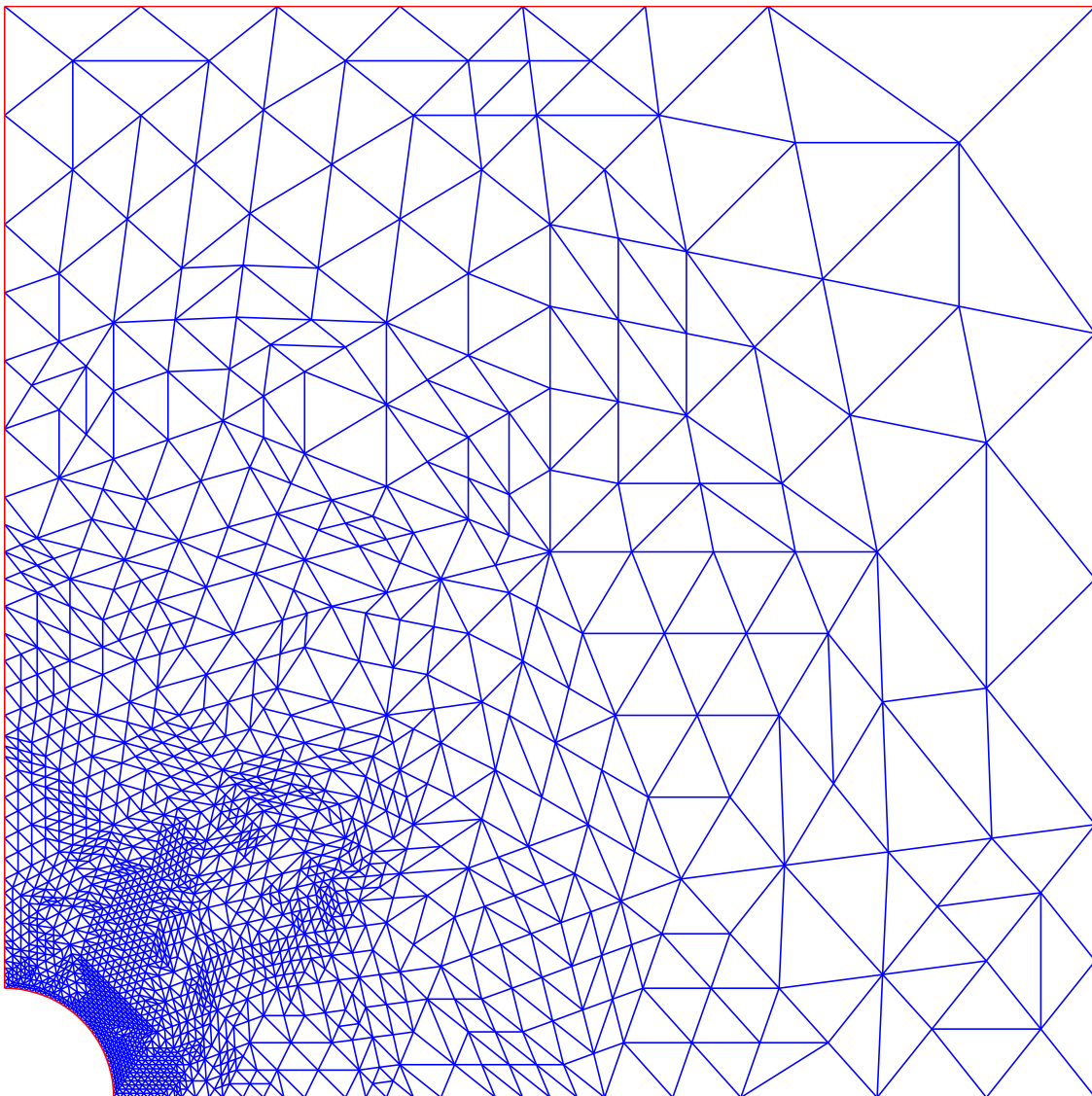

Figure 6.13: *An adaptive mesh after four adaptive refinement steps. In each step the mesh around the center hole was automatically refined for a better approximation of its circle shape. In this example the benchmark was subjected to a surface traction* $\mathbf{g} = 350$ *MPa.*
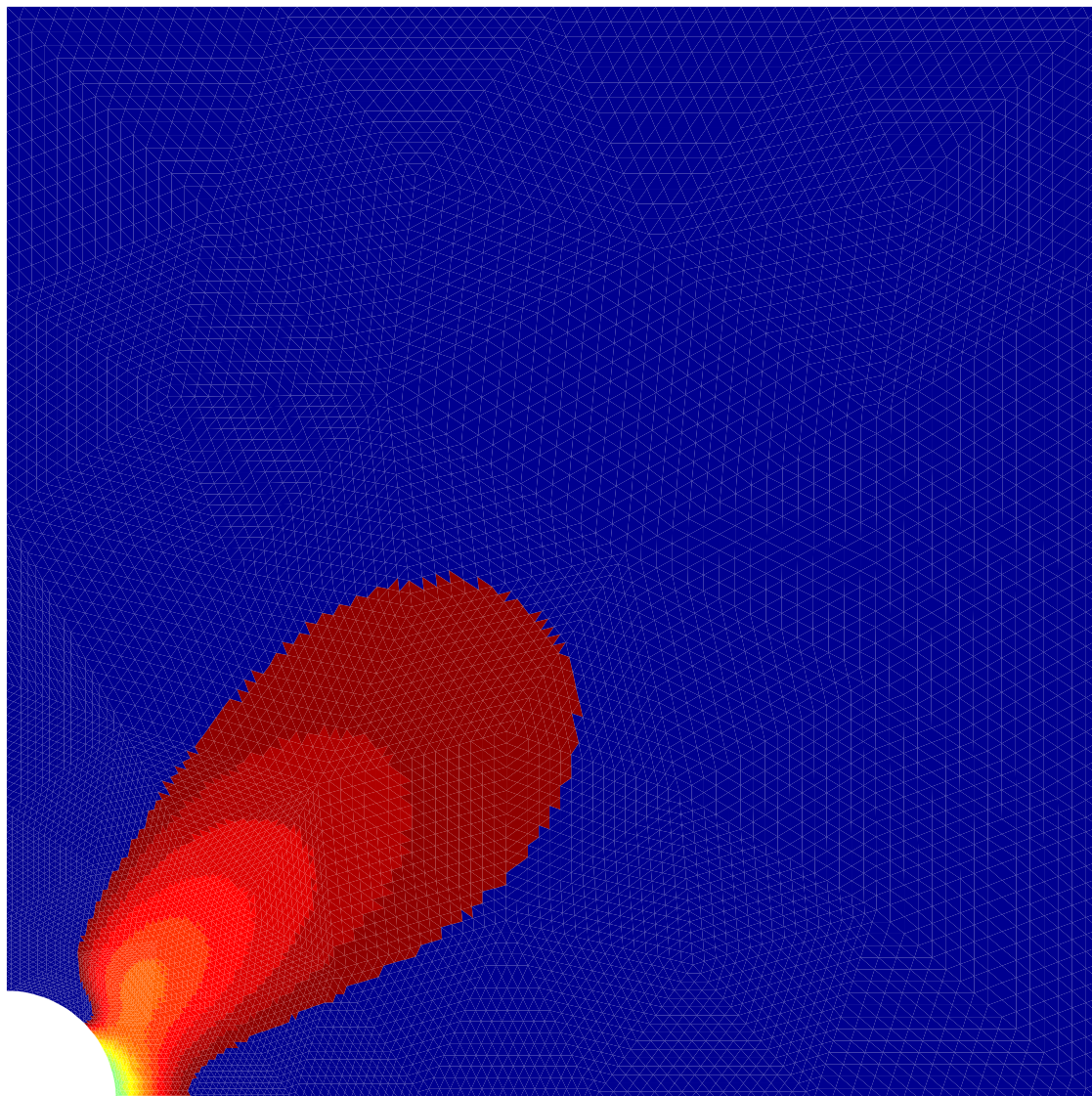
Figure 6.14: *This figure shows the plastic region in the elastoplastic benchmark problem. The blue color indicates the elastic region while the colors from yellow to red indicate the plastic region for growing surface tractions* **g** *up to* **g** $= 425$ *MPa.*

Bibliography

[ACZ'99]   J. ALBERTY, C. CARSTENSEN, D. ZARRABI: *Adaptive Numerical Analysis in Primal Elastoplasticity with hardening.* Comp. Meth. Appl. Mech. Eng., Vol. **127**, pp. 345-356 (1995).

[ABD'84]   D.N. ARNOLD, F. BREZZI, J. DOUGLAS: *PEERS: A new Mixed Finite Element for Plane Elasticity.* Japan J. Appl. Math., Vol. **1**, pp. 347-367 (1984).

[AFW'97]   D.N. ARNOLD, R.S. FALK, R. WINTHER: *Preconditioning in H(div) and Applications.* Math. Comp., Vol. **66**, No. 219, pp. 957-984 (1997).

[Ar'81]   D.N. ARNOLD: *Discretization by Finite Elements of a Model Paramter Dependent Problem.* Numer. Math., Vol. **37**, pp. 405-421 (1981).

[B'98]   U. BRINK: *Adaptive Gemischte Finite Elemente in der Nichtlinearen Elastostatik und deren Kopplung mit Randelementen.* Dissertation, Universität Hannover (1998).

[BF'91]   F. BREZZI, M. FORTIN: *Mixed and Hybrid Finite Element Methods.* Springer (1991).

[BGS'02]   M.A. BARIENTOS, G.N. GATICA, E.P. STEPHAN: *A Mixed Finite Element Method for Nonlinear Elasticity: Two-Fold Saddle Point Approach and A Posteriori Error Estimate.* Numer. Math. **91**, pp. 197-222 (2002).

[BKNSW'95] D. BRAESS, O. KLAAS, R. NIEKAMP, E. STEIN, F. WOBSCHAL: *Error Indicators for Mixed Finite Elements in 2-Dimensional Linear Elasticity.* Comput. Methods Appl. Mech. Eng., Vol. **127**, pp. 345-356 (1995).

[Bl'97]   R. BLAHETA: *Convergence of Newton-Type Methods in Incremental Return Mapping Analysis of Elasto-Plastic Problems.* Comp. Meth. Appl. Mech. Eng., Vol. **147**, pp. 167-185 (1997).

[Br'97]   D. BRAESS: *Finite Elements. Theory, Fast Solvers, and Applications in Solid Mechanics.* 2$^{\text{nd}}$ Edition. Cambridge (1997).

[BR1'78]   I. Babuska, W.C Rheinboldt: *A Posteriori Error Estimates for the Finite Element Method.* Int. J. Numer. Methods Eng., Vol. **12**, pp. 1597-1615 (1978).

[BR2'78]   I. Babuska, W.C Rheinboldt: *Error Estimates for Adaptive Finite Element Computations.* SIAM. J. Numer. Anal., Vol. **15**, pp. 736-754 (1978).

[BS1'92]   I. Babuska, M. Suri: *On Locking and Robustness in the Finite Element Method.* SIAM. J. Numer. Anal., Vol. **29**, pp. 1261-1299 (1992).

[BS2'92]   I. Babuska, M. Suri: *Locking Effcts in the Finite Element Approximation of Elasticity Problems.* Numer. Math., Vol. **62**, pp. 439-463 (1992).

[BV'96]   D. Braess, R. Verfürth: *A Posteriori Error Estimators for the Raviart-Thomas Element.* SIAM J. Numer. Anal., Vol **33**, No. 6, pp. 2431-2444 (1996).

[BW'85]   R.E. Bank, A.Weiser: *Some A Posteriori Error Estimates for Elliptic Partial Differential Equations.* Math. Comput., Vol **44**, pp. 283-301 (1985).

[Bz'74]   F. Brezzi: *On the Existence, Uniqueness and Approximation of Saddle-Point Problems Arising from Lagrangian Multipliers.* Math. Model. Numer. Anal., Vol **8**, pp. 129-151 (1974).

[Ca'97]   C. Carstensen: *A Posteriori Error Estimates for the Mixed Finite Element Method.* Math. Comput., Vol. **66**, No. 219, pp. 465-476 (1997).

[CD'98]   C. Carstensen, G. Dolzmann: *A Posteriori Error Estimates for Mixed FEM in Elasticity.* Numer. Math., Vol. **81**, No. 2, pp. 187-209 (1998).

[CDFH'00]   C. Carstensen, G. Dolzmann, S.A. Funken, D.S. Helm: *Locking-Free Adaptive Mixed Finite Element Methods in Linear Elasticity.* Comput. Methods Appl. Eng., Vol. **190**, No. 13-14, pp. 1701-1718 (2000).

[Co'94]   T.F. Coleman: *Linearly Constrained Optimization and Projected Preconditioned Conjugate Gradients.* SIAM Proc. Appl. Math., Vol **72**, pp. 188-222 (1994).

[CKS'04]   Z. Cai, J. Korsawe, G. Starke: *An Adaptive Least Squares Mixed Finite Element Method for the Stress-Displacement Formulation of Linear Elasticity.* Numer. Meth. Part. Diff. Eq., Vol **21**, to appear (2004).

[CS'03]   Z. Cai, G. Starke: *First-Order System Least Squares for the Stress-Displacement Formulation: Linear Elasticity.* SIAM J. Numer. Anal., Vol **41**, pp. 715-730 (2003).

[DL'76]   G. Duvaut, J.L. Lions: *Inequalities in Mechanics and Physics.* Springer (1976).

[Do'96]   W. Dörfler: *A Convergent Adaptive Algorithm for Poisson's Equation.* SIAM J. Numer. Anal., Vol **33**, No. 3, pp. 1106-1124 (1996).

[Ge'00]   A. Geilenkothen: *Theorie und Implementierung eines elementbasierten algebraischen Mehr-Gitter-Verfahrens.* Diplomarbeit, Universität Essen (2000).

[Ge'03]   A. Geilenkothen: *Constraint Preconditioning for Linear Systems in Elasticity.* Proceedings in Applied Mathematics and Mechanics (PAMM), Vol. **2**, pp. 481-482 (2003).

[GHN'98]   N.I.M. Gould, M.E. Hribar, J. Nocedal: *On the Solution of Equality Constrained Quadratic Programming Problems Arising in Optimization.* Rutherford Appleton Laboratory, Technical Report RAL-TR-1998-069 (1998).

[GS'02]   G.N. Gatica, E.P. Stephan: *A Mixed-FEM Formulation for Nonlinear Incompressible Elasticity in the Plane.* Numer. Meth. Part. Diff. Eq., Vol. **18**, pp. 105-128 (2002).

[Gl'84]   R. Glowinski: *Numerical Methods for Nonlinear Variational Problems.* Springer (1984).

[He'95]   H. Heuser: *Lehrbuch der Analysis. Teil 2.* 9th Edition. Teubner (1995).

[HR'99]   W. Han, B.D. Reddy: *Plasticity: Mathematical Theory and Numerical Analysis.* Springer (1999).

[Jo'77]   C. Johnson: *A Mixed Finite Element Method for Plasticity Problems with Hardening.* SIAM J. Numer. Anal., Vol. **14**, No. 4, pp. 575-583 (1977).

[Jo'78]   C. Johnson: *On Plasticity with Hardening.* J. Math. Anal. Appl., Vol. **62**, No. 4, pp. 325-336 (1978).

[JS'04]   F. Jarre, J. Stoer: *Optimierung.* Springer (2004).

[KGW'00]   C. Keller, N.I.M. Gould, A.J. Wathen: *Constraint Preconditioning for Indefinite Linear Systems.* SIAM J. Matrix Anal. Appl., Vol. **21**, No. 4, pp. 1300-1317 (2000).

[KS'04]   A. Klawonn, G. Starke: *A Preconditioner for the Equations of Linear Elasticity Discretized by the PEERS Element.* Numer. Linear Algebra Appl., Vol. **11**, pp. 493-510 (2004).

[KSSM'94]   O. Klaas, J. Schröder, E. Stein, C. Miehe: *A Regularized Dual Mixed Element for Plane Elasticity Implementation and Performance of the BDM Element.* Comput. Methods Appl. Mech. Eng., Vol. **121**, pp. 201-209 (1994).

[Lo'02]   M. Lonsing: *A Posteriori Fehlerschätzer für Gemischte Finite Elemente in der Linearen Elastizität.* Dissertation, Ruhr-Universität Bochum (2002).

[LoV'04]   M. Lonsing, R. Verfürth: *A Posteriori Error Estimators for Mixed Finite Element Methods in Linear Elasticity.* Numer. Math., Vol. **97**, No. 4, pp. 757-778 (2004).

[LV'98]   L. Luksan, J. Vlcek: *Indefinitely Preconditioned Inexact Newton Method for Large Sparse Equality Constrained Nonlinear Programming Problems.* Numer. Linear Algebra Appl., Vol. **5**, pp. 219-247 (1998).

[Me'99]   A. Meister: *Numerik linearer Gleichungssysteme. Eine Einführung in moderne Verfahren.* Vieweg (1999).

[Re'50]   E. Reissner: *On a Variational Theorem in Elasticity.* J. Math. Phys., Vol. **29**, pp. 90-95 (1950).

[RPD'03]   M. Rappaz, M. Bellet, M. Deville: *Numerical Modeling in Materials Science and Engineering.* Springer (2003).

[QSS'02]   A. Quarteroni, R. Sacco, F. Saleri: *Numerische Mathematik 1.* Springer (2002).

[S+'02]   E. Stein (Editor) et. al.: *Error-controlled Adaptive Finite Elements in Solid Mechanics.* Wiley (2002).

[SH'98]   J. Simo, T.R. Hughes: *Computational Inelasticity.* Springer (1999).

[SKSM'97]   J. Schröder, O. Klaas, E. Stein, C. Miehe: *A Physically Nonlinear Dual Mixed Element Formulation.* Comput. Methods Appl. Mech. Eng., Vol. **144**, pp. 77-92 (1997).

[SR'90]   E. Stein, R. Rolfes: *Mechanical Conditions for Stability and Optimal Convergence of Mixed Finite Elements for Linear Plane Elasticity.* Comput. Methods Appl. Mech. Eng., Vol. **84**, pp. 77-95 (1990).

[Ve'96]   R. Verfürth: *A Review of A Posteriori Error Estimation and Adaptive Mesh-Refinement Techniques.* Wiley-Teubner (1996).

[Ve'97]   R. Verfürth: *A Review of A Posteriori Error Estimation Techniques for Elasticity Problems.* Bericht 223, Ruhr-Universität Bochum (1999).

[Ve'99]   R. Verfürth: *Error Estimates for some Quasi-Interpolation Operators.* Math. Model. Numer. Anal., Vol. **33**, pp. 695-713 (1999).

[Wa'68]   K. Washizu: *Variational Methods in Elasticity and Plasticity.* Pergamon Press (1968).

[WH'99]   B.I. Wohlmuth, R.H. Hoppe: *A Comparison of A Posteriori Error Estimators for Mixed Finite Element Discretizations by Raviart-Thomas Elements.* Math. Comp., Vol. **68**, pp. 1347-1378 (1999).

[Wie1'99]   C. Wieners: *Orthogonal Projections onto Convex Sets and the Application to Problems in Plasticity.* Bericht des SFB 404, Universität Stuttgart (1999).

[Wie2'99]   C. Wieners: *Theorie und Numerik der Prandtl-Reuß-Plastizität.* Habilitationsschrift, Universität Stuttgart, SFB 404 (1999).

[ZZ'87]   J.Z. Zhu, O.C. Zienkiewicz: *A Simple Error Estimator and Adaptive Procedure for Practical Engineering Analysis.* Int. J. Numer. Methods Eng., Vol. **24**, pp. 337-357 (1987).

[ZZ'88]   J.Z. Zhu, O.C. Zienkiewicz: *Adaptive Techniques in the Finite Element Method.* Commun. Appl. Numer. Methods, Vol. **4**, No. 2, pp. 197-204 (1988).

Lebenslauf

Persönliche Daten

11.07.1972	geboren in Mülheim an der Ruhr
seit 07.05.2001	verheiratet

Schule und Zivildienst

1979 - 1983	Grundschule an der Hölterstraße in Mülheim an der Ruhr
1983 - 1992	Otto–Pankok–Gymnasium in Mülheim an der Ruhr
04.06.1992	Erwerb der Allgemeinen Hochschulreife
01.08.1994 - 31.10.1995	Zivildienst in den Christophorus–Werkstätten für Behinderte in Essen

Berufliche Ausbildung

01.08.1992 - 06.06.1994	Ausbildung zum Bankkaufmann bei der Sparkasse Essen
06.06.1994	Erwerb des Kaufmannsgehilfenbriefes

Studium

01.10.1995 - 22.12.2000	Studium der Mathematik mit Nebenfach Betriebswirtschaftslehre an der Universität Essen
18.03.1998	Erwerb des Vordiploms im Studiengang Mathematik
22.12.2000	Erwerb des Diploms im Studiengang Mathematik
01.01.2001 - 31.12.2003	Doktoranden–Stipendiat im Graduiertenkolleg "Interaktion von Modellbildung, Numerik und Software–Konzepten für technisch–wissenschaftliche Problemstellungen" (GRK 615) an der Universität Hannover
03.05.2004	Promotion zum Doktor der Naturwissenschaften

Berufliche Tätigkeiten

07.06.1994 - 30.09.1995	Angestellter im Service–Team der Sparkasse Essen
seit 01.01.2004	Wissenschaftlicher Mitarbeiter am Institut für Angewandte Mathematik (IfAM) der Universität Hannover